PEOPLE'S DEMOCRATIC REPUBLIC OF ALGERIA MINISTRY OF HIGHER EDUCATION AND SCIENTIFIC RESEARCH

University Kasdi Merbah Ouargla

Faculty of Hydrocarbons and Renewable Energies and Earth and Universe Science

, **Department of Renewable Energies**

N° d'ordre :

N° de série :

THESIS

Presented for obtaining the 3rd cycle Doctorate Diploma

By:

Sabrina Horr

Option: Renewable Energy

Title of the thesis

Study and numerical simulation of thermo-mass transfer in solid oxide fuel cell (SOFC)

Defended on: 15 / 11 /2022

In front of the jury composed of:

Prof. Abdelmadjid DOBBI	Univ.Ouargla	**President**
Prof. Bachir BOUCHEKIMA	Univ.Ouargla	**Examiner**
Prof. Slimane BOUGHALI	Univ.Ouargla	**Examiner**
Prof. Boubeker BENHAWA	Univ.El Oued	**Examiner**
A.Prof. Abdelmalek ATIA	Univ.El Oued	**Examiner**
A.Prof. Hocine MAHCENE	Univ.Ouargla	**Supervisor**

Academic year: 2021/2022

Table of contents

Abstract

In this thesis, a 3D, steady-state numerical model has been developed to analyze the performance of solid oxide fuel cell SOFC. The model is used the finite volumes method to evaluate the optimal operating points as well as the optimal design. However, our resolution was carried out by ANSYS FLUENT software, the results involves the performance curves (j-V), H_2 and H_2O mass fraction, fuel utilization, Ohmic losses, activation losses, and concentration losses for different physical and geometric parameters. Moreover, we proposed a new design to understand the flow field effects on overall fuel cell performance.

The results have shown that increasing the operating temperature, pressure, and porosity improved the performance. While the anode supported had significantly better performance than cathode and electrolyte supported. The results also showed that a significant improvement in the power density for a fixed voltage (V=0.6 V). Clearly, we were able to improve the performance starting from the initial operating parameters. The optimized model shows that the use of the optimal parameters compared to the initial operating parameters increases the power density from 1.416 A/cm^2 to 1.801 A/cm^2. We have also change the thickness of the anode from the 0.7 mm value to the optimal 0.3 mm value. With making the electrolyte layer thin is necessary to diminish the Ohmic overpotential and improve the cell performance. Moreover, the results shows the sinusoidal design gave a better distribution of velocities and temperatures than the single flow, which improved the transport of hydrogen of the cell.

The results shows the best configuration and calculates the optimal operating parameters allowing maximum power production, and this could be useful in choosing the best configuration for certain applications requiring the greatest achievable performance. Our model was verified using previous works in literature and gives a suitable agreement.

Key Words: SOFC fuel cell, ANSY FLUENT, Performance, Overpotentials, Fuel utilization

Résumé

Dans cette thèse, un modèle numérique 3D en régime permanent a été développé pour analyser les performances de la pile à combustible à oxyde solide SOFC. Le modèle utilise la méthode des volumes finis pour identifier les points de fonctionnement optimaux ainsi que la configuration optimale. Cependant, notre résolution a été effectuée par le logiciel ANSYS FLUENT, les résultats présents : les courbes de performance (j-V), la distribution de fraction massique H_2 et H_2O, le taux de l'utilisation du carburant, les pertes ohmiques, les pertes d'activation et les pertes de concentration pour différents paramètres physiques et géométriques. De plus, nous avons proposé une nouvelle configuration pour comprendre les effets du champ d'écoulement sur les performances de la pile à combustible SOFC.

Les résultats ont montré que l'augmentation de la température de fonctionnement, de la pression et de la porosité améliorait les performances. Alors que l'anode supportée avait des performances nettement meilleures que la cathode et l'électrolyte supportés. Les résultats ont également montré une amélioration significative de la densité de puissance pour une tension fixe (V=0,6 V). De toute évidence, nous avons pu améliorer les performances à partir des paramètres de fonctionnement initiaux. Le modèle optimisé montre que l'utilisation des paramètres optimaux par rapport aux paramètres de fonctionnement initiaux augmente la densité de puissance de 1,416 A/cm^2 à 1,801 A/cm^2. Nous avons également changé l'épaisseur de l'anode de la valeur de 0,7 mm à la valeur optimale de 0,3 mm. En rendant l'épaisseur d'électrolyte mince, il est nécessaire de diminuer la surtension ohmique et d'améliorer les performances de la cellule. De plus, les résultats montrent que la configuration sinusoïdale a donné une meilleure répartition des vitesses et des températures que la configuration unique, ce qui a amélioré le transport de l'hydrogène de la cellule.

Les résultats présentent la meilleure configuration et calcule les paramètres de fonctionnement optimaux permettant une production d'énergie maximale, ce qui pourrait être utile pour choisir la meilleure configuration pour certaines applications nécessitant les meilleures performances réalisables. Notre modèle a été vérifié avec la littérature et donne un accord convenable.

Mots clés : pile à combustible SOFC, ANSYS FLUENT, performances, losses, utilisation de carburant

الملخص

في هذه الأطروحة ، تم تطوير نموذج رقمي ثلاثي الأبعاد ثابت الحالة لتحليل أداء خلية وقود الأكسيد الصلب SOFC. يستخدم النموذج طريقة الأحجام المحدودة لتقييم نقاط التشغيل المثلى بالإضافة إلى التصميم الأمثل. تم تنفيذ حلنا بواسطة برنامج ANSYS FLUENT ، والنتائج تشمل: منحنيات الأداء (j-V) ، و جزء الكتلة H_2 و H_2O ، واستخدام الوقود ، والفقد الأومي ، وخسائر التنشيط ، وفقدان التركيز لوسائط فيزيائية وهندسية مختلفة. علاوة على ذلك ، اقترحنا تصميمًا جديدًا لفهم تأثيرات مجال التدفق على الأداء الكلي لخلايا الوقود.

أظهرت النتائج أن زيادة درجة حرارة التشغيل والضغط والمسامية حسنت الأداء. في حين أن القطب الموجب المدعوم كان له أداء أفضل بكثير من دعم الكاثود والإلكتروليت. كما أظهرت النتائج تحسناً معنوياً في كثافة القدرة لجهد ثابت (V = 0.6 فولت). بوضوح ، تمكنا من تحسين الأداء بدءًا من معلمات التشغيل الأولية. يوضح النموذج الأمثل أن استخدام المعلمات المثلى مقارنة بمعلمات التشغيل الأولية يزيد من كثافة الطاقة من 1.416 أمبير / سم ^{2} إلى 1.801 أمبير / سم ^{2}. لقد قمنا أيضًا بتغيير سمك الأنود من قيمة 0.7 مم إلى القيمة المثلى 0.3 مم. من الضروري جعل طبقة المنحل بالكهرباء رقيقة لتقليل الجهد الأومي الزائد وتحسين أداء الخلية. علاوة على ذلك ، أظهرت النتائج أن التصميم الجيبي أعطى توزيعًا أفضل للسرعات ودرجات الحرارة مقارنةً بالتدفق الأحادي ، مما أدى إلى تحسين نقل الهيدروجين في الخلية.

تُظهر النتائج أفضل تكوين وتحسب معلمات التشغيل المثلى التي تسمح بأقصى إنتاج للطاقة ، وقد يكون ذلك مفيدًا في اختيار أفضل تكوين لتطبيقات معينة تتطلب أفضل أداء يمكن تحقيقه. تم التحقق من نموذجنا باستخدام الأعمال السابقة.

الكلمات المفتاحية: خلية الوقود SOFC، ANSYS FLUENT، الأداء، الخسائر،استخدام الوقود

Dedications

We dedicate this work to:

My mother and my father;

My husband and my son;

My thesis director Hocine Mahcene;

All my family and all those who contributed to complete this work

Sabrina Horr

Nomenclatures

A_V	reactive surface area per unit volume, m^2m^{-3}
c_p	specific heat capacity, J kg^{-1} K^{-1}
e	the thickness,mm
D	gas diffusivity, m^2 s^{-1}
E^0	the theoretical potential difference under standard conditions,V
E	the ideal standard potential,V
E_{act}	Activation energy, J mol^{-1}
$E_{Nernest}$	Nernst potential, V
F	faraday's constant, C mol^{-1}
j_0	The exchange current density in the electrodes,A m^{-2}
j_L	the limit current density,A m^{-2}
j	The exchange current density,A m^{-2}
J	The current density, A m^{-2}
K	equilibrium constant
k_f, k_b	reaction constants,s^{-1}
k_{an}	Pre-exponential factor anodic, $\Omega^{-1}m^{-2}$
k_{cat}	Pre-exponential factor cathodic,$\Omega^{-1}m^{-2}$
κ	The permeability,m^2
M	The molar mass, g/mol
n	the number of electrons transferred
P	the pressure,Pa
P^0	the reference pressure,Pa
P_{H_2}	the partial pressures of hydrogen,Pa
P_{O_2}	the partial pressures of oxygen,Pa
P_{H_2O}	the partial pressures of water,Pa
$P_{H_2,TPB}$	the partial pressures of hydrogen at the electrolyte/electrode interfaces,Pa
$P_{H_2,TPB}$	the partial pressures of oxygen at the electrolyte/electrode interfaces,Pa
$P_{H_2O,TPB}$	the partial pressures of water at the electrolyte/electrode interfaces,Pa
$P_{H_2,f}$	the partial pressures of hydrogen at the anodic channel,Pa
$P_{O_2,a}$	the partial pressures of oxygen at the cathodic channel,Pa
$P_{H_2O,f}$	the partial pressures of water at the anodic channel,Pa
R	universal gas constant, J mol^{-1} K^{-1}
S_T	source term,Kg m^{-3} s^{-1} ,W m^{-3}
$S_{H_2,an}$	Hydrogen source term at the anode,Kg m^{-3} s^{-1}
$S_{O_2,cat}$	Oxygen source term at the cathode,Kg m^{-3} s^{-1}
$S_{H_2O,an}$	Water source term at the anode,Kg m^{-3} s^{-1}
S_u	The darcy source terms following x,Kg m^{-2} s^{-2}
S_v	The darcy source terms following y,Kg m^{-2} s^{-2}
S_w	The darcy source terms following z,Kg m^{-2} s^{-2}

T	temperature, K
u	velocity following x,m s^{-1}
v	velocity following y,m s^{-1}
V_{cell}	cell potential, V
w	velocity following z,m s^{-1}
X	mass fraction
ΔC_{pr}	Deference of specific heats, J mol^{-1} K^{-1}
ΔG	Gibbs free energy change,J mol^{-1}
ΔG_0	the standard Gibbs energy, J mol^{-1}
ΔH	the enthalpy change,J mol^{-1}
ΔS	the entropy change,J mol^{-1} K^{-1}
ΔS_0	the standard entropy change,J mol^{-1} K^{-1}
α	the electron transfer coefficient
η	The overpotentials,V
λ_{eff}	Effective thermal conductivity,W $m^{-1}K^{-1}$
σ	the conductivity of electrodes and electrolyte,$\Omega^{-1}m^{-1}$
μ	fluid viscosity, kg m^{-1} s^{-1}
ρ	Density, kg m^{-3}
ε	porosity
∅	Exchange potential,V

Subscripts and Superscripts

0	standard state
an	Anode
act	Activation
cat	Cathode
$conc$	Concentration
eff	Effective
el	Electronic
ele	Electrolyte
k	species
i_0	Ionic
LSM	Cathode material
MEA	Membrane-Electrode-Assembly
Ni-YSZ	Anode material
OCV	open-circuit voltage
Ohm	Ohmic
SOFC	solid oxide fuel cell
TPB	Three-phase boundary length
YSZ	Electrolyte material

List of Figures

List of Tables

General introduction

Currently, the energy problem and the increase in the level of pollution are major problems across the world. Therefore the development of new energy production systems must therefore be considered. A possible new source is the fuel cell. It is certainly not without disadvantages, but it has fewer of them than (non-renewable) oil.

A fuel cell uses the chemical energy of hydrogen and oxygen to produce electricity, without pollution. The other products are simply pure water and heat. Scientists have already and continue to develop different types of fuel cells, characterized by the nature of the gases and the electrolyte used, thus determining its optimal operating characteristics.

Concerning our work, we are interested in the SOFC fuel cells type. The latter consists of the anode, the solid electrolyte, and the cathode. It produces electrical energy by an electrochemical process at high operating temperature (600-1000°C). Where the fuel is oxidized at the anode and liberated electrons go to the cathode for oxygen reduction through an external circuit. The O^{2-} ions will cross a solid electrolyte, it is at its interface with the anode that a chemical reaction will take place. Electrons, heat and water will be released. It is within this system; anode, electrolyte, and cathode that transfer phenomena of electrical charges, mass and heat occur. SOFC fuel cell performance relies on these transfer modes. It is they who limit losses such as activation overvoltages, concentration overvoltages at the electrodes and Ohmic overvoltages in the electrodes and electrolyte.

Much research has focused on modeling and simulating the phenomena that occur within the fuel cell, as experiments are expensive and time-consuming. Moreover, the research has focused on developing new materials and designs in order to eliminate the problems associated with SOFC fuel cells and enhance performance. So to evaluate the performance of the SOFC fuel cell and optimize the different geometric parameters as well as the design we chose the numerical simulation.

Our thesis is organized as follows:

Chapter 1, after a brief historical review. A general presentation of fuel cells and their applications. Then we presented a detailed description of the SOFC fuel cell, specifying its constituent materials, the elements of the fuel cell as well as geometric configurations, and finally their performance.

Chapter 2 was devoted to the presentation of a bibliographical review on numerical modeling work, mass and heat transfer phenomena in solid oxide fuel cells. Comprehensive bibliographical research is created particularly on the various expressions of the tension and the various overvoltages used.

Chapter 3 was devoted to the presentation of the physical domain. Then we will present the mathematical model which describes the phenomena of heat and mass transfer in the heart of the SOFC type fuel cell. A three-dimensional model within the part of this thesis will be detailed and the implementation of the boundary conditions to fully understand the internal phenomena in the fuel cell as well as the steps of resolution and implementation of its simultaneous model at the ANSYS FLUENT software.

chapter 4 we started with a validation of our model, then we presented the modeling results in order to illustrate the influence of physical parameters (temperature, pressure, fuel utilization, mass fraction) and geometric parameters (thicknesses electrodes and electrolyte and porosity) on the performance of the SOFC cell as well as an evaluation of the various overvoltages (ohmic, activation, and concentration losses), in order to locate the optimal operating points. Then we ended this last chapter with a design that improves the performance of the SOFC fuel cell.

In a conclusion, the integration of this simulation in the ANSYS FLUENT software for the study and simulation of fuel cells will be very beneficial for understanding the physical, chemical, and electrochemical phenomena that occur to optimize the operation and performance of SOFC fuel cells.

Chapter I: Fuel Cells and performance

Introduction

With the increase in energy consumption and declining reserves of fossil fuels, it is important to find new alternative solutions. In this context, we often talk about fuel cells appearing as one of the interesting solutions for the future because of the absence of polluting discharge when used. In 1839 the first fuel cell was discovered by Sir William Grove [1], who performed the reverse reaction of water electrolysis. Despite their benefits and large usage profile, widespread adoption of fuel cells has not been an important breakthrough in those years. Until, to be returned and continue the concept in advancing fuel cell in the early 1990s, which restored research in the field of fuel cells, to become one of the greatest leading renewable energy sources. In the 21st century fuel cells have been incorporated into numerous domains, particularly in transportation (automobiles, buses, tractors, trains, and ships) and stationary use (homes, hospitals, schools, etc).

Fuel cells are electrochemical generators that convert the chemical energy of a fuel, such as hydrogen, into electrical energy. The use of pure hydrogen as fuel theoretically leads to a non-polluting cell since the only product generated by the cell is water. Depending on the operating temperature, several types of fuel cells can be distinguished, each type having its own characteristics.

In this thesis, we will focus on the SOFC fuel cell type. This type of fuel cell is currently much studied because the applications are multiple as much in the stationary field as in the automotive and portable fields.

I.1 Hydrogen technology

Faced with the incessant increase in energy consumption and the environmental problems it raises, it is urgent to make societal choices. Two solutions are proposed. One is to reduce overall energy consumption. Several governments, aware of this situation, reached an agreement in Japan in 1997 and signed the Kyoto Protocol which aims to reduce and stabilize CO_2 emissions for the period 2008-2012, at values corresponding to 1990. Unfortunately, we know the limits of these agreements. The second solution is to develop

new technologies that are more favorable to the environment. Hydrogen energy appears to be one of the most promising solutions because it has several interesting characteristics:

- Efficient energy: compared to oil or coal, hydrogen of equivalent weight releases about 3 times more energy than oil, about 6 times more energy than coal.
- Clean energy: production of water without pollution.
- Reliable source: hydrogen is very abundant and very accessible in nature.

Due to the many advantages, hydrogen is very environmentally friendly energy. Research into new user technologies has been encouraged and undertaken, to develop systems for converting or producing electrical energy. Fuel cells appear to be one of the best solutions for converting hydrogen into electrical energy.

I.2 Classification of fuel cells

The main distinguishing characteristic is depending on the material used as the electrolyte, there are different types of fuel cells. Further, the second characteristic used to classify fuel cells is their operating temperature. Where operating temperatures represent a significant role in deciding on suitable fuel. **Table I.1** groups together the various fuel cells developed as well as their characteristics and their operating conditions. [1,2]

Table I.1: Fuel Cells Types.

Fuel cell type	Electrolyte	Mobile ion	Fuel	oxidant	Operating Temperature
Alkaline Fuel Cell (AFC)	Mobilized or Immobilized Potassium Hydroxide in asbestos matrix	OH^-	H_2	O_2(pure)	50-200°C
Proton exchange membrane fuel cell (PEMFC)	Hydrated Polymeric Ion Exchange Membranes	H^+	H_2(pure or reformed)	Air	40-100°C
Direct methanol *fuel cells* (DMFC)	Polymeric membrane Proton conductor	H^+	Methanol	Air	60-100°C
Phosphoric Acid Fuel Cell (PAFC)	Immobilized Liquid Phosphoric Acid in SiC	H^+	H_2(pure or reformed)	Air	205°C

Molten Carbonate Fuel Cell (MCFC)	Immobilized Liquid Molten Carbonate in LiAlO2 Nickel	CO_3^{2-}	H_2(pure or reformed)	Air	650°C
Solid Oxide Fuel Cell (SOFC)	Perovskites (Ceramics)	O^{2-}	H_2(pure or reformed)	Air	500-1000°C

From this table, we can classify fuel cells, according to the operating temperature, into three categories: high-temperature fuel cells (600-1000 ° C), medium-temperature fuel cells (≈ 100-300 °C), and low-temperature fuel cells (≤100 ° C).

High-temperature fuel cells are essentially solid oxide cells (SOFC), and molten carbonate cells (MCFC). These kinds of fuel cells are commonly applied for fixed applications where constant power generation is required. This is due to its large temperature changes which need a long time to start up.

Phosphoric acid cells (PAFC) and alkaline fuel cells (AFC) are distinguished by their medium temperature. These kinds of fuel cells are commonly applied for both fixed and mobile applications.

Proton exchange membrane cells (PEMFC) and direct methanol cells (DMFC) are distinguished by their low operating temperature. Which makes it different from other cells in that they can be run directly after start-up and at low-temperature conditions. This makes them very suitable for mobile applications that require instant power generation.

After this global presentation on fuel cells, we will be interested in solid oxide fuel cells (SOFC) in this thesis.

I.3 Fuel cell applications

The fuel cell can be used in almost any situation where electrical power is required. In order of size, three types of applications are generally distinguished. Stationary applications are aimed at the supply of electrical energy in large or small networks and simultaneously thermal energy. In vehicles, they are used to drive or supply electricity for onboard devices. Finally, portable applications cover a wide range of electrical devices:

computers, camcorders, telephones, and more. In addition to these major areas niche applications.[3]

- **Stationary**

In stationary applications, the fuel cell delivers electrical energy to places where a grid is not available or where the simultaneous production of heat and electricity (cogeneration) allows high efficiency. Another concept of decentralized production is emerging today. These are virtual power plants built using a large number of fuel cells scattered throughout the fueled area. In the first case. Supplying fuel (usually pressurized hydrogen) is less expensive than establishing a continuous cable supply. The fuel cell replaces the diesel generator usually used. The gain in efficiency is often less important than reducing noise and maintenance. Hydrogen can also be produced on site by wind turbines or photovoltaic panels. Cogeneration allows energy production with very high efficiency because the losses are recovered in the form of heat. The fuel cell can replace a gas boiler in a building. In this case, it will be supplied with city natural gas. A large number of demonstration plants with an output ranging from 1 kW for single-family houses to a few hundred kW for residences have been installed in different countries. A set of small domestic power plants networked and controlled from a control center can bring energy production closer to the point of consumption and therefore reduce losses in the grid while enjoying the benefits of cogeneration[4].

- **Transport**

In the automotive sector, reducing CO_2 emissions requires the use of clean technologies. Fuel cells are an innovative solution for automotive traction, complementary to battery-powered vehicles already on the market.

Used in vehicles, fuel cells can help reduce pollution and improve driving behavior. The higher efficiency compared to an internal combustion engine reduces the energy requirement of the vehicle. In addition, depending on the fuel used (hydrogen, natural gas), it may be locally low-polluting or even non-polluting. Relocation of the discharges to the fuel production area may be of interest in particular for vehicles used in urban areas. Finally, hydrogen is a vector for storing electrical energy to replace a battery.

Recently, 100% electric vehicles equipped with Lithium (Li) batteries have been introduced to the market [4–7].

- **Portable**

Portable applications are small power systems (less than 1 kW) supplying objects intended to be transported. This involves powering electronic devices such as telephones or laptops. For portable applications, fuel cells compete with batteries. We hope to gain autonomy time and be able to recharge depleted energy reserves more quickly. The batteries used in this field must be extremely robust and not very sensitive to external conditions. In addition, strong constraints of size and weight are imposed. It is important to note that portable applications are the only application where the user can expect significant gains in terms of convenience and for which they are willing to pay the price. A large number of prototypes have been made. Methanol is the preferred fuel for small applications because it is liquid and can be easily transported. The authorization for the air transport of methanol cartridges has just been obtained by Smart Fuel Cell. Besides civilian applications, the US military is working on systems with an output of around 50 W to equip soldiers.[4,5]

I.4 Solid Oxide Fuel Cells (SOFCs)

We will only be interested here in SOFC fuel cell type. This type of fuel cell is currently very studied because of its benefits and its great profile of use in the stationary field. However, some scientific problems in the core of the cell remain to be overcome. The downside is that they are only conductive at high temperatures. The system must therefore be heated. However, the final efficiency remains high if we consider the co-generation of electricity and heat.

I.4.1 SOFC Operating principle and components

A SOFC fuel cell consists of a negatively charged electrode (anode), a positively charged electrode (cathode), an electrolyte sandwiched between the two electrodes (these three components are named the membrane electrode assembly (MEA)), and interconnections to separate the oxidizing and combustible gases in addition to collecting the electrons. A SOFC is named a single cell if it contains only one cell of MEA. But if it contains a multi-cell of MEA with a series or parallel design we call it SOFC stack. Moreover, the interface between electrode and electrolyte in which the electrochemical reaction occurs is named

the triple-phase boundary (TPB).in addition, the anode is supplied with hydrogen or a mixture of gases (fuel), and the cathode is supplied with air (oxidizer)[2, 3]. **Figure I.1**

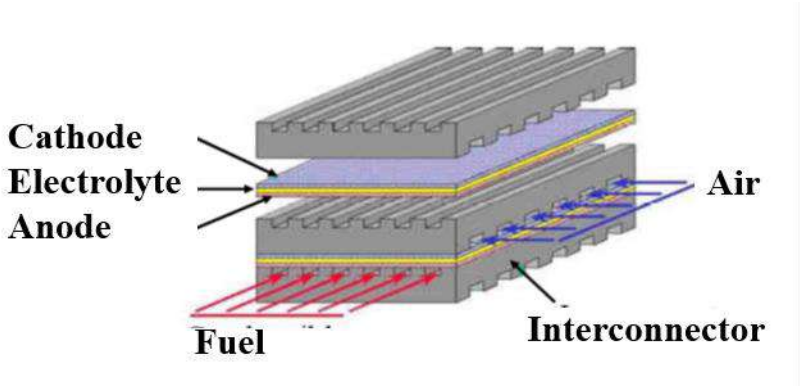

Figure I.1: SOFC components[9]

This type of cell operates at a temperature above 500 ° C for efficiency of around 70%.

The operation of SOFC begins with the arrival of the fuel and the oxidant respectively at the anode and the cathode. Hydrogen is introduced from the anode side and oxygen is introduced from the cathode side, in opposite directions, towards the interfaces with the electrolyte. Under favorable conditions, two chemical reactions will take place at the electrode/electrolyte interfaces (TPB). Oxygen ions resulting from the chemical reaction at the cathode/electrolyte interface migrate through a dense solid electrolyte. The electrodes must also have electronic conductivity to be able to transport the electronic fluxes from the collector to the reaction sites or from the latter to the electron collector **Figure I.2**.[10]

The electrochemical reduction of oxygen at the cathode leads to the formation of oxide ions which diffuse through the ionically conductive electrolyte to reach the anode material where the electrochemical oxidation of the fuel occurs with simultaneous production of electricity, water, and heat according to the two reactions (**I.1**) and (**I.2**).[10]

$$\frac{1}{2}O_2 + 2e^- \rightarrow O^{2-} \qquad \textbf{(I.1)}$$

$$H_2 + O^{2-} \rightarrow H_2O + 2e^- \quad \textbf{(I.2)}$$

The electrochemical model is based on the assumption that the overall chemical reaction occurs within the cell. The overall reaction is similar to that of combustion, but no combustion occurs in the SOFC cell, the gases not being in direct contact.[10]

$$H_2 + \frac{1}{2}O_2 \rightarrow H_2O + \text{Heat} \quad \textbf{(I.3)}$$

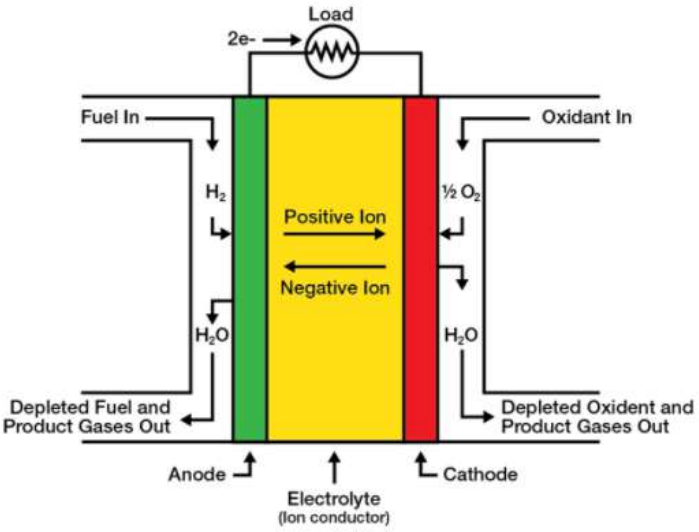

Figure I. 2: Principle of operation of a SOFC fuel cell [11].

I.5 The different materials of the SOFC fuel cell

Currently, the materials used are quite varied, but there is always a part for innovation in this field. Anywhere chemically stable materials at high temperatures must be used to avoid chemical reactions occurring between them thus avoiding the formation of insulating phases. So, all research in this field is focused on finding original materials or technological solutions in order to increase the conductivity and lifetime of elements of the cell and to produce electricity with less costly systems to manufacture. The characteristics and properties of the various constituent elements of the cell are described below.

I.5.1 Electrolyte materials

SOFC fuel cells are made of a dense, gas-impermeable solid electrolyte. Its main role is to conduct the oxide ions from the cathode to the anode and to block the electrons in order to avoid any risk of a short circuit. The most known material of electrolytes is yttrium stabilized zirconia, YSZ. However, recent studies retain the zirconia stabilized with scandium which has better properties. Other compounds such as ceria, perovskites (Lanthanum gallates (LSGM)), and hydroxyapatites have also been widely studied.

I.5.1.1 Doped zirconium oxides

a. yttrium-doped zirconia electrolytes (YSZ)

The most often electrolyte is yttrium stabilized zirconia (YSZ). It consists of ZrO_2 doped with 8 to 10 mol% Y_2O_3. Has a purely ionic conductivity for temperatures above 800 ° C[12]. It is very chemically stable compared to the other components of the cell and resists very well in the oxidizing environment than in a reducing environment. It is still the most widely used electrolyte today. The only problem with this zirconia is its low ionic conductivity at the target operating temperatures (600-700 ° C) which makes it difficult to use with large thicknesses (> 100 μm). To overcome this problem, several studies have been carried out to reduce the thickness of the electrolyte, to the detriment of its mechanical properties. Another solution also consists in playing on the nature and the rate of substituent (yttrium, scandium, etc.).[2, 8]

b. scandium-doped Zirconia electrolytes (ScSZ)

Likewise, scandium dopants are used in place of yttrium because of better results in improving the performance of the electrodes and having better ionic conductivities. Scandium-doped zirconia is, therefore, a very interesting material as an electrolyte for SOFC, but it has been ruled out from an industrial point of view because of its high cost. In parallel, many studies are carried out to develop and implement new materials showing good ionic conductivity at a lower temperature (500-700 ° C), such as ceria doped with gadolinium (GDC), lanthanum gallate (LSGM), etc.[9, 10]

I.5.1.2 The doped ceria electrolytes

Another family of electrolyte materials that is the ceria CeO2 was doped under low partial pressures of oxygen for stability. Usually substituted by gadolinium (GDC) and samarium (SDC) for rates between 10 and 20 mol%[16]. Knowing that ceria doped with gadolinium at a content of 10 mol% gives better electrochemical performance because it has high conductivity and the largest range of ionic conductivity according to the partial pressure of oxygen[17]. In addition, the doped ceria electrolytes have a conductivity of approximately 10 times higher than those YSZ and even that ScSZ for operating temperatures between 600- 800 ° C. But, despite these materials being good in the electrolytic field for SOFCs, they have a major inconvenience: the cerium changes the degree of oxidation in a reducing atmosphere (partial reduction of Ce^{4+} to Ce^{3+}) for operating temperatures of around of 500-600 ° C[18]. Therefore to avoid the risk of electrolyte reduction. One solution consists in placing an electronic barrier on the surface of the GDC which is a thin layer of YSZ on the anodic side, so as not to penalize the properties of the electrolyte. Knowing that the mechanical strength of the micrometric layers of YSZ is facilitated by close coefficients of expansion between GDC and YSZ($\alpha_{YSZ} \approx 10.5 \times 10^{-6} K^{-1}, \alpha_{GDC} \approx 13 \times 10^{-6} K^{-1}$). In addition, ceria at low temperatures resides in its very good thermomechanical and chemical compatibility with anode and cathode materials, such as cobaltites or lanthanum strontium-doped manganite (LSCF or LSM)[19].

I.5.1.3 Lanthanum gallates (LSGM)

Lanthanum gallates exhibit a Perovskite, their chemical formula is $La_{0,9}Sr_{0,1}Ga_{0,8}Mg_{0,2}O_3$. Lanthanum gallates (LSGM) have greater ionic conductivity than YSZ which is about ten times in the desired temperature range (of the order of 1.7 10-1 $\Omega^{-1}cm^{-1}$ at 800°C). Despite, LSGM being stable under an oxidizing atmosphere but it has many disadvantages such as more expensive gallium oxide materials, its volatilization under low partial pressures of oxygen, a high synthesis temperature, and chemical reactivity with electrode materials.[20]

I.5.1.4 Hydroxyapatites

They have a general formula $A_{10-x}(MO_4)_6O_2$ where A is rare earth, alkaline earth, or transition metal cation and M is silicon or germanium. Several studies have demonstrated the benefit of rare earth silicon apatites, which have open structures, with channels capable

of promoting mobility by oxide ions. They have very good ionic conduction properties superior to those of YSZ. Unfortunately, the difficulties in synthesizing these materials which require high temperatures (1600 ° C) make them less interesting for the moment.[21]

I.5.2 Cathode materials

The cathode is the site of oxygen reduction. It is porous to allow gaseous oxygen to diffuse to the point of reaction. The gas is absorbed and then dissociated and reduced to ions due to the presence of oxygen vacancies. In addition, to aid in the reduction of oxygen, the material must be an electronic conductor. Therefore the researchers interested in using materials must exhibit interesting electronic conduction properties and good catalytic activity with regards to the oxygen reduction reaction. The main materials studied are presented below.

I.5.2.1 The perovskites

the most common cathode materials for SOFC type fuel cells are perovskites of general form ABO_3 where the element A is rare-earth (La, Pr, Nd, Gd) and the atom B is a transition metal (Ni, Co, Cu, Al, Mn…). The perovskites have many cathode materials that were employed by various research groups. The major perovskite families of compounds most generally studied as cathode material are described below.

a. Lanthanum manganite $LaMnO_3$

Lanthanum Manganite is a perovskite oxide for operating temperatures in the order of 1000 ° C. This material depends on several parameters such as the temperature or the partial pressure of oxygen. However, it is stable in an oxidizing atmosphere. Doping generally with strontium is carried out on the sites of lanthanum. $LaMnO_3$ can be associated with an electrolyte of YSZ. On the other hand, $LaMnO_3$ doped with strontium $La_{1-x}Sr_xMnO_3$ (LSM) cannot be associated with YSZ.[22]

b. Lanthanum manganites doped with strontium (LSM)

The most generally developed as cathode materials for SOFC type fuel cells is LSM (lanthanum manganite) oxide with a perovskite structure for high temperatures above 800 ° C. Its chemical formula is $La_{1-x}Sr_xMnO_3$. LSM has very good catalytic oxygen reduction activity and its electrical conductivity at high temperature, stable chemically, relatively

high activity, and its coefficient of expansion agrees well with that of zirconia stabilized with yttrium oxide, commonly used as an electrolyte. The main disadvantage of this material is its exclusively electrical conductivity, which limits the oxygen reduction reaction at the interface with the electrolyte. Moreover, it forms non-conductive phases at high temperatures with the electrolyte. Eventually, this material lost its interest due to the use of higher temperatures. Therefore replaced by other materials with better low-temperature characteristics.[13,17]

c. Lanthanum cobaltites (LSC/LSCF)

They are mixed conductors (electronic and ionic) such as Lanthanum strontium cobaltite (La, Sr) CoO_3 (LSC) or Lanthanum strontium cobalt ferrite (La, Sr) (Co, Fe) O_3 (LSCF). This material is suitable for working at intermediate temperatures (<700 ° C) but its incompatibility with YSZ remains a major obstacle to its use. LSCF-type materials exhibit good ionic (about 0.18 S/cm at 900 °C) and electronic (150 S/cm at 700 °C) conduction properties, compared to the LSC-type materials which show conductivity lower electronics. In addition, these materials have very high surface exchange coefficients with oxygen, which greatly reduces the overvoltage. However, in these cathode materials, cobaltites like lanthanum manganite exhibit reactivity with YSZ, which results in the formation of the $SrZrO_3$ phase or the precipitation of ZrO_2. Because of all these disadvantages, many scientists researchers have focused on a type of material exhibiting very good ionic and electrical properties as well as good compatibility with common electrolyte materials at intermediate temperatures (IT).[18]

d. The copper-based perovskites of type LSCu

Other popular electrode material families are copper-based perovskites for operating temperatures of the order of 700 ° C its chemical formula is $La_{1-x}Sr_xCuO_{3-\delta}$. The ionic conductivity increases with the rate of strontium. In addition, it does not react with YSZ at temperatures below 800 ° C, on the other hand, the formation of $SrZrO_3$ is noticed at 900 ° C. However, the thermal expansion coefficient (TEC) seems to pose a problem of this family of compounds, which is higher than that of zirconia. [24]

I.5.3 Anode materials

The anode is the site of the chemical oxidation reaction of hydrogen, but it is also used to collect electrons. It is porous to convey the fuel to the electrolyte/anode interface, it is also used to evacuate the water formed in the form of water vapor. And must have several characteristics: chemically stable, have good catalytic activity, present good ionic conductivity to be able to conduct the oxide ions to the reaction sites, as well as good electronic conductivity to ensure the circulation of the electrons produced by the oxidation to the external circuit. The anode material must also be stable under the conditions of functioning. A wide range of developed materials as an anode for SOFC has been considered.

I.5.3.1 Cermet Ni / YSZ

The most SOFC anode material use is nickel and yttria zirconia cermet (Ni-YSZ), this composite is used in high-temperature SOFCs (1000 ° C). Polarization studies have shown that nickel exhibits the lowest overvoltage of all catalysis materials at 1000 ° C, whereas YSZ gives structural stability and thermal expansion. In addition, the electrical conductivity of the anode material certainly depends on the proportion of the two phases (YSZ and Ni) but also on the size of the particles, the distribution of the two constituents, and the continuity of each phase. Consequently, the mixture of Ni-YSZ plays an important role in the performances. A study has demonstrated in this sense the complicated relationship between the preparation parameters and the overvoltage of the Ni-YSZ cermet, concluding on the need to ultimately obtain good performance, two separate networks to ensure the connections Ni-Ni and YSZ-YSZ must be in place. This layer must be structured so that the contact between YSZ and Ni is optimal, taking into account the porosities which can be an obstacle to the conductivity. Thus the best use of the composition, microstructure as well as thickness of Ni-YSZ provide good electrocatalytic and electrochemical performance for hydrogen oxidation and demonstrate high electrical conductivity.

The disadvantage of Ni-YSZ is that the long use of nickel as a catalyst causes carbon formation when a hydrocarbon is used as a fuel instead of hydrogen.[20, 21]

I.5.3.2 Cermet Co-YSZ

To solve the problems Ni-YSZ has been replaced nickel with copper, which is a poor catalyst for carbon formation and has better resistance to pollution by sulfides. In addition to its mechanical resistance in a reducing atmosphere. Cobalt is another suitable oxide for SOFC cells as long as it resists the reducing atmosphere and remains unoxidized compared to nickel. The disadvantage of cobalt is its higher cost than that of nickel, which makes its use limited.[9]

I.5.3.3 Cermet Ru-YSZ.

Also to solve the problems of poisoning of anodes by carbon or sulfides, further research focusing on the development of new anode materials such as Cermet Ru-YSZ. Was developed because of their very high catalytic activity for internal reforming with negligible carbon deposition during reforming. However, it's very high cost makes its use limited.[22]

I.5.4 Interconnector materials

The interconnectors are used for gas distribution, electron collection, and the evacuation of reaction products. The interconnector materials have good electronic conductivity and have a high thermal conduction coefficient in order to dissipate heat. As well as stable in reducing and oxidizing media. Lanthanum chromites ($LaCrO_3$) are the most used materials at high-temperature in the past. Since they are stable under reducing and oxidizing atmospheres. They are also compatible with the other components of the cell from a chemical point of view and in terms of coefficient of thermal expansion. Currently, Chromium-based alloys are the most efficient compared to ceramic materials. Because they have good corrosion resistance through the formation of a protective oxide layer (Cr_2O_3).[27]

I.6 The different geometries of existing SOFC fuel cells

There are several types of configurations for SOFCs which can be categorized mainly into three categories: planar, tubular, and monolithic configurations. The variety of configurations is important. As well as each configuration offer different performance: they all have advantages and disadvantages which are often a compromise between manufacturing cost, ease of stacking and therefore being able to produce stacks of varying

sizes or even ease in the resolution of gas chamber sealing problems which is a very important point for fuel cells.

I.6.1 Planar geometry

Planar geometry is newer and the easiest to design compared to other geometries **Figure I.3**. Each element making up a single cell is flat in shape and thin. The planar geometry has several advantages, in particular: the internal resistance of the devices does not depend on the surface of the cells but only on their thickness due to the conduction being made perpendicular to the plane of the cells, The ease of manufacture makes the systems flexible and inexpensive since the cell components, electrolytes, electrodes or interconnectors can be manufactured separately to avoid co-sintering. It is therefore also possible in this case to integrate metal components as for the interconnectors. Therefore, the quality controls of the different elements are easier because of their great independence from each other. With all these advantages, it also has drawbacks: sealing problems due to the expansion of materials in high temperatures. Therefore, high-temperature gaskets have been proposed for sealing between the compartments. Compressive gaskets (gold gasket), ceramic (glass), or cement, and finally, deteriorate the cells due to mechanical stresses and chemical reactions, thereby reducing performance.[22]

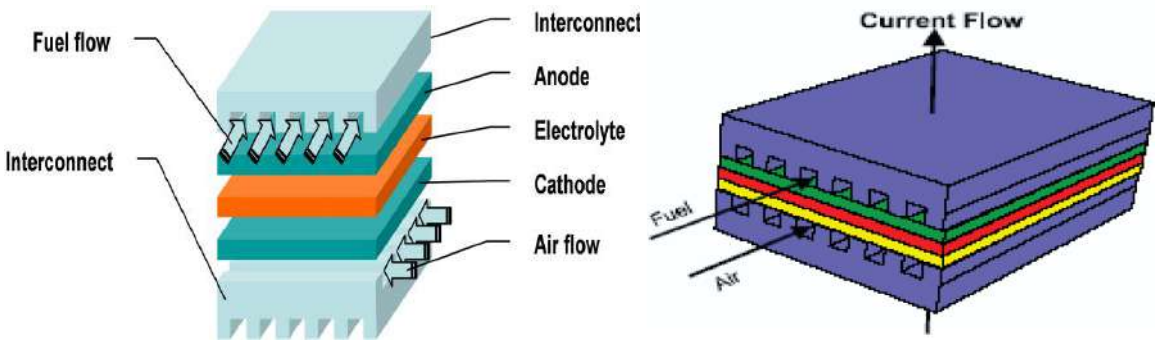

a- cross-flow **b-co-flow**

Figure I.3: Schematic Solid oxide fuel cell planar geometry[23, 24]

I.6.2 Tubular geometry

For more than 30 years, Siemens-Westinghouse has been developing tubular technology SOFCs with support from the US Department of Energy. This tubular geometry consists of a ceramic tube **Figure I.4**. Air is sent to the inside of this tube, and fuel to the outer surface. Part of the periphery of the tube is not covered by the material of the anode, but by a metallic material, after interconnection, which allows connecting one cell to another to increase the power. The tubular geometry has several advantages, in particular: each cell is independent of the others and the layers are deposited on thick support therefore the structure is robust, being able to put the seals in a zone at a lower temperature, thus reducing the consequences of mechanical stresses resulting from thermal stresses and thus improving the reliability of these systems. And finally, the performance degradation is very low. With all these advantages, it also has disadvantages: the long path of the current through the electrodes, in addition to an unnecessary additional weight due to the electrode support which decreases the electric power supplied, and the high cost of manufacture which can limit their use.[22]

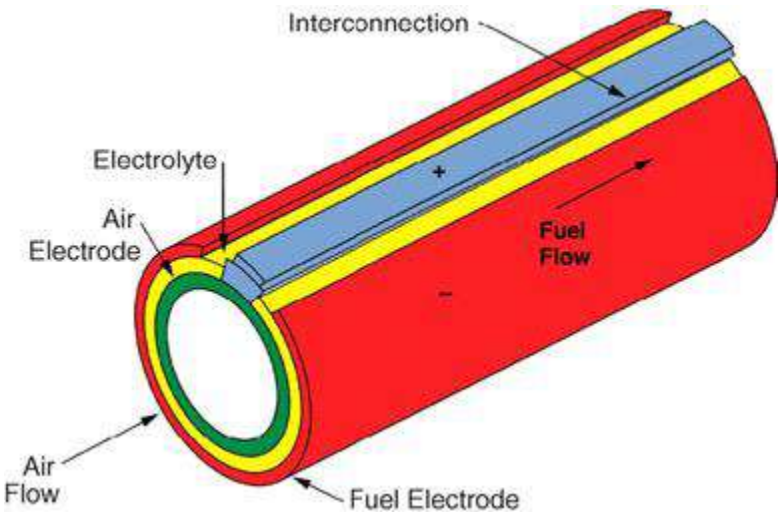

Figure I.4: Schematic Solid oxide fuel cell tubular geometry[29]

I.6.3 Monolithic geometry

The great advantage of this geometry is that it allows the cell to be compacted. It was developed by the laboratory: Argonne National Laboratory (US) in 1984. The monolithic geometry consists of a flat part and a wavy part. We find the cathode-electrolyte anode

trilogy **Figure I.5**. The oxidizing and fuel gas channels circulate in the wavy part. The interconnection plates are much thinner which saves volume and achieves a much higher overall system energy density. The monolithic geometry has several advantages, in particular: presents small dimensions, a large active surface as well as a high current density leading to obtaining high power densities due to the low internal resistance. With all these advantages, it also has drawbacks: obtaining the very nested structure which therefore requires a co-firing of the whole, in addition to the sealing problems due to the expansion of the materials in high temperatures.[17, 25]

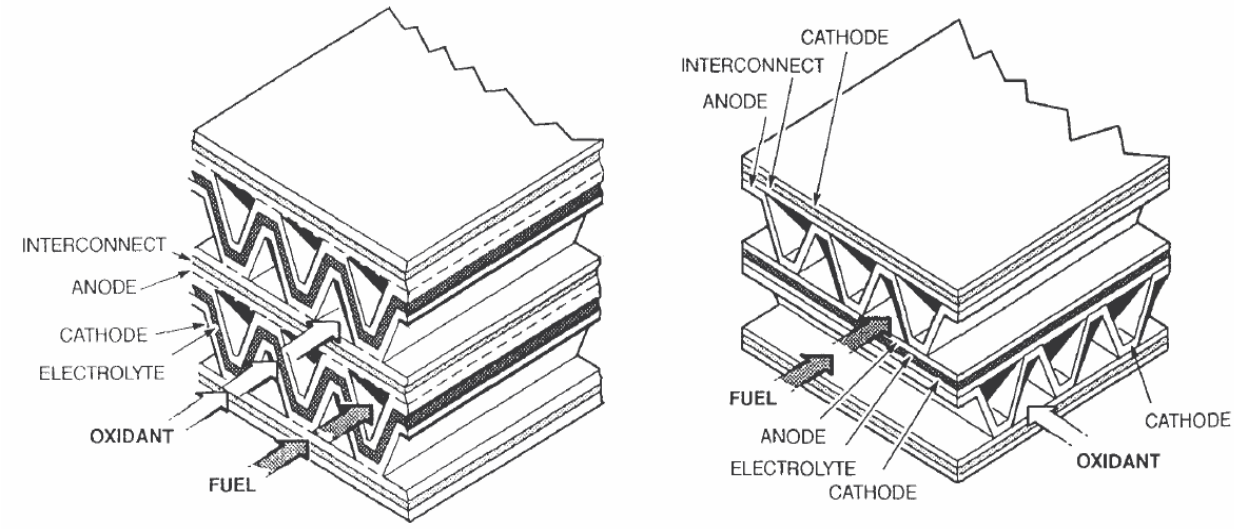

a- co-flow **b-cross-flow**

Figure I.5: Schematic Solid oxide fuel cell monolithic geometry[30]

I.7 The different support structures of planar type SOFCs

Generally, SOFC fuel cells have three structures depending on the type of support used:

- electrolyte supported operating around 900-1050 °C
- anode supported operating around 700-800 °C
- cathode supported operating around 500-700 °C

The advantage of the electrode as the support structure with thin electrolyte minimizes the Ohmic loss considerably and enables lower operating temperature and higher performance.

Figure I.6 shows the three structures for planar cells [31]. The advantages and disadvantages of cells using different structural supports are listed in **Table I.2**.

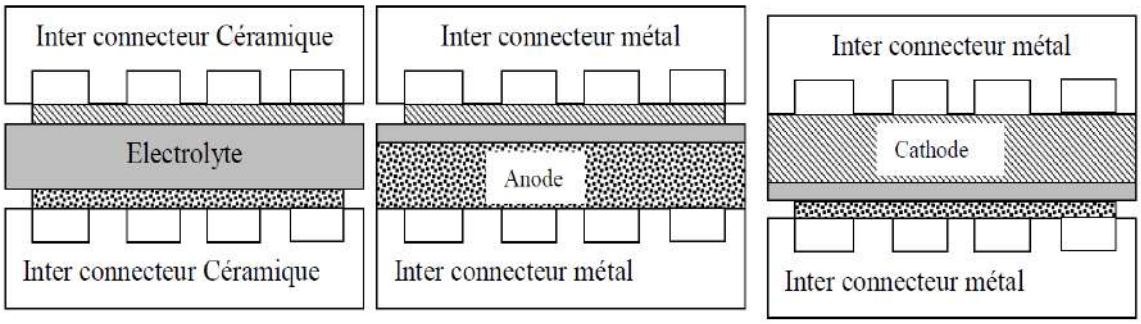

Electrolyte supported	Anode supported	Cathode supported
Cathode ≈50 µm	Cathode ≈50 µm	Cathode ≈300-1500 µm
Electrolyte ≥100 µm	Electrolyte ≤ 20 µm	Electrolyte ≤ 20 µm
Anode ≈50 µm	Anode ≈300-1500 µm	Anode ≈50 µm

Figure I.6: Different support structure of planar type SOFCs[32]

Table I.2: Main advantages and disadvantages of the different types of structural support[13].

Support	Advantages	Disadvantages
Anode	Highly conductive anode Low operating temperatures (fine electrolytes)	Potential re-oxidation of the anode Mass transport limitation (strong thicknesses)
Electrolyte	Strong structural support (dense) Better mechanical behavior compared to the anode (re-oxidation) and cathode (reduction)	Very high resistance due to the low ionic conductivity of the electrolyte (high thicknesses) Requires high operating temperatures
	No oxidation but a reduction	Lower conductivity

Cathode	cathode potential Low operating temperatures (fine electrolytes)	Mass transport limitation (strong thicknesses)

I.8 Advantages and Disadvantages of SOFC Fuel Cells

Fuel cells are usually offered as the solution of the future in the domains of electric power generation, automotive. This attraction is justified by heir many advantages: The solid electrolyte permits the SOFC cell can be taken in various configurations, like planar, tubular, or monolithic geometries. In addition, fuel cells can have different sizes, they can therefore also be arranged in different places with a minimum of space. With no moving parts, the fuel cell operates without noise pollution. As a result, fuel cells may very well be near residential areas. Moreover, the solid electrolyte avoids the problem of corrosion in the cell and evades flooding in the anode and cathode. Emit less harmful gases like Co2. Important electrical efficiency around 40-50% and great power generation around 10-100000 KW. Therefore can be easily exploited in cogeneration with or without a gas turbine. The overall efficiency can then reach 80% due to its high operating temperature. However there are also disadvantages which are as follows: High-temperature fuel cells are schematic of two types, cylindrical or planar. For the cylindrical, manufacturing costs are high but there are fewer problems for the systems because the stacking is done with cells that are mechanically independent of each other and because the sealing is done in a cold zone. For planar cells, the manufacturing costs are less important, but the problems appear for the realization of the systems because the stacks are made by mechanically connecting the cells and the seals are made in a hot zone. Also, the high temperature caused thermal expansion mismatches between materials.[3]

I.9 New features of the SOFC solid electrolyte cell

Fuel cells have undergone several developments in recent years, which have mainly affected the geometry of the cell and the materials constituting these elements.

I.10 SOFC performance and thermodynamic

I.10.1 Electromotive force

The electromotive force is expressed as the change in Gibb's free energy during the reaction between hydrogen and oxygen. The maximum electrical work provided by a fuel cell working at constant temperature and pressure is given by the change in Gibbs free energy of the reaction:[2]

$$W_{ele} = \Delta G = -nFE \quad \textbf{(I.4)}$$

From where

$$E = -\frac{\Delta G}{nF} \quad \textbf{(I.5)}$$

Where then is the number of electrons participating in the reaction, F (C mol^{-1}) is Faraday constant, and E is the ideal potential of the cell.

If we consider the case where the reactants and products are in the standard state, then[2]:

$$\Delta G^0 = -nFE^0 \quad \textbf{(I.6)}$$

If the water formed is in liquid form, the theoretical voltage of an H_2 / O_2 fuel cell is[2]:

$$E^0 = -\frac{\Delta G^0}{nF} = -\frac{237.34}{2 \times 96.485} = 1.23\ V \quad \textbf{(I.7)}$$

For a general reaction we have[2]:

$$\alpha A + \beta B \rightarrow cC + \delta D \quad \textbf{(I.8)}$$

The change of Gibbs free energy is expressed by[2]:

$$\Delta G = \Delta G^0 + RT\ ln\frac{C^c D^\delta}{A^\alpha B^\beta} \quad \textbf{(I.9)}$$

Substituting equation (I.1) and (I.3) in equation (I.6) gives the relation[2]:

$$E = E^0 + \frac{RT}{nF} ln \frac{C^c D^\delta}{A^\alpha B^\beta} \quad \textbf{(I.10)}$$

Which is the general form of the Nernst equation.

The Nernst equation provides a relationship between the ideal standard potential and the ideal equilibrium potential for other temperature and pressure conditions the Nernst expression for the reaction $H_2 + ½O_2 \rightarrow H_2O$ takes the form[2]:

$$\mathrm{E_{Nernst}} = E^0 + \frac{\mathrm{RT}}{\mathrm{2F}} \ln\left(\frac{\mathrm{P_{H_2}}.\mathrm{P_{O_2}^{0.5}}}{\mathrm{P_{H_2O}}}\right) \quad \textbf{(I.11)}$$

Where P (Pa) terms are the partial pressures of reacting species, R (J mol^{-1} K^{-1}) is the universal gas constant, T (K) the temperature and E^0(V) is the theoretical potential difference under standard conditions.

When a current flows in the external circuit, the voltage of the cell is lower than the theoretical voltage. This is due to irreversible losses. Many sources contribute to irreversible losses in a fuel cell. Losses often referred to as polarization, come primarily from three sources: activation polarization, Ohmic polarization, and concentration polarization. These losses cause, for a cell of ideal potential E, a drop in voltage V as shown in **Figure I.7**.[33]

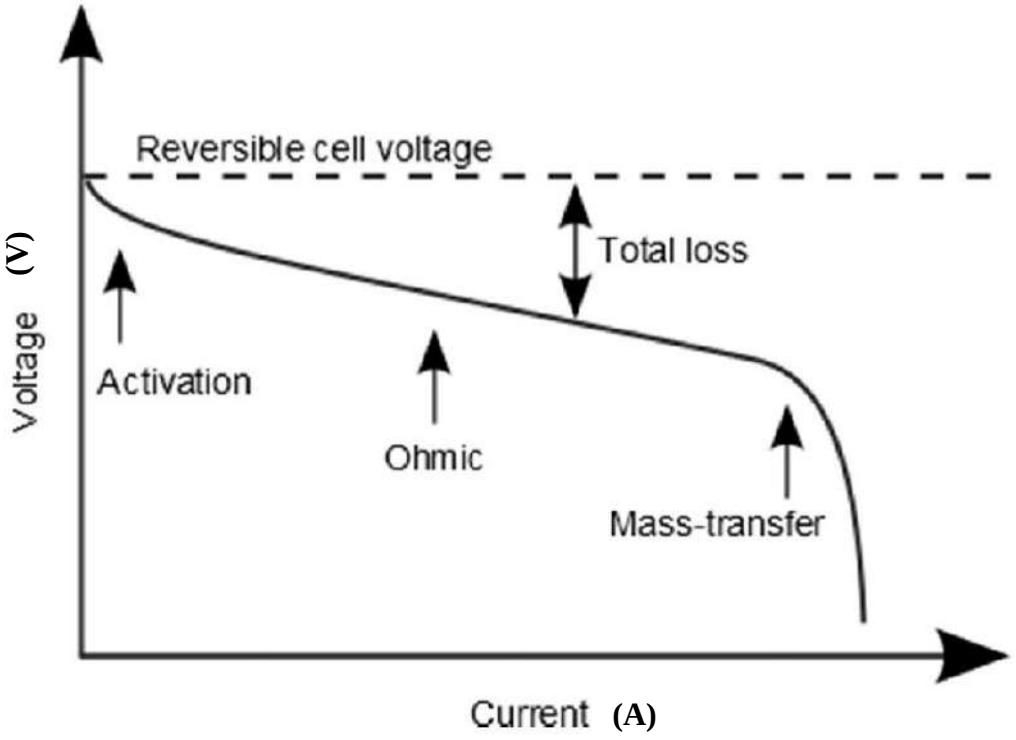

Figure I.7: Losses curve in a SOFC fuel cell[33]

As can be seen in **Figure I.7**, can be divided the curve three parts where each part is dominated by various types of loss mechanisms.

- At low current density, the activation losses are dominant.
- For medium intensities, the Ohmic losses, which are directly proportional to the current density, then become predominant over a wide range of current density.
- And finally, at high current densities, losses due to mass transfer become dominant.

So it is necessary to know these losses to enhance the wanted operating conditions of a cell.

Another performance indicator is given by the voltage and the power density. These are based on the current density and measured as a product of current and voltage:

$$Power\ density = j \times V \qquad \textbf{(I.12)}$$

Power density varies with the current drawn. The power density normally increases as the amount of current drawn is raised, up to a certain point, after which the power density reduces with the raise of current being drawn. This can easily be seen on a j-V curve as in **Figure I.8** which presents a view of the trend of paper research about fuel cells in the range of power electronics.

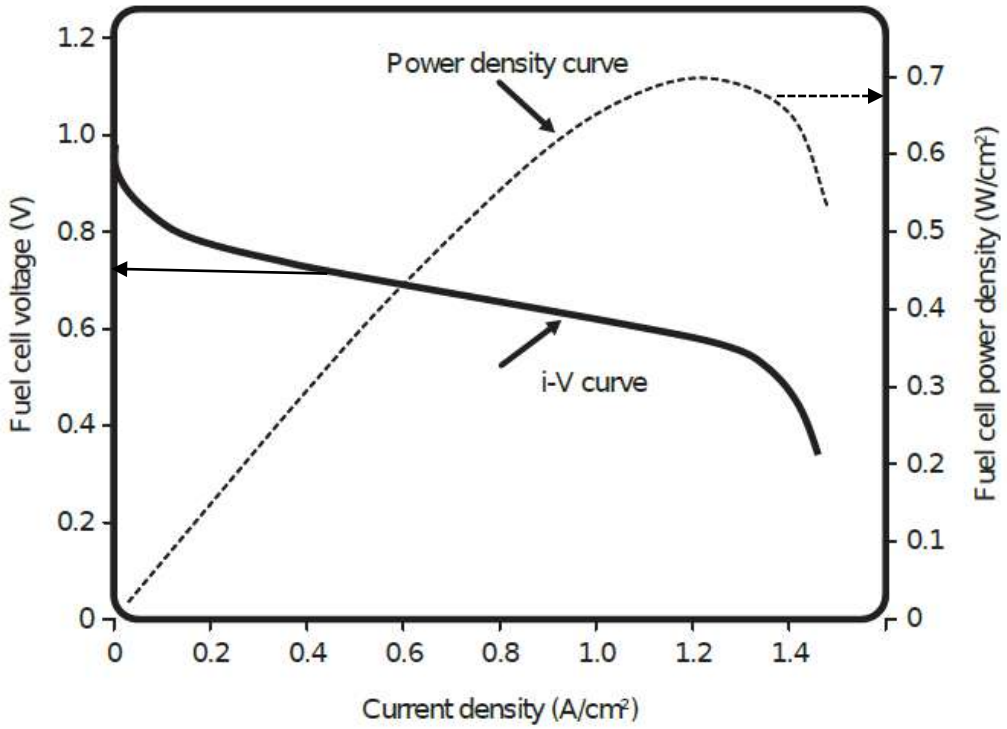

Figure I.8: j-V curve for fuel cell combined with power density curve[34]

I.10.2 Fuel cell efficiency

SOFC fuel cell performance is influenced by operating parameters (temperature, pressure, gas composition, fuel utilization, and current density) as well as other factors and cell design. These parameters directly influence overvoltage and the mechanical strength of the electrodes. From a thermodynamics point of view. The thermal efficiency of an energy transformation process is defined as follows[35]:

$$\eta = \frac{reacted\ fuel}{supplied\ fuel} \qquad \textbf{(I.13)}$$

For a chemical process like a fuel cell, it is difficult to quantify the energy supplied in the form of chemical reactants. The benchmark generally used is the energy released during the combustion of the reactants.

In the ideal case of an electrochemical converter such as a fuel cell, with Gibbs free energy which indicates the maximum electrical energy that can be produced in a fuel cell, it is possible to give an upper limit for efficiency. This quantity is called the ideal efficiency, operating reversibly, is then[35]:

$$\eta_{ideal} = \frac{\Delta G}{\Delta H} \qquad \textbf{(I.14)}$$

Where $\Delta H$is the enthalpy change.

If we compare this efficiency with that of other energy conversion modes. For an internal combustion engine operating according to a Carnot cycle, the efficiency is written[35]:

$$\eta_c = \frac{T_h - T_c}{T_h} \qquad \textbf{(I.15)}$$

Based on a temperature difference between a cold source (T_c) at 25 ° C and a hot source (T_h) at the operating temperature of the cell, we obtain **Figure I.9**.

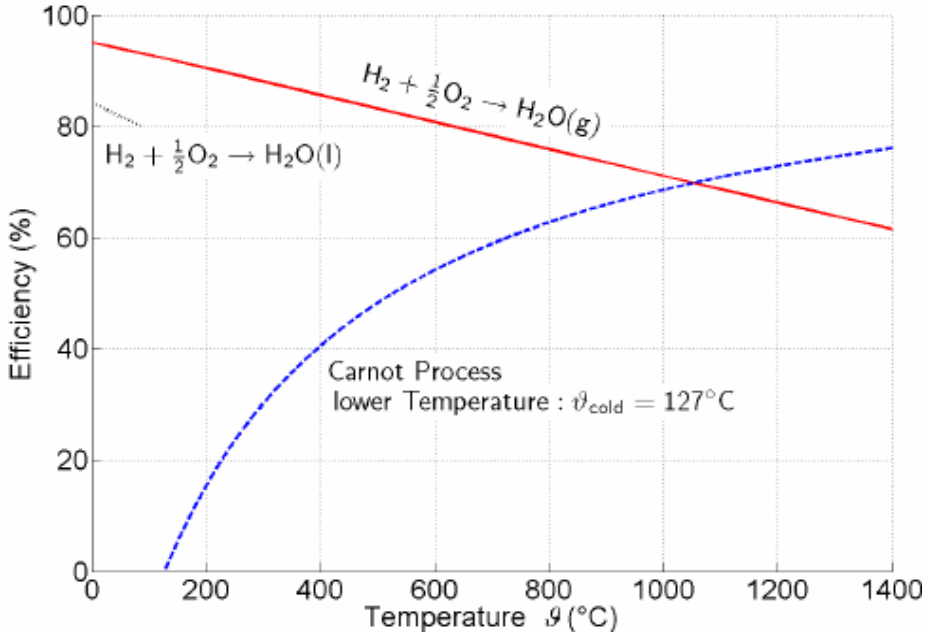

Figure I.9: Comparison of the Efficiency of the fuel cell process and the Carnot process[36]

We then see that the fuel cell has better efficiency than the heat engine. For low temperatures. In other words, the fuel cell makes it possible to exceed the principle limits of the heat engine.[37]

I.10.3 Effect of Pressure

SOFCs, present an improved performance by rising cell pressure. However, the cell can operate at different pressures ranging from atmospheric pressure up to several bars. For a process considered isothermal and based on the change in Gibbs free energy can be written[2]:

$$\left(\frac{\partial E}{\partial P}\right)_T = -\frac{\Delta V}{nF} \qquad \textbf{(I.16)}$$

Experimental tests were carried out by Siemens Westinghouse on an AES 4 cell over a pressure range of 1 to 15 atm at an operating temperature close to 1000 ◦C. The experimental results **Figure I.10**:

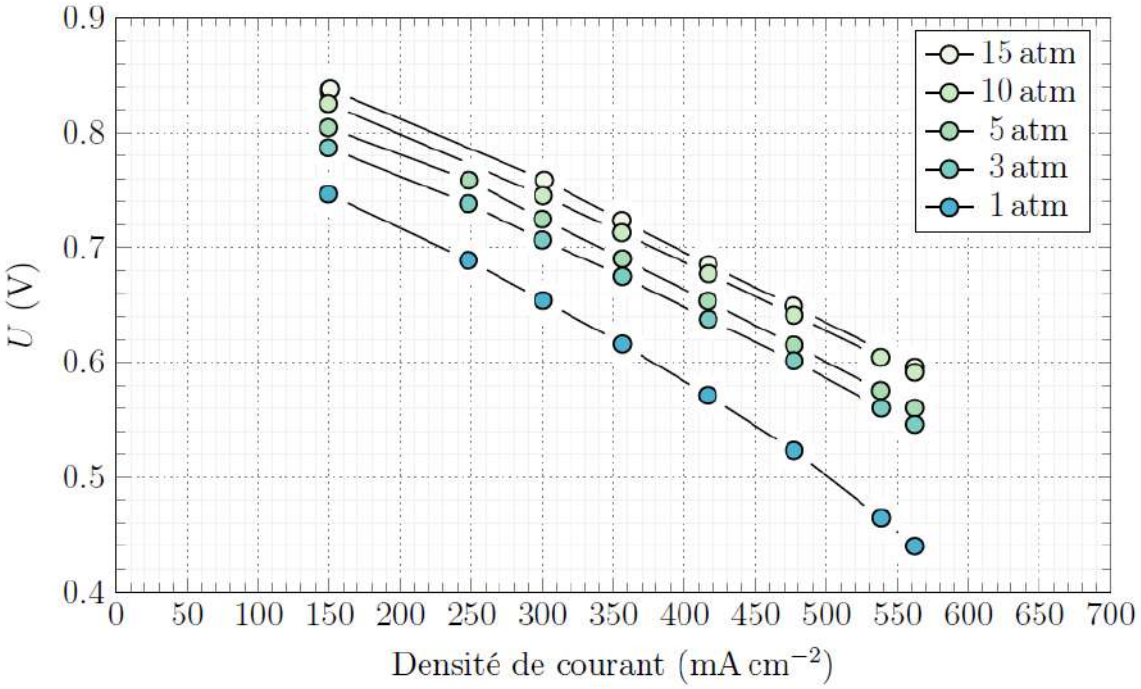

Figure I.10: Influence of pressure on the voltage of a cell operating with 89% H_2 + 11% H_2O at the anode and in the air at the cathode[38]

I.10.4 Effect of temperature

As the operating temperature of the fuel cell increases, the Ohmic overvoltages decrease and the current density increases[39]. In the open circuit we write[2]:

$$\left(\frac{\partial E}{\partial T}\right)_P = \frac{\Delta S}{nF} \qquad \textbf{(I.17)}$$

Where ΔS is the entropy change

I.10.5 Fuel utilization

Fuel utilization factor (U_F) is described as the ratio between the mass fraction consumed of fuel flow and the mass fraction of fuel flow that does not react (output). However, this factor is utilized to describe the cell efficiencies due to having a significant impact on them.

$$U_F = \frac{X_{H_2}^{in} - X_{H_2}^{out}}{X_{H_2}^{out}} \qquad \textbf{(I.18)}$$

Where $X_{H_2}^{in}$ and $X_{H_2}^{out}$ are the input and output mass fraction of hydrogen respectively.

Conclusion

This first chapter made it possible to present the fuel cell, especially the solid oxide fuel cell (SOFC) as a whole, it should be remembered that it is an excellent energy converter; and because it will help solve, if not reduce energy and environmental problems, sooner or later she should prevail. It also has a great future for powering electric vehicles, for example.

The technical maturity of the fuel cell has not been reached yet, at least in relation to the expectations of its users. The main difficulties are its geometric configuration, its construction materials, and the environment in which this system operates. It is, therefore, necessary to combine it with even more efficient systems to optimize its performance.

Chapter II: Bibliographic study

Introduction

The fuel cell technology with emphasis on solid oxide fuel cells (SOFC) has gotten attention in the past two decades as clean energy and it has become an alternative to fossil energy at this time. The SOFC fuel cell is an electrochemical cell that is used to produce electrical energy by the reaction whereby hydrogen and oxygen combine to form water that can be converted into electrical energy and heat by the fuel cell. A significant development in SOFC modeling has led to an enhanced with knowledge of related heat and mass transfer phenomena in SOFCs. The latter has been the topic of several mathematical and numerical models which will satisfy all the performance requirements in fuel cells. The creation of mathematical models of the fuel cell depends on a series of assumptions in order to simplify the numerical resolution and not for the accuracy of the study of the model. Assumptions that neglect some phenomena and address others considerably diminish the accuracy and usefulness of the model.

Other scientific work has taken into account the detailed SOFCs' operation, components, and layouts as voltage, operating temperature, fuel utilization, the configuration of the cell (planar or tubular), the dimensions of the electrolyte and electrodes, the type of construction metals, the manufacturing technology of the cell. All these studies are directed focused on one objective which is to improve the efficiency of fuel cells.

A comprehensive literature review and an analysis of current models of the SOFC fuel cell are presented and a summary of the concerns work published. This was necessary to start our numerical calculations.

II.1 State of the art on numerical studies of transfer phenomena in fuel cells

Achenbach[40]**.** Studied with time-dependent the effects of flow manifolding by utilizing differential and finite equations that allow determining heat and mass transfer in SOFCs. The researchers found that the counter-flow design has an impact in improving the performance compared to cross and co-flow. Moreover, he reached an important estimation that thermal radiation may be an important factor of heat transfer at a high operating temperature within several configurations.

Wuxi et al. [41]**.** Present a 3D SOFC stacks based on CFD calculations to examine the impact of geometric parameters such as the dimension of the channel, the repeating cell height and the width of the manifold on the flow improvement. The simulation results showed that the ratio of the outlet to the inlet manifold width was affected significantly by the flow uniformity. Moreover, the small fuel flow velocity and small pressure change in the manifold lead to uniform fuel flow distribution compared to the airflow distribution.

Valery et al. [42]**.** Proposed a modified planar SOFC fuel cell with internal reforming. The developed SOFC model is created in gambit pre-processing software and executed in the commercial CFD code FLUENT with source terms (user-defined functions (UDF)). The study combined parallel flow and a new flow field design. The simulation analysis confirmed that the newly modified anode configuration enhanced the performance cell and realized a more uniform distribution of species concentration, velocity, and current density.

Saied M et al.[43]**.** In this work, a 3D mathematical model for a planar SOFC fuel cell was introduced and the analysis was executed using Ansys Fluent 17.2. The model involves electrochemistry, charge transport, conservation of mass, momentum, and energy. in order to enhance the cell performance was proposed diverse flow fields including helical, modified parallel design, traditional parallel, single-entry serpentine, double-entry serpentine, and triple-entry serpentine. SOFC operating at temperatures 1023 K and electrolyte materials used in the cell are stabilized yttrium-zirconia (YSZ). the model compared diverse flow fields suggested. Their results noted that the triple-entry serpentine configuration achieved regular distributions for fuel and oxygen and presented better performance compared to other designs. As a result, give a high current with a percentage increase of 5.18%.

Huang et al. [44]**.** Considered a new design using short guide vanes equally spaced around the feed header of the double-inlet/single-outlet flows of rib-channel interconnects to examine the flow uniformity in several interconnectors and its impact on cell performance. They established that the new design enhanced the degree of flow uniformity in interconnects and achieved a greater value of peak power density. Moreover, their studies show a strong impact of Re_{Fuel} and Re_{Air} on cell performance at suitable ranges in order to

achieve a greater value of peak power density while maintaining an economical fuel utilization rate with lower temperature changes in the single-cell stack.

Lin et al.[45]**.** Its objective is to develop a model estimating the influence of rectangular ribs on the concentration polarization of planar SOFCs as a function of various physical and geometrical parameters involved in order to suggest its optimized structure to enhance cell performance. The study showed that the best rib design was achieved by reducing the overall concentration and Ohmic polarization of the ribs. and this last is influenced significantly by the electrical resistance and must be between 1/3 and 2/3 of the channel width.

Qiuwan S et al.[46]**.** A 3D mathematical model was performed to simulate the effect of geometry. The mass, momentum, species, energy, and charge conservation equations are solved using the finite-volume method. The model performed numerical studies examining the performance of SOFC with and without rectangular obstacles. This attempt indicated that the fuel cell with obstacles enhanced the cell performance as it attained better current density, species concentration, and temperature distribution.

Zitouni B et al[47]**.** Construct a two-dimensional model for a planar solid oxide fuel cell, to study the cause of increasing the temperature under different structure geometry with taking into account the effect of heat source. For three type structure configuration a simulation program written in FORTRAN language has been integrated for SOFC of planar type. Where the electrode and electrolyte part discretized using the central-difference scheme. The result indicates an increment in the temperature in the electrode and electrolyte due to the joule effect. Moreover, at anode supported all the hydrogen mass transfer arrives at the anode/electrolyte interface. Similarly, the water produced at all interface.

Mustafa ilbas et al[48]**.** Presented a 3D model of a planar solid oxide fuel cell (SOFC) to study the effect of cathode and electrolyte supported on SOFC cell performance numerically using a finite element method (FEM) implemented in code Comsol. The model predicts the polarization and power curves where the electrolyte materials used in the components are yttria-stabilized zirconia (YSZ: 8 mol%Y2O3-ZrO2) where the anode and cathode materials are nickel oxide (NiO)/YSZ and La0.60Sr0.40FeO3-d (LSF)

respectively. The numerical result indicates raising the operating temperature and pressure improved the performance. While the cathode supported shows the better performance compared to the electrolyte supported. Furthermore at range temperature 600-1000 °C at the cathode supported the average of current density and power density increased by 53%, 56% respectively. Moreover, the average of current density and power density increased by 20%, 22% respectively when the pressure range from 1-5 atm. In this work shows that the power density of a cathode supported cell type LSF is higher than an electrolyte supported cell type YSZ.

S Koch el al[49]**.** Presented a study to examine the degradation of anode supported (AS) SOFC cell under several operating conditions (the fuel gas composition, the operating temperature, and the current density) at two different temperatures 750 °C and 850°C. Where the anode and cathode materials are Ni-YSZ and LSM respectively. The study shows the higher degradation rates at high current densities as result a more water content produced for some temperatures and current densities. Can be said the degradation rate reduced the voltage. Thus, the cell deteriorates.

H Severson[50]**.** A mathematical transport model for an anode supported solid oxide fuel cell type planar was performed and the analysis was executed through the use of an internal program that can help the researcher understand the influence of different parameters on fuel cell performance. The configuration is co-flow with steady-state and adiabatic boundary conditions for terminal anode and cathode. The electrochemical model implemented in FORTRAN is based on the finite volume method (FVM). The model was taken out a detailed parameter study, at both the anode and cathode in order to predict the performance of AS-SOFC, the ohmic overpotentials, concentration overpotentials, activation overpotentials, and diffusion coefficient for various electrolyte thickness, pore size, porosities, and temperature. The model uses the stabilized yttrium-zirconia (YSZ) as electrolyte materials, LSM and Ni-YSZ as cathode and anode materials respectively with thicknesses 20, 50, and 500 μm respectively. The result shows rising pore sizes reduce concentration overpotential, and as result the Knudsen diffusion coefficient is improved. And therefore diminishes the concentration overpotential due to raises the porosity. Where

found the Ohmic and activation overpotential diminishes as temperature rise Contrary to concentration overpotential which is directly proportional to temperature.

A Shukla et al[51]**.** A parametric study was performed to examine the impact of current density, fuel utilization, and recirculation ratio on the performance of SOFC fuel cells. The author studies thermodynamic modeling based on gas turbine SOFC-GT by using waste heat from the gas turbine to preheat the air entering the SOFC where the fuel is natural gas. The SOFC fuel cell work on syn-gas at operating temperature 1150 K. The assumptions for this study are isothermal conditions, a Steady-state analysis, and radiative heat transfer effects are ignored. The result summarized that a lower recirculation ratio and higher fuel utilization factor improved the performance by 2.4%. The study confirm the combination of the SOFC with gas turbine enhances the performance.

A. K. Samantaray et al[52]**.** Performed a study in order to develop maximum energy and exergy efficiency by using a cascaded optimization algorithm. The paper includes a Steady-State Model, the after-burner, and the heat exchangers. Whereas, the second law of thermodynamics is applicable to the SOFC fuel cell in this research to get the large irreversibilities. Formed an algorithm with the help of Matlab in order to calculate the steady-state value of various variables like temperatures, pressures, mass flow rates, voltage, fuel utilization, air utilization, and power. The main conclusion of their investigation indicates that the fuel utilization for maximum efficiency operation decreases with increment in current density. Moreover, a linear relationship between mass flow rate and current density which leads to maximum system efficiency at constant fuel utilization.

W Cameron Tanne et al[53]. Examined theoretically the effect of porous composite electrode by taking different parameters like porosity, intrinsic charge-transfer resistance, and electrode/electrolyte thickness. The experimental results show the intrinsic charge-transfer resistance diminishes as the thickness of the electrode raises. On another side to ensure negligible concentration losses use a fine microstructure with a fine electrode at porosity sufficient.

M Farnak et al[54]**.** Evaluated the performance of SOFC fuel cell experimentally utilizing partial oxidation reforming of natural gas. An experimental study based on the design of the experiment (DOE) was performed to attain the maximum performance of SOFCs. The

model uses methane CH4 as fuel. The paper focused on several parameters including methane and oxygen flow rates as well as Re number of fluid flow and air ratio in order to maximize the peak power density (PPD). Where the methane flow rate range varies between 50-150 sccm and the oxygen flow rate range between 10-30 sccm. The results of this model led to some useful conclusions which are still applicable to fuel cell investigation. Where they concluded that the maximum peak power density when the Reynolds (Re) number of fluid flow around 10 and O2/CH4 ratios between 0.2-0.4.

Z Khalid et al[55]**.** Investigate theoretically and analytically the efficiency of the SOFC fuel cell. To evaluate the effect of various material and functional conditions on the cathode diffusion polarization and its impact on exergy efficiency. This research is a continuation of his previous work which deals to investigate the anode diffusion polarization of the SOFC. In his mathematical model, an iterative approach is used for solving the continuity equations and thermal equations and using the calculation of a finite differences method (FDM) to discretize the partial differential equations for mass and energy. The model includes various parameters to study the cathode diffusion polarization on cell efficiency we mention among them the porosity, tortuosity, pore diameter, temperature, pressure. The model led to some useful results which are still applicable to fuel cell study across a high temperature range. Their results summarized that when the cathode porosity is between 0.35-0.38, the SOFC temperature range between 850°c-950°c, the thickness of the cathode between 0.01-0.02 cm, and the pressure range between 3-5 bars achieve the optimum peak exergy efficiency at the range of 0.35-0.38.

S Lee et al[56]**.** Present a 3D numerical study to test the impact of fuel utilization on heat and mass transfer on planar AS-SOFC stack. The developed model has solved the charge, mass, momentum, species, and energy conservation equation using COMSOL multi-physics with the relative tolerance of 10^{-4} for solving the fully-coupled nonlinear equation. The Butler-Volmer equation is treated and the derivation and applicability of various approximations are examined. The SOFC model includes the Ni-YSZ anode layer, YSZ electrolyte, and LSCF–GDC composite cathode layer besides the gas flow channel is a counter-flow. Numerical simulation results revealed that increasing fuel utilization

produces a small and non-uniform reaction zone at the inlet fuel which leads to an increase in the oxygen pressure consequently reducing the electrochemical potential gradient.

J Zhang et al[57]**.** Study the several electrolyte materials under low-temperature SOFC fuel cell (500°C). They used YSZ, GDC, and ScSZ as electrolyte materials for the comparison of their ionic conductivities. Furthermore, this investigation was an experimental study. The result indicates that the GDC has higher ionic conductivities than YSZ and ScSZ. These experimental results show that the model developed can be reasonably and applicable to the design of the cell. In addition, helps the manufacturer to choose the best electrolyte thickness in SOFC application.

D Feng et al[58]**.** Manifested some success with a 1D SOFC fuel cell where developed an algorithm analytical to predict the overpotential in anode and cathode SOFC. Steady-state model, temperature, and pressure are uniforms throughout the positive and negative electrode, and the ideal gases applicable for species. Based on the Butler-Volmer equation and linear model of Fick's diffusion to calculate the total overpotential. Firstly the algorithm validated in Matlab for an electrolyte supported and thin anode layer SOFC. The result is acceptable for the conventional linear approximation (CLA) and power-law (PL) approach for enhancing the performance. Nevertheless, He concluded that an algorithm gave fast and accurate results to predict the overpotential and species concentrations.

S Dong et al[59]**.** Established a 3D numerical analysis of the solid oxide fuel cell stack to predict current density, temperature, Ohmic and activation overpotentials, voltage versus power, and reactants distribution to verify the flow uniformity and to measure the electrochemical reactions in the stack. The stack consists of five cells. A commercial CFD tool was employed, solving the equation of mass, momentum, and energy. Steady-state is presented, the flow is laminar and incompressible, mass and heat transfer are included beside the radiative heat is negligible. The model composes a 3 cases with different volume flow rates for calculating the performance of the stack at a temperature of 1073 K. They concluded that while the temperature increases progressively, the flow rates of the reactants are reduced which led to increasing the utilization rates of the SOFC stack. It is necessary to predict the performance of the SOFC stack before the manufacture to advance improvements in design for the planar SOFC stacks.

F Calise[60]**.** Based on finite volume finite developed a tubular SOFC fuel cell capable of performing calculations for radiative heat transfer and exergy analysis inside the SOFC cell. After a description of the basic geometry and general assumptions and simplifications for the calculation of temperature, pressure, chemical composition, electrical parameters, and exergy destruction rates, heat transfer by radiative for tubular SOFC. The chemical, electrochemical, electrical, and thermodynamic parameters were input and simulated using code MATLAB to solve a non-linear equation. This model demonstrates the importance of the radiation heat transfer in tubular SOFC whereas this latter contributed to 70% to the radial transfer in the SOFC tube and its air injection tube. This model is used to predict the correct operating conditions and optimal design.

W Kong et al[61]**.** Examine a structural design of the SOFC cell by developing a new interconnector design in order to raise the performance of SOFC. The model compared two different designs which are the X-type interconnector and the conventional interconnector. Various parameters such as porosity, pressure, temperature, conductivity..etc are examined to testify the advantage of this novel design. They show that among various parameters, the configuration of the X-type interconnector was better compared to the conventional interconnector design. It showed the best gas distribution in SOFC and superior porosity and conductivity. Thus, it led to an increase in the performance of the SOFC cell. This work was adopted in the software COMSOL multiphysics.

G Min et al[62]**.** Developed a thermodynamic system analysis to simulate the performance of a solid oxide fuel cell stack under different operating conditions and design factors. Current density, fuel utilization, air utilization, pressure, and steam to carbon ratio were calculated with the model in different regions. The model discretizes the SOFC stack in 1D to facilitate the thermodynamic balance calculation and predict the electrochemical performance. The overpotentials equation based on the Butler-Volmer equation is explained and the derivation and applicability of different approximations are studied. The model tested all parameters in detail and discussed. The authors show that great fuel utilization operation, low air utilization, and low current density is suitable for high 1st and 2nd law efficiencies. In addition, obtain a performance higher than 50% and exit gas temperature lower than 900℃. This model is characterized by the advantage of faster run

time for simulations compared to a complex three-dimensional model by solving almost so many details moreover choose the optimum parameter of the SOFC stack without doing expensive experiments.

A Raj et al[63]**.** The purpose of this study is tested temperature, stoichiometry, and Cathode humidity for planar SOFC using COMSOL software. The model includes the mass, momentum and charge balance, secondary current, and Butler–Volmer equations. The simplified assumptions and related omissions that each of these approaches involves are also analyzed. The polarization curve was adopted in this study that generally accepted as a measure of the important efficiency of the fuel cell. The result shows the performance enhances at raised temperature while the cathode humidity is observed to negatively affect the performance so it is necessary to Neglecting the humidification of the cathode. Moreover, the influence of anode stoichiometry has become insignificant on the performance of SOFC cells under all operating conditions.

H Xu et al[64]**.** A 2D numerical analysis has been developed to study the influence of electrolyte porosity on the SOFC cell. Furthermore, suggested a novel design of tubular SOFC in order to achieve the optimum performance. The model use CGO as electrolyte materials with a supported thickness of 2mm, while the anode and cathode materials are Ni-CGO and BSCF, respectively with thickness layer is 55 μm and 25 μm, respectively. The model use CH_4 as inlet fuel and O_2 as an air inlet. The model uses many assumptions discussed in the paper to facilitate the solution and speed up the calculation. The finite element analysis is used for discretizing the governing equations and implemented in software COMSOL. The output result for the electrolyte-supported SOFC includes effects of electrolyte porosity, the effect of anode inlet CH_4 mole fraction, the effect of inlet gas flow rate, and the effect of a novel design. The result shows that a great electrolyte porosity could be only possible for thick electrolytes and the raises of CH_4 mole fraction lead to improve the performance. While reducing the electrode inlet gas flow rate leads to a decrease in the current density and uses the higher rate of CH_4. In addition, the new design was found to contribute to enhancing the performance of the tubular SOFC fuel cell.

D.A. Noren et al[65]**.** Several authors give different expressions for activation losses in solid oxide fuel cell models. This paper explains how to obtain losses through the Butler-

Volmer equation. Acknowledging that there are many expressions in the literature used to calculate the activation losses, among which we mention the Tafel equation, the Butler-Volmer equation, and the linear-current potential equation. The paper discussed the importance of calculating the activation losses based on the Butler–Volmer equation at low temperature in order to predict the current-voltage of the cell. The authors note that the implicit Butler–Volmer equation is favored in resolving activation losses because of its simplicity and provides more precise results in numerical technique.

A. Akkaya[66]**.** In this research, a tubular SOFC fuel cell was presented and the analysis was performed through the use of an internal program that can help the researcher comprehend the impact of various parameters on the performance of the fuel cell. In the model, electrochemical kinetics, gas dynamics and energy transport, and species are coupled. The model predicts the Ohmic, activation, and concentration polarization curves for several operating conditions (such as temperature, pressure, and current density) and various cell component properties (such as thickness layer, pore size) in order to assist in getting the optimal performance of tubular SOFC. Additionally, electrolyte materials used in components are Yttria-stabilized zirconia (YSZ) and anode materials are the Ni/YSZ. Fick's law, Ohm's law, and the Butler–Volmer equation are applied to resolve the polarization terms. The simplified assumptions and related omissions that each of these approaches involves are also analyzed. As a conclusion of this research must study carefully operating conditions to attain the optimal performance of tubular SOFC cells. Consequently, their setting during operation improves the performance considerably. Moreover, the concentration polarization is a significant key connected with limiting current density.

Y Wang et al[67]**.** The model analyzes the effect of operating pressure on cell characteristics which includes the cell performance, temperature, fuel utilizations, air ratios and flow arrangement distribution in two cases: case1: using partly pre-reformed gas and case2: syngas. The anode-supported structure composed Ni-yttria- stabilized zirconia (Ni-YSZ), the electrolyte structure composed YSZ electrolyte, and the cathode structure composed lanthanum strontium manganite (LSM). The model is established to several hypotheses presented in the paper. This model presented the heat and mass coupling,

electron and ion transport, and internal reforming reactions, while the coupled equation is described and solved using the software FLUENT. Moreover, a user-defined function (UDF) has been written for electronic and ionic potential, multi-component diffusion coefficients, and internal reforming reactions. They show that among various parameters, the great pressure improves the distributions of species, temperature, and internal reforming reactions in case1 compared to the case2. Besides, the case1 it gave better results in improving performance for flow arrangement distribution.

D Cui et al[68]**.** Described a tow-dimensional, steady-state simulation tool which ignores radiative transfer for the anode supported tubular solid oxide fuel cells (AST-SOFC). The model described is intended to simulate several parameters taking into account examining the electrical and species transport for various geometries of the AST-SOFC in order to enhance the performance. The AST-SOFC operates at 800 °C under the cell operating voltage of 0.7 V. The equations which governing are solved simultaneously by the commercial software, COMSOL. The main conclusion of their investigation developing the geometry design of tubular SOFCs can enhance the current distribution, causing the cell performance better.

M Kamvar et al[69]**.** presented a comparative study between various support types configuration on a planar single-chamber solid oxide fuel cell (SC-SOFC) with a steady-state and time-dependent two-dimensional model, it includes the equations describing the transport of chemical and electrochemical processes of mass, species, and energy, it ignores the thermal diffusion, the equations are solved by code CFD based on the finite element method. Their results revealed that the anode-supported and cathode-supported cells show the better performance compared to the electrolyte supported.

II.2 Different Expressions voltage and losses modeling

According to the bibliographic research carried out, several authors give different expressions for the Nernst voltage (E_{Nernst}) and overvoltage. These later have different expressions. This is what we explain in the following.

II.2.1 Pakalapati model

The overall reaction for the formation of water from hydrogen and oxygen, in a SOFC fuel cell is given by[70]:

$$H_2 + \frac{1}{2} O_2 \rightarrow H_2O \quad \textbf{(II.1)}$$

The Nernst potential for this reaction, for a fuel cell operating at atmospheric pressure, is given by:

$$\mathrm{E_{Nernst}} = -\frac{\Delta \mathrm{G_0}}{2\mathrm{F}} - \frac{\mathrm{RT}}{2\mathrm{F}} \ln\left(\frac{\mathrm{X_{H_2O}}}{\mathrm{X_{H_2}}.\mathrm{X_{O_2}^{0.5}}}\right) \quad \textbf{(II.2)}$$

where $\Delta \mathrm{G_0}$ is the standard Gibbs energy exchanged for the water formation reaction. In general, for the electrochemical reaction, the exchanged standard Gibbs energy is linked to a constant which is called the equilibrium constant K , according to Pakalapati[70]

$$\Delta \mathrm{G_0} = -RTln(K) \quad \textbf{(II.3)}$$

$$\mathrm{K}=k_f/k_b \quad \textbf{(II.4)}$$

Where k_f, k_b are reaction constants estimated by Bieberie and Gauckler

The cathodic and anodic losses are given by[70]:

$$\mathrm{J} = \mathrm{J_{0,cat}}\left(\frac{C_{O_2}}{C^*_{O_2}}\exp\left(\alpha^f_{cat} f \eta_{\mathrm{cat}}\right) - \frac{C_{O^-}}{C^*_{O^-}}\exp\left(-\alpha^b_{cat} f \eta_{\mathrm{cat}}\right)\right) \quad \textbf{(II.5)}$$

$$\mathrm{J} = \mathrm{J_{0,an}}\left(\frac{C_{H_2} C_{O^-}}{C^*_{H_2} C^*_{O^-}}\exp\left(\alpha^f_{an} f \eta_{\mathrm{an}}\right) - \frac{C_{H_2O}}{C^*_{H_2O^-}}\exp(-\alpha^b_{an} f \eta_{\mathrm{an}})\right) \quad \textbf{(II.6)}$$

With $\mathrm{J_{0,cat}}$, $\mathrm{J_{0,an}}$ are the cathodic and anodic exchange current density, respectively and $C_{O_2}, C^*_{O_2}, C_{O^-}, C^*_{O^-}$ are oxygen concentrations and oxygen ions respectively (the asterisk represents the reference concentration).

The relationship between current, overvoltage following the **Tafel** approach at cathode and anode is given respectively by the expressions[70]:

$$\eta_{cat} = \frac{1}{\alpha_{cat}^{f} f} \ln\left(\frac{j}{j_{0,cat}}\right) \quad \textbf{(II.7)}$$

$$\eta_{an} = \frac{1}{\alpha_{an}^{f} f} \ln\left(\frac{j}{j_{0,an}}\right) \quad \textbf{(II.8)}$$

The ohmic losses are given by the expression:

$$\eta_{\mathrm{Ohm}} = \mathrm{jR}_{\mathrm{Ohm}} \quad \textbf{(II.9)}$$

Where $R_{Ohm}$is the effective resistance of the cell

II.2.2 Aguiar model

The Nernst tension is given as a function of the partial pressures of the three species and the temperature [71]:

$$\mathrm{E}_{\mathrm{Nernst}} = E^{0} - \frac{\mathrm{RT}}{2\mathrm{F}} \ln\left(\frac{\mathrm{X}_{\mathrm{H_2O}}}{\mathrm{X}_{\mathrm{H_2}}.\mathrm{X}_{\mathrm{O_2}}^{0.5}}\right) \quad \textbf{(II.10)}$$

The expression of the cell's potential takes the form[71]:

$$\mathrm{V}_{\mathrm{cell}} = \mathrm{E}_{\mathrm{Nernst}} - \eta_{\mathrm{Ohm}} - \eta_{\mathrm{act,an}} - \eta_{\mathrm{act,cat}} - \eta_{\mathrm{con,an}} - \eta_{\mathrm{con,cat}} \quad \textbf{(II.11)}$$

Ohmic losses $\eta_{Ohm}$are due to the electrical resistances of the three solid parts of the cell. This voltage drop is significant and increases linearly with the current density i. According to Ohm's law, Ohmic losses are expressed as follows[71]:

$$\eta_{\mathrm{Ohm}} = \mathrm{iR}_{\mathrm{Ohm}} \quad \textbf{(II.12)}$$

Concentration overpotentials are caused by gas diffusion in the porous electrodes. These losses are a function of the partial pressures of the gases produced and the gases reacting at the level of the channels and at the level of the electrode/electrolyte interfaces. Concentration losses at the anode and cathode take the following forms[71]:

$$\eta_{con,an} = \frac{RT}{2F} Ln\left(\frac{\mathrm{X}_{\mathrm{H_2O,TPB}}.\mathrm{X}_{\mathrm{H_2,f}}}{\mathrm{X}_{\mathrm{H_2O,f}}.\mathrm{X}_{\mathrm{H_2,TPB}}}\right) \quad \textbf{(II.13)}$$

$$\eta_{con,cat} = \frac{RT}{4F} Ln\left(\frac{X_{O_2,a}}{X_{O_2,TPB}}\right) \quad \textbf{(II.14)}$$

To calculate the concentration losses, the relation between the partial pressures of the three species H_2O, H_2, O_2 at the interface (triple contact point) and the current density is necessary. The partial pressures of the three species at the electrolyte/electrode interfaces are a function of the partial pressures of these species at the level of the channels, they are expressed as follows[71]:

$$P_{H_2,TPB} = P_{H_2} - \frac{RTe_{an}}{2FD_{eff,an}} j \quad \textbf{(II.15)}$$

$$P_{H_2OTPB} = P_{H_2O} + \frac{RTe_{an}}{2FD_{eff,an}} j \quad \textbf{(II.16)}$$

$$P_{O_2,TPB} = P - \left(P - P_{O_2,a}\right).exp\left(\frac{RTe_{cat}}{4FD_{eff,cat}.P} j\right) \quad \textbf{(II.17)}$$

With $D_{eff,an}$represents the average diffusion coefficient of hydrogen and water vapor in the anode and $D_{eff,cat}$represents the average diffusion coefficient of oxygen in the cathode.

The activation losses are caused by the kinetics of the reactions in the electrodes. It is at higher temperatures that this type of loss is lower. Their expressions are given by non-linear equations (Butler-Volmer equation) [71]:

$$\eta_{act,an} = \frac{RT}{\alpha nF} Ln\left(\frac{H_{2,f}}{H_{2TPB}} . \frac{j}{j_{0,an}}\right) \quad \textbf{(II.18)}$$

$$\eta_{act,cat} = \frac{RT}{\alpha nF} Ln\left(\frac{O_{2,a}}{O_{2TPB}} . \frac{j}{j_{0,cat}}\right) \quad \textbf{(II.19)}$$

With α the transfer coefficient (generally α=0.5), n the number of electrons transferred and j_0 exchange current density in the electrodes which are expressed by[71]:

$$\mathrm{j_{0,an}} = \mathrm{k_{an}} \frac{RT}{nF} \exp\left(-\frac{\mathrm{E_{act,an}}}{\mathrm{RT}}\right) \quad \textbf{(II.20)}$$

$$\mathrm{j_{0,cat}} = \mathrm{k_{cat}} \frac{RT}{nF} \exp\left(-\frac{\mathrm{E_{act,cat}}}{\mathrm{RT}}\right) \quad \textbf{(II.21)}$$

II.2.3 A.C. Burt model

This electrochemical model is based on the consideration of the global reaction in a fuel cell[72]:

$$H_2 + \frac{1}{2} O_2 \rightarrow H_2 O_g \quad \textbf{(II.22)}$$

The Nernst potential is given by the following expression[72]:

$$\mathrm{E_{Nernst}} = E^0 + \frac{\mathrm{RT}}{\mathrm{2F}} \ln\left(\frac{\mathrm{X_{H_2}} . \mathrm{X_{O_2}^{0.5}}}{\mathrm{X_{H_2O}}}\right) + \frac{\mathrm{RT}}{\mathrm{2F}} \ln\frac{P}{P^0} \quad \textbf{(II.23)}$$

Where P and P^0 are respectively the pressure and the reference pressure. The reversible potential at standard conditions is related to the standard Gibbs energy[72]:

$$E^0 = \frac{\Delta \mathrm{G^0}}{\mathrm{2F}} \quad \textbf{(II.24)}$$

The potential of the cell is calculated according to the Nernst potential and the various losses (ohmic losses, activation losses, and those of concentration) [72]:

$$\mathrm{V_{cell}} = \mathrm{E_{Nernst}} - \eta_{\mathrm{Ohm}} - \eta_{\mathrm{act}} - \eta_{\mathrm{con}} \quad \textbf{(II.25)}$$

These losses are related to the current density. The activation overvoltage is defined by an empirical relation represented by the different forms of Tafel's equations[72]:

$$\eta_{act} = \frac{RT}{\alpha nF} Ln \frac{j}{j_0} \quad \textbf{(II.26)}$$

The ohmic and concentration losses are expressed as follows[72]:

$$\eta_{Ohm} = jR_{Ohm} \quad \textbf{(II.27)}$$

$$\eta_{Con} = \frac{RT}{nF} ln\left(1 - \frac{j}{j_L}\right) \quad \textbf{(II.28)}$$

Where $j_0$represents the exchange current density, j_L the limit current density and α the transfer coefficient (α=0.5), $R_{Ohm}$the total resistance of the cell.

These calculation models are summarized in **Table II.1**:

	Nernst potential	**Ohmic loss**	**Activation loss**	**Loss of concentration**
Pakalapati model	$E_{Nernst} = -\frac{\Delta G_0}{2F} - \frac{RT}{2F}\ln\left(\frac{X_{H_2O}}{X_{H_2}.X_{O_2}^{0.5}}\right)$	$\eta_{Ohm} = jR_{Ohm}$	/	/
Aguiar model	$E_{Nernst} = E^0 - \frac{RT}{2F}\ln\left(\frac{X_{H_2O}}{X_{H_2}.X_{O_2}^{0.5}}\right)$	$\eta_{Ohm} = iR_{Ohm}$	/	/
A.C. Burt model	$E_{Nernst} = E^0 + \frac{RT}{2F}\ln\left(\frac{X_{H_2}.X_{O_2}^{0.5}}{X_{H_2O}}\right) + \frac{RT}{2F}\ln\frac{P}{P^0}$	$\eta_{Ohm} = jR_{Ohm}$	$\eta_{act} = \frac{RT}{\alpha nF} Ln \frac{j}{j_0}$	$\eta_{Con} = \frac{RT}{nF} ln\left(1 - \frac{j}{j_L}\right)$

Loss of anodic activation	**Loss of anodic concentration**
$\eta_{an} = \frac{1}{\alpha_{an}^f f}\ln\left(\frac{j}{j_{0,an}}\right)$	

$\eta_{act,an} = \frac{RT}{\alpha nF} Ln\left(\frac{H_{2,f}}{H_{2TPB}} . \frac{j}{j_{0,an}}\right)$	$\eta_{con,an} = \frac{RT}{2F} Ln\left(\frac{X_{H_2O,TPB} . X_{H_2,f}}{X_{H_2O,f} . X_{H_2,TPB}}\right)$
/	/

Loss of cathodic activation	**Loss of cathodic concentration**
$\eta_{cat} = \frac{1}{\alpha_{cat}^{f} f} \ln\left(\frac{j}{j_{0,cat}}\right)$	
$\eta_{act,cat} = \frac{RT}{\alpha nF} Ln\left(\frac{O_{2,a}}{O_{2TPB}} . \frac{j}{j_{0,cat}}\right)$	$\eta_{con,cat} = \frac{RT}{4F} Ln\left(\frac{X_{O_2,a}}{X_{O_2,TPB}}\right)$
/	/

Table II.1: Summary of three models.

Conclusion

A literature review study under several operating and design conditions, the different expressions of the voltage and polarizations of the SOFC fuel cell was carried out. In addition, the physical, chemical, and electrochemical processes inside the cell are taken into account. The exchange current density in expressions of activation loss takes on different values and forms of expression. A possibility of choosing between the approach of Tafel or that of Butler-Volmer exists for the losses of activation. Furthermore, Ni-YSZ cermet, YSZ, and Lanthanum Strontium Manganite (LSM) are the generally utilized materials for the anode, electrolyte, and cathode respectively. Besides, various flow fields design influence the distribution of the temperature, pressure, fuel utilization, and reaction rate. The performance of the SOFC stack as a function of each type of overvoltage is compared for a certain calculation model found in the literature.

In the end, a comprehensive literary study was presented about the various calculations in order to improve the performance of the SOFC fuel cell at different operating conditions

and geometric configurations. Moreover, a comparative study is made on a few selected simulation works and discussed.

Chapter III: Mathematical formulation and numerical procedure

Introduction

The research of SOFC fuel cells has been steadily rising during the last ten years. Where the problem of developing and creating new geometries has generated a lot of interest. However, examining the performance of SOFC fuel cells requires understanding and studying the physical, chemical, and electrochemical phenomena that occur in these cells. The experiments in these studies are possible but they are very expensive, given the very high cost of the materials and equipment necessary for carrying out the manipulations, as well as the duration of the tests, which is generally long. Therefore, we have chosen to use modeling and simulation to solve this problem in order to predict the performance of this type of cell according to the physical parameter and operating conditions.

During its operation, the SOFC fuel cell is subjected to several phenomena: material transport[73], heat transfer[74], and electrochemical[75]–[77]. These phenomena interact and act directly on the performance of the fuel cell.

To be able to build the mathematical model of a cell with planar geometry, we must first define a macroscopic geometric design, on which we place the coordinate system and define the system of equations composing our model.

III.1 Physical Domain

Our field of study is represented in **Figure III.1**, characterized by its dimensions, it is a plane geometry of a cell of the SOFC model which comprises two porous diffusion layers (GDLs) inside which are the so-called active or catalytic reaction zones (CLs), delimited on the outside by the channels of the incoming gases (fuel and oxidizer) and on the inside by a dense and purely impermeable solid area called the electrolyte (EL), the whole GDLs -EL is commonly referred to as Membrane-Electrode-Assembly (MEA). Hydrogen and oxygen react at the anode and produce water, heat, and current. So two distinguished fluids flow, the first that of the porous medium characterized by a transfer of mass and heat by diffusion, the second convective that of the zone of the channels where the gases are assimilated as ideal gases. Our simulation would be applied at the level of a single cell in order to be able to determine the performance of the latter, then generalized to the sized prototype in order to acquire the power desired by the fuel cell.

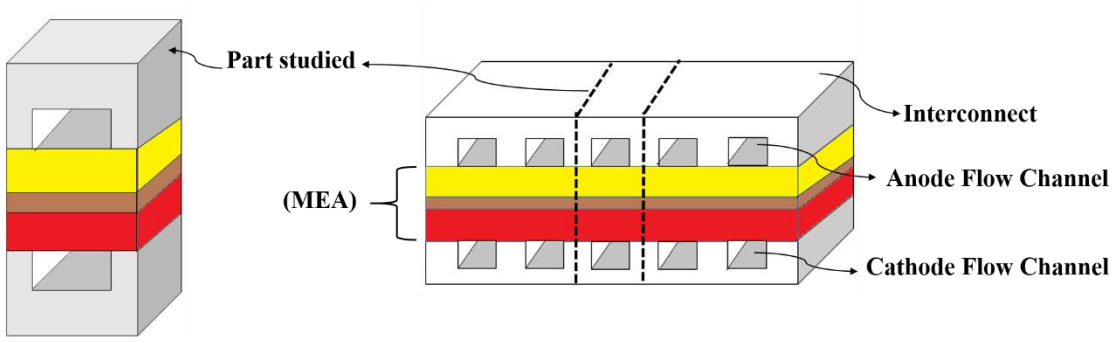

Figure III.1: Three-dimensional SOFC fuel cell of the study area.

The choice of the field of study is an important step in our study, this choice is based on considerations of repeatability, symmetry, and simplicity. Thus, we must define a geometric design on all the parts that we were interested in in our study.

a. Material

The choice of an electrode and electrolyte under these conditions is above all a compromise that will make it possible to keep the performance of the fuel cell at the same level over a long period of use. In our field of study we choose Ni-YSZ as anode material, LSM as cathode material where we assume that this material is isotropic and that the pore size is greater than the average free path of the gas molecules, and yttrium-doped zirconia (YSZ) has been widely employed as an electrolyte material to achieve sufficient conductivity of oxygen ions in the electrolyte. **Figure III.2** shows the used material diagram of central part of a MEA (Membrane – Electrode Assembly) with Porous Anode, Dense Electrolyte, and Porous Cathode layers.

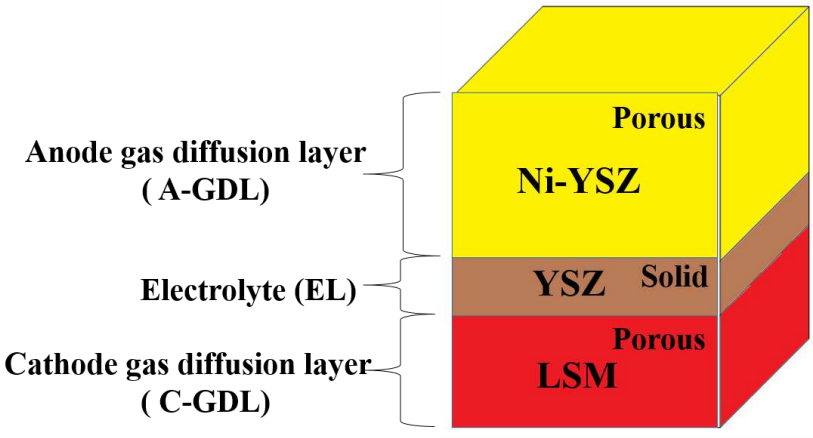

Figure III.2: Membrane-Electrode-Assembly (MEA) materiel of the field of study.

b. Flow field direction

The direction of flow is very sensitive to performance. From the bibliography research, we choose the anode and cathode gas flows are opposite (flow counter-current) in our study as indicated in **Figure III.3**.

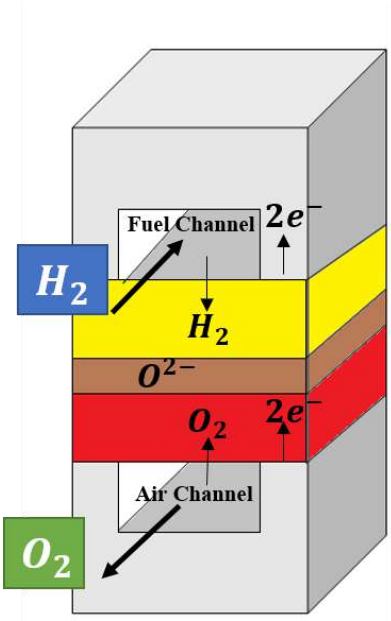

Figure III.3: Flow field direction of the field of study

c. Gas channel geometry

The flow field configuration has a vital effect on the performance of the fuel cell and is the key factor in SOFC design optimization. Therefore, further studies on new field designs are recommended to obtain more acute and reliable results on cell performance. Thus, a new flow field based on a sinusoidal flow has been proposed and studied, and compared with the single flow field as shown in **Figure III.4**.

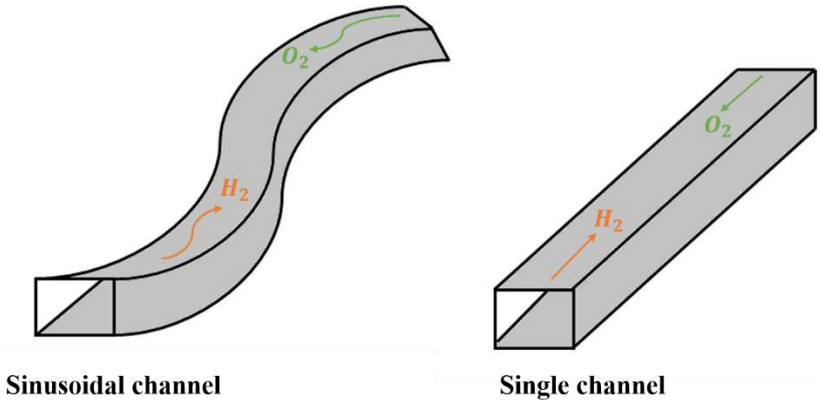

Figure III.4: Illustration of the gas channels geometry of the field of study

III.2 The assumptions of the model

The three-dimensional modeling of a cell, taking into account all the physical phenomena, represents a major problem. For this purpose, the governing equations of these phenomena become very complicated, which makes the resolution very difficult at all levels (the calculation time, numerical errors, etc.).

So it clearly appears that the introduction of the hypotheses is necessary in order to simplify the system of equations and to make the problem less difficult. Consequently, we made the following assumptions:

- The flow is permanent $\frac{\partial}{\partial t} = 0$.
- The calculation is three-dimensional 3D.
- Reactant gases and products are assimilated as ideal gases.
- Radiative heat transfer is negligible.

- The porous medium is homogeneous isotropic.
- The flow in the porous medium (the electrodes) is laminar.

III.3 Mathematical formulation of the problem

The study of the performance of a fuel cell requires the modeling of many phenomena in the different parts of the SOFC cell such as, the flow of the reactants, the heat transfer, the consumption of the reactants and their transport. In order to simulate all these phenomena, the mathematical model used in this work is based on two models: the mass and heat transfer model, and the electrochemical model. The first represents the phenomena of transfer of momentum, heat and species in the different parts of the cell (channels, gas diffusion layers, and membrane). The second represents the process of redox reactions of reactants in the catalyst layers and also serves to quantify the source terms of the transfer model equations. All of these models plan to explain the fundamental processes occurring in the fuel cell system and therefore serve as a tool for the design and optimization of different cell components.

III.4 Heat and mass transfer model

To study the different phenomena, we use a stationary three-dimensional model containing the conservation equations for the momentum of energy and species, expressed in Cartesian coordinates as follows:

III.4.1 Energy equation

III.4.1.1 Electrolyte

SOFCs have a solid electrolyte, an ionic conductor and an electronic insulator. Ion conduction takes place by diffusion which is a thermally activated phenomenon, hence the three-dimensional energy equation is written [3]:

$$\frac{\partial}{\partial x}\left(\lambda_{eff\ el}\frac{\partial T}{\partial x}\right)+\frac{\partial}{\partial y}\left(\lambda_{eff\ el}\frac{\partial T}{\partial y}\right)+\frac{\partial}{\partial z}\left(\lambda_{eff\ el}\frac{\partial T}{\partial z}\right)+S_T=0 \qquad \textbf{(III.1)}$$

Source term

The source of energy that exists in the electrolyte of a SOFC cell is due to ohmic losses; it is expressed as follows[3]:

$$S_T = S_{Ohmic} = \frac{j^2}{\sigma_{el}} \quad \textbf{(III.2)}$$

III.4.1.2 The electrodes

Three-dimensional energy equation is written [3]:

$$\frac{\partial}{\partial x}\left(\left(\rho C_p u\right)_{Fluid} T\right) + \frac{\partial}{\partial y}\left(\left(\rho C_p v\right)_{Fluid} T\right) + \frac{\partial}{\partial z}\left(\left(\rho C_p w\right)_{Fluid} T\right) = \frac{\partial}{\partial x}\left(\lambda_{eff}\frac{\partial T}{\partial x}\right) + \frac{\partial}{\partial y}\left(\lambda_{eff}\frac{\partial T}{\partial y}\right) + \frac{\partial}{\partial z}\left(\lambda_{eff}\frac{\partial T}{\partial z}\right) + S_T \quad \textbf{(III.3)}$$

Source term

In order to accurately model heat transfer in a SOFC fuel cell, special attention must be paid to the evaluation of heat sources in the cell that are directly related to Ohmic losses, activation losses, and electrochemical reactions. The densities of the exchange current, the total energy source, and the different sources; Ohmic, and activation are expressed by the following **Tables (III.1)** and **(III.2).**

Table III.1: The densities of the exchange current [78][47][77]

	Anode	**Cathode**
The densities of the exchange current	$j_{0,a} = k_a \frac{RT}{nF} \exp\left(-\frac{E_{act,a}}{RT}\right)$	$j_{0,c} = k_c \frac{RT}{nF} \exp\left(-\frac{E_{act,c}}{RT}\right)$

TableIII.2: Source terms corresponding to the conservation equation energy in the GDL[39][3]

	GDL	
	Anode side	**Cathode side**
Source Ohmic (W/m^3)	$S_{Ohmic} = \frac{j^2}{\sigma_{an}}$	$S_{Ohmic} = \frac{j^2}{\sigma_{ca}}$

Source activation (W/ m^3)	$S_{act} = \frac{RT}{\alpha nF} Ln\left(\frac{j}{j_{0,an}}\right) j$	$S_{act} = \frac{RT}{\alpha nF} Ln\left(\frac{j}{j_{0,ca}}\right) j$
Total source (W/m^3)	$S_T = S_{Ohmic} + S_{act}$	$S_T = S_{Ohmic} + S_{act}$

A part of the reaction is not completely transformed to electricity. Consequently the heat generation created due the contribution entropy heat which given as:

$$S_T = \frac{T.\Delta S.j}{2F} \quad \textbf{(III.4)}$$

Where ΔS was the entropy change defined as [47]:

$$\Delta S = \Delta S_0 + \int_{298}^{T} \frac{\Delta C_{pr}}{T} dT \quad \textbf{(III.5)}$$

$$C_{pr} = C_{pH_2O} - C_{pH_2} - 0.5C_{pO_2} \quad \textbf{(III.6)}$$

III.4.2 Continuity equation

The continuity equation is a mathematical representation of the fundamental notion of fluid dynamics which is the conservation of mass, we use a stationary and gas ideal with flow laminar[79]

$$\frac{\partial \rho u_k}{\partial x} + \frac{\partial \rho v_k}{\partial y} + \frac{\partial \rho w_k}{\partial z} = 0 \quad \textbf{(III.7)}$$

k: Designates H_2, O_2, H_2O

III.4.3 Species conservation equations

At the anode

The effect of current density on hydrogen consumption at the anode is taken into account by an additional term in the mass balance equation, which is the source term. The hydrogen

mass conservation equation in the fuel cell anode takes into account two fluxes, diffusive and convective, and takes the following form,[3]

$$\frac{\partial}{\partial x}\left((\rho u)X_{H_2}\right)+\frac{\partial}{\partial y}\left((\rho v)X_{H_2}\right)+\frac{\partial}{\partial z}\left((\rho w)X_{H_2}\right)= \quad \textbf{(III.8)}$$
$$\frac{\partial}{\partial x}\left(D_{eff,H_2}\frac{\partial X_{H_2}}{\partial x}\right)+\frac{\partial}{\partial y}\left(D_{eff,H_2}\frac{\partial X_{H_2}}{\partial y}\right)+\frac{\partial}{\partial z}\left(D_{eff,H_2}\frac{\partial X_{H_2}}{\partial z}\right)+$$
$$S_{H_2,an}$$

The same thing for the mass of water vapor is transported by diffusion and convection in the anode of the pile. The effect of current density on the production of water vapor in the anode is taken into account by an additional source term in the mass balance equation, the equation for the mass concentration of water is given by[3]:

$$\frac{\partial}{\partial x}\left((\rho u)X_{H_2O}\right)+\frac{\partial}{\partial y}\left((\rho v)X_{H_2O}\right)+\frac{\partial}{\partial z}\left((\rho w)X_{H_2O}\right)= \quad \textbf{(III.9)}$$
$$\frac{\partial}{\partial x}\left(D_{eff,H_2O}\frac{\partial X_{H_2O}}{\partial x}\right)+\frac{\partial}{\partial y}\left(D_{eff,H_2O}\frac{\partial X_{H_2O}}{\partial y}\right)+$$
$$\frac{\partial}{\partial z}\left(D_{eff,H_2O}\frac{\partial X_{H_2O}}{\partial z}\right)+S_{H_2O,an}$$

At the cathode

The quantity of oxygen is transported by diffusion and convection in the cathode of the cell. The current density effect on oxygen consumption at the cathode is taken into account by an additional term in the source in the mass balance equation, the oxygen mass conservation equation is given by[3]:

$$\frac{\partial}{\partial x}\left((\rho u)X_{O_2}\right)+\frac{\partial}{\partial y}\left((\rho v)X_{O_2}\right)+\frac{\partial}{\partial z}\left((\rho w)X_{O_2}\right)= \quad \textbf{(III.10)}$$
$$\frac{\partial}{\partial x}\left(D_{eff,O_2}\frac{\partial X_{O_2}}{\partial x}\right)+\frac{\partial}{\partial y}\left(D_{eff,O_2}\frac{\partial X_{O_2}}{\partial y}\right)+\frac{\partial}{\partial z}\left(D_{eff,O_2}\frac{\partial X_{O_2}}{\partial z}\right)+$$
$$S_{O_2,cat}$$

Source term

The source terms, which are applicable at the interface electrode-electrolyte, are obtained from Eqs. (III.11)-(III.14), calculated as [9–12] :

$$S_T = S_{H_2} + S_{H_2O} + S_{O_2} \quad \textbf{(III.11)}$$

$$S_{H_2} = -\left(\frac{J_a}{2F}\right) M_{H_2} \quad \textbf{(III.12)}$$

$$S_{H_2O} = +\left(\frac{J_a}{2F}\right) M_{H_2O} \quad \textbf{(III.13)}$$

$$S_{O_2} = -\left(\frac{J_c}{4F}\right) M_{O_2} \quad \textbf{(III.14)}$$

Where the local current density is defined by the Butler-Volmer formula[77]:

$$J_a = J_{0,a} A_V \left(\exp\left(\alpha \frac{2F\eta_{act,a}}{RT}\right) - \exp\left(-(1-\alpha)\frac{2F\eta_{act,a}}{RT}\right)\right) \quad \textbf{(III.15)}$$

$$J_c = J_{0,c} A_V \left(\exp\left(\beta \frac{4F\eta_{act,c}}{RT}\right) - \exp\left(-(1-\beta)\frac{4F\eta_{act,c}}{RT}\right)\right) \quad \textbf{(III.16)}$$

F: Faraday's constant;

M: The molar mass of the species;

J: Current density;

A_V: Reactive surface area per unit volume.

III.4.4 Momentum conservation equation

The conservation of motion equation is written in the stationary, gas ideal, and three-dimensional case[84][79]:

Along the x axis[84][79]:

$$\rho_k u_k \frac{\partial u_k}{\partial x} + \rho_k v_k \frac{\partial u_k}{\partial y} + \rho_k w_k \frac{\partial u_k}{\partial z} = \frac{\partial}{\partial x}\left(\mu_k \frac{\partial u_k}{\partial x}\right) + \frac{\partial}{\partial y}\left(\mu_k \frac{\partial u_k}{\partial y}\right) + \frac{\partial}{\partial z}\left(\mu_k \frac{\partial u_k}{\partial z}\right) + S_{u,k} \quad \textbf{(III.17)}$$

$$S_{u,k} = -\varepsilon \frac{\mu_k}{\kappa_m} u_k \quad \textbf{(III.18)}$$

Along the y axis[84][79]:

$$\rho_k u_k \frac{\partial v_k}{\partial x} + \rho_k v_k \frac{\partial v_k}{\partial y} + \rho_k w_k \frac{\partial v_k}{\partial z} = \frac{\partial}{\partial x}\left(\mu_k \frac{\partial v_k}{\partial x}\right) + \frac{\partial}{\partial y}\left(\mu_k \frac{\partial v_k}{\partial y}\right) + \frac{\partial}{\partial z}\left(\mu_k \frac{\partial v_k}{\partial z}\right) + S_{v,k} \quad \textbf{(III.19)}$$

$$S_{v,k} = -\varepsilon \frac{\mu_k}{\kappa_m} v_k \quad \textbf{(III.20)}$$

Along the z axis[84][79]:

$$\rho_k u_k \frac{\partial w_k}{\partial x} + \rho_k v_k \frac{\partial w_k}{\partial y} + \rho_k w_k \frac{\partial w_k}{\partial z} = \frac{\partial}{\partial x}\left(\mu_k \frac{\partial w_k}{\partial x}\right) + \frac{\partial}{\partial y}\left(\mu_k \frac{\partial w_k}{\partial y}\right) + \frac{\partial}{\partial z}\left(\mu_k \frac{\partial w_k}{\partial z}\right) + S_{wk} \quad \textbf{(III.21)}$$

$$S_{w,k} = -\varepsilon \frac{\mu_k}{\kappa_m} w_k \quad \textbf{(III.22)}$$

The source terms S_u, S_v and S_w in gas diffusion layers model the behavior of the porous medium and they are based on Darcy's law.

ε: The porosity;

κ: The permeability of each porous medium in the cell;

μ_k: The viscosity;

m: designates anode or cathode.

Table III.3: Physical properties of different porous media.

Physical properties	Porosity (ε)	Permeability (κ)
GDL	0.3	2.10^{-10}
channels	1	/

III.5 Electrochemical model

The actual fuel cell potential is affected by voltage drops (losses) caused by electrochemical reactions and concentration differences. Therefore, the cell voltage is given by the expression[10–14]:

$$V_{cell} = E_{Nernst} - \eta_{Ohm} - \eta_{act} - \eta_{con} \quad \textbf{(III.23)}$$

V_{cell}: Actual voltage of a single cell;

E_{Nernst}: Thermodynamic (ideal) potential of each cell and represents the reversible voltage;

η_{Ohm}: Ohmic polarization of the anode and the cathode;

η_{act}: Activation polarization of the anode and cathode,

η_{con}: Concentration polarization of the anode and cathode.

The Nernst equation is also an open-circuit voltage (OCV); its value is related to the gas composition, the operating pressure, the operating temperature… etc. It is defined by Eq (III.24), [15–18]:

$$E_{Nernst} = -\frac{\Delta G}{2F} + \frac{RT}{2F}\ln\left(\frac{P_{H_2}.P_{O_2}^{0.5}}{P_{H_2O}}\right) \quad \textbf{(III.24)}$$

T: the operating temperature;

P: The partial pressures of reacting species;

R : The gas constant;

F : Faraday number;

ΔG: The Gibbs free energy.

Where $P_{H_2O} = pX_{H_2O}$, $P_{H_2} = pX_{H_2}$, $P_{O_2} = pX_{O_2}$

p: The atmospheric pressures;

$X_{H_2O}, X_{H_2}, X_{O_2}$: The mass fraction of steam, hydrogen and oxygen, respectively.

III.5.1 Activation Polarization

The activation overpotential is caused by sluggish electrode kinetics at the reaction site although it affected the temperature. In order to obtain the activation can be calculated as[39]:

$$\eta_{act} = \frac{RT}{\alpha nF} Ln \frac{j}{j_0} \quad \textbf{(III.25)}$$

α : The electron transfer coefficient,

n: The electron number

j_0: The exchange current density.

III.5.2 Ohmic polarization

The Ohmic losses η_{Ohm}: are due to the electrical resistances of the three solid parts of the cell. According to Ohm's law, the ohmic losses are expressed as follows by[93][86]:

$$\eta_{Ohm} = jR_{Ohm} \quad \textbf{(III.26)}$$

j: The current density

R_{Ohm} :The ohmic resistance of the cell and can be calculated as[86]:

$$R_{Ohm} = \frac{e_{an}}{\sigma_{an}} + \frac{e_{ele}}{\sigma_{ele}} + \frac{e_{cat}}{\sigma_{cat}} \quad \textbf{(III.27)}$$

$e_{an}, e_{cat}, e_{ele}, \sigma_{an}, \sigma_{cat}, \sigma_{ele}$ Are respectively represents the thickness and conductivity of electrodes and electrolyte used in our study, **Table III.4**

Part	Anode	Cathode	Electrolyte
Conductivity $\sigma(\Omega.m^{-1})$	$\frac{9.0 \times 10^7}{T} e^{-1150/T}$	$\frac{4.0 \times 10^7}{T} e^{-1200/T}$	$3.34\times 10^4 e^{-10300/T}$

Table.III.4: Electrical conductivity used [8, 24, 25]

III.5.3 Concentration polarization

The concentration overpotential is caused by the transport of reactant species through porous electrodes. In the SOFC cell, the concentration overpotential can be defined as[39]:

$$\eta_{Con} = \frac{RT}{nF} ln\left(1 - \frac{j}{j_0}\right) \quad \textbf{(III.28)}$$

The cell performance is given by voltage and power density. The latter are a function of the current density:

$$P(j) = V_{cell}.j \quad \textbf{(III.29)}$$

III.5.4 Charge transport

The electrons and ions transport should be considered in SOFC to solve the charge conservation equation. Where the electronic charge occurs in the electrodes and interconnectors. While ionic charge only exists in the electrodes and electrolyte. Thus governing equations for the charge by Ohm's law are as follows [11–14, 27]:

Electronic charge balance

Anode electrode layer[27] $\nabla.(\sigma_a \nabla \emptyset_{el}) = -J_a A_V$ **(III.30)**

Cathode electrode layer[27] $\nabla.(\sigma_c \nabla \emptyset_{el}) = -J_c A_V$ **(III.31)**

Ionic charge balance:

Electrolyte layer[27] $\nabla.(\sigma_{ele} \nabla \emptyset_{i0}) = 0$ **(III.32)**

Anode electrode layer[27] $\nabla.(\sigma_a \nabla \emptyset_{i0}) = J_a A_V$ **(III.33)**

Cathode electrode layer[27] $\nabla.(\sigma_c \nabla \emptyset_{i0}) = J_c A_V$ **(III.34)**

Where, σ_a and σ_c(s m^{-1}) are the electrical conductivity for anode and cathode, respectively. While J_a and J_c are the volumetric current densities of anode and cathode; based on the Butler-Volmer equation shown in Eqs. (III.15) and (III.16).

III.6 Boundary conditions

On all the external surfaces and all the directions, the boundary conditions are of the Neumann type, except at the entrance of the channels where we take a constant temperature and mass fraction of species whose conditions are of the Dirichlet type.

Refer to **Figure III.5**, at the inlet channel (anode and cathode), mass flow, temperature, and mass fraction of species were specified. At the outlet channel (anode and cathode) the pressure is specified. At the channel walls and extremities MEA considered adiabatic surfaces. At the intersection between the gas channel and electrodes, the cell potential was defined. At the cathode side, we set $\emptyset_{elec} = V_{cell}$, and at the anode side $\emptyset_{elec} = 0$

Nevertheless, cell zone conditions must be defined for each zone. Besides, to converge the solution it is very necessary to determine the electrode channel-gdl intersection as an interface to pass the flow through the porous zone. Details regarding the type of the zones presented in **Figure III.5** is shown in **Table III.5**.

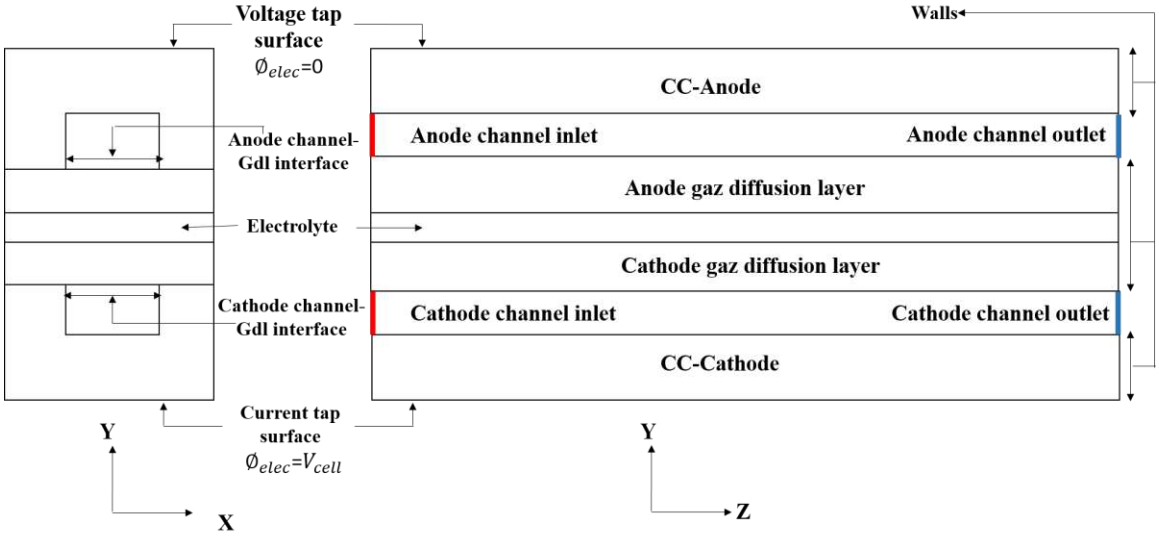

Figure III.5: Boundaries of the cell for the 3D model.

Table III.5: Cell zone condition.

Zone name	Zone type	Porous?
Anode CC	Solid	-
Cathode CC	Solid	-
Anode GDL	Fluid	Yes
Cathode GDL	Fluid	Yes
Anode gas channel	Fluid	No
Cathode gas channel	Fluid	No

III.7 Numerical simulation

III.7.1 Choice of the simulation tool

Fuel cell designing and studying have two ways, the first one is an experimental study and the second is modeling and numerical simulation. The experimental study is more trusted but very costly and requires special laboratory. Numerical simulation is less in cost compared to the experimental. Among the different modeling strategists and tools available, the computational fluid dynamic is a prevailing special interest.

It is very interesting to have a simulation environment that includes the possibility of coupling different physical phenomena, this is the case of our studied model. We chose the Ansys Fluent which presents different physical modules, among which we find fluid mechanics, heat transfer, electricity, electromagnetism, chemistry, and structural mechanics. It also offers the possibility of combining several physical phenomena during the same numerical simulation.

This numerical program uses the finite volume method to model a wide variety of physical phenomena characterizing a real problem. It will also be a design tool thanks to its ability to manage complex geometries.

III.7.2 Steps of the Simulation under ANSYS Fluent

The modeling and numerical simulation process under ANSYS Fluent involve several steps as shown in **Figure III.6.**

- ✓ Geometry creation
- ✓ Mesh generation (choose the size of the elements to use for the mesh as well as the different types of mesh that exist)
- ✓ Choose the initial and boundary conditions of your model for each physics used.
- ✓ Select the appropriate material(s) from the model
- ✓ Solving technique (set solver parameters and launch calculations in the studies directory)
- ✓ Post processing (display the desired results in the most meaningful way in the result directory.)

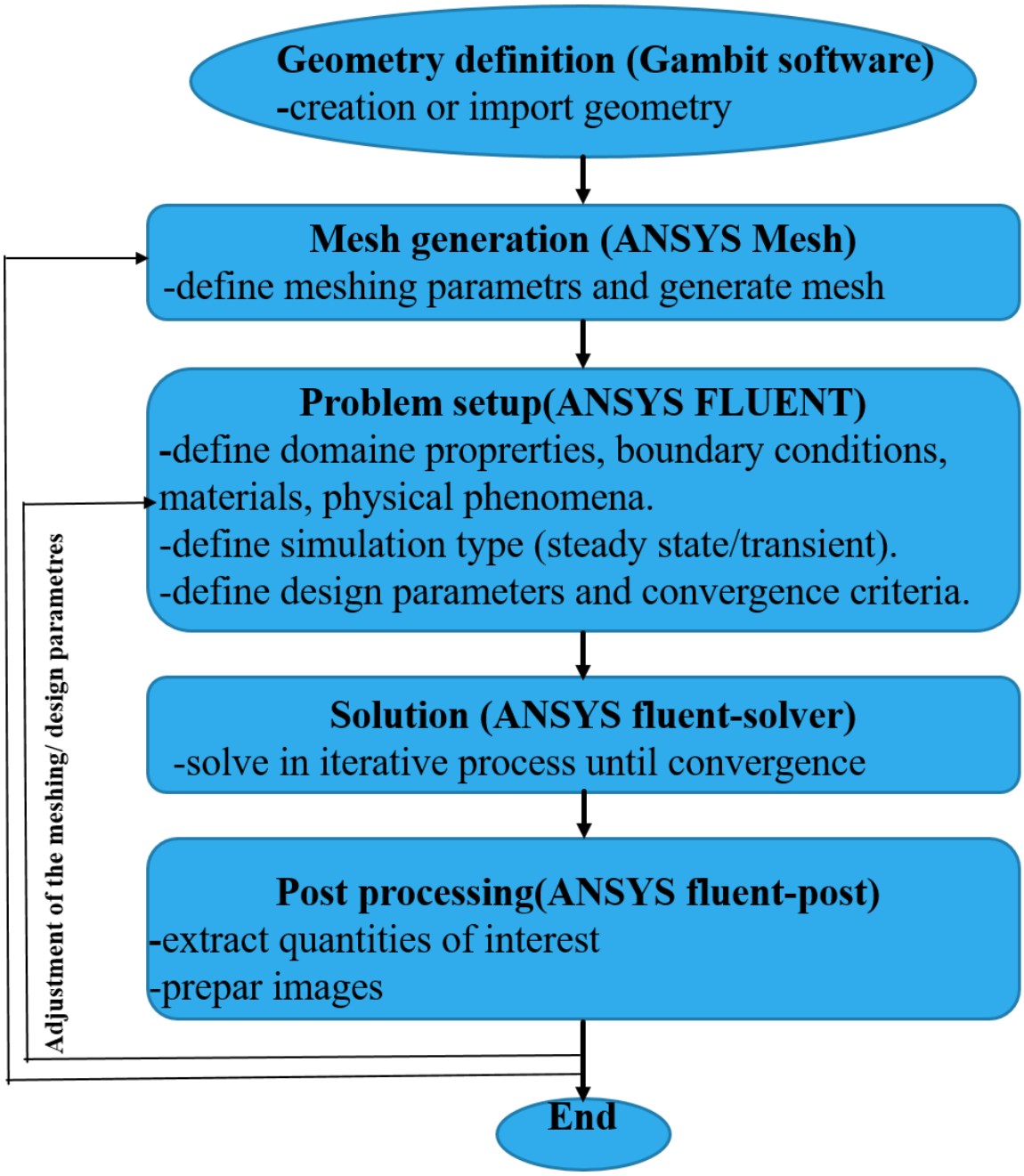

Figure III.6: Simulation steps under ANSYS Fluent.

Conclusion

In this chapter, we elaborated on the phenomena which govern the operation of the cell and we developed the various mathematical equations in the various parts of the selected cell.

The bibliographical study allowed us to choose the physical and mathematical model governing the heat and mass transfer phenomenon in the different parts of the SOFC stack. The mathematical model is more interested in the different types of heat source; due to Ohmic loss, heat source due to loss of activation, heat source due to loss of concentration, and heat source due to chemical reactions as well as to the dimensions of the electrodes and the electrolyte. In this chapter, we expose the numerical simulation procedure adopted for the resolution of these governing equations

Chapter IV: Interpretation and discussion of results

Introduction

Several studies have shown that the performance of SOFC fuel cells is strongly influenced by operating conditions such as temperature, pressure, and structural parameters such as electrode and electrolyte thickness and porosity. Therefore, SOFC fuel cell performance analysis should consider these parameters to achieve optimal operation.

In this chapter, we present a complete set of results according to 3 dimensions with a CFD calculation tool, then we will show the results of our modeling and numerical simulation concerning the evolution of the various parameters characterizing the performance of the SOFC fuel cell. The results that will be obtained to be classified into two parts:

Part A will allow:

-Evaluated the effect of temperature, pressure, and porosity field is made according to the effect of different types of heat sources: This is the heat source due to Ohmic, activation, and concentration and that due to the reaction chemical. In order, to illustrate the importance of the various overpotentials on the cell performance at deferent parameters.

-The impact of fuel utilization and the change of the hydrogen mass fraction along the anode flow channel at various parameters

-Evaluated the influence of supporting layer thickness (AS, CS, and ES) on the polarization and power density curves and studied the overpotentials at three different structures with the impact of fuel utilization

Part B will allow

-To propose new geometry to improve the performance of the fuel cell and evaluated the losses.

Part A: Study of the effects of operating parameters on the performance of the SOFC cell and optimization of operating conditions

IV.1 Description the geometry

The proposed AS-SOFC fuel cell for the current study is shown in **Figure IV.1**. The geometrical SOFC single cell described in the work was executed in the commercial software GAMBIT (Version 2.4.6). It is composed of the fuel-flow channel, anode gas diffusion layer (A-GDL), anode catalyst layer (A-CL), electrolyte, cathode catalyst layer (C-CL), cathode gas diffusion layer (C-GDL), air-flow channel, and anode and cathode collectors. We will be interested in a supposedly homogeneous temperature equal to T=1123 K and the geometric configuration adopted is the supported anode. All details about the dimensions and cell components are presented in **Table IV.1**[78]. At the cathode part, oxygen particles are distributed from GDL to the electrode/electrolyte interface (triple phase boundary (TPB)), where they are reduced and pass through the electrolyte to the anode as expressed in Eq. (IV.1). At the anode part, hydrogen gas particles are distributed from GDL through TPB where they find oxygen ion and react with them to form water and produce an electron as expressed in Eqs. (IV.2) and (IV.3).

$$\frac{1}{2}O_2 + 2e^- \rightarrow O^{2-} \quad \textbf{(IV.1)}$$

$$H_2 + O^{2-} \rightarrow H_2O + 2e^- \quad \textbf{(IV.2)}$$

$$H_2 + \frac{1}{2}O_2 \rightarrow H_2O + \text{Heat} \quad \textbf{(IV.3)}$$

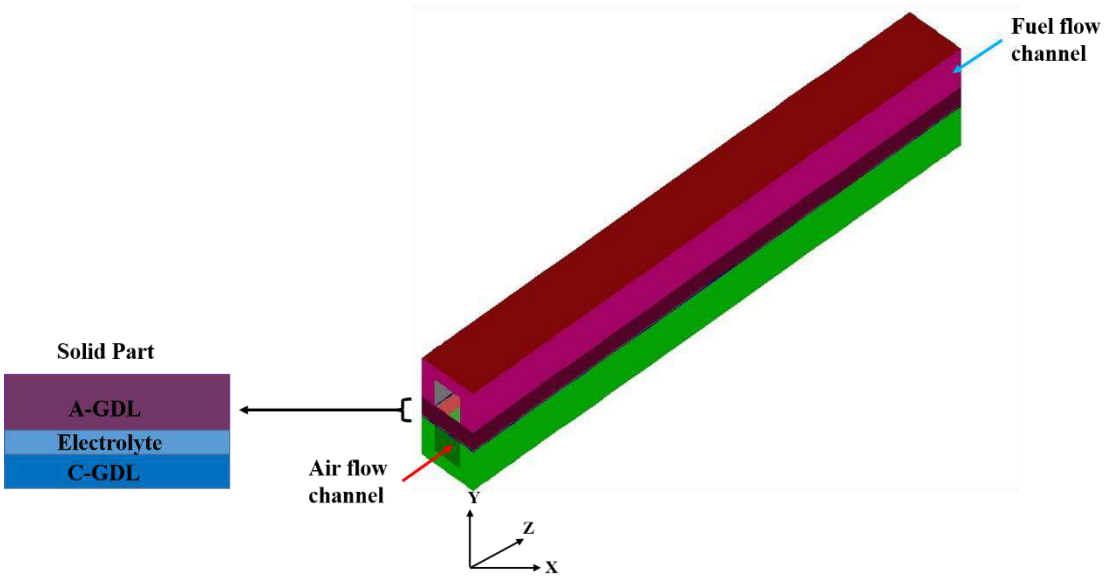

Figure IV.1: Schematic view of SOFC cell designs.

Table IV.1: Geometrical Parameters.

Zone	Dimension
Cell width (mm)	2
Cell length (mm)	19
Anode thickness (mm)	0.700
Cathode thickness (mm)	0.05
Electrolyte thickness (mm)	0.01
Channel height (mm)	1
Channel width (mm)	1
Current collector height (mm)	1.5

IV.1.1 Parametric study

Among the most tedious parts of model development is determining the correct parameters for the model, which will ultimately determine the accuracy of the results. Furthermore writing the model requires knowledge of the thermophysical properties of the various materials constituting the core of the cell (Figure IV.2). All the parameters used for our modeling are listed in the following **Table IV.2**.

Table IV.2: Specifications of the Case Study.

		Value	Unit	Ref
Anode GDL (Ni-YSZ)	Porosity	0.3		[96]
	specific heat	377	$J\ kg^{-1}K^{-1}$	[97][94]
	Thermal conductivity	11	$W\ m^{-1}K^{-1}$	[98]
	Density	4200	$kg\ m^{-3}$	[96][97]
	Anodic transfer coefficient	2		[96][94]
	Cathodic transfer coefficient	1		[96][94]
	Electron conductivity	$\frac{9.0 \times 10^7}{\mathrm{T}} \mathrm{e}^{-1150/\mathrm{T}}$	$s\ m^{-1}$	[99]
Cathode GDL (LSM)	Porosity	0.3		[96]
	Specific heat	377	$J\ kg^{-1}K^{-1}$	[97] [98]
	Thermal conductivity	2.37	$W\ m^{-1}K^{-1}$	[98]
	Density	6350	$kg\ m^{-3}$	[96][97]
	Anodic transfer coefficient	1.4		[96][94]
	Cathodic transfer coefficient	0.6		[96][94]
	Electron conductivity	$\frac{4.0 \times 10^7}{T} e^{-1200/T}$	$s\ m^{-1}$	[99]
Electrolyte (YSZ)	Specific heat	2000	$J\ kg^{-1}K^{-1}$	[97][98]
	Thermal conductivity	2.7	$W\ m^{-1}K^{-1}$	[98]
	Density	6010	$kg\ m^{-3}$	[96][97]
	Electronic conductivity	$3.34\times 10^4 e^{-10300/T}$	$s\ m^{-1}$	[99]
Interconnect (metal)	Specific heat	300	$J\ kg^{-1}K^{-1}$	[98]
	Thermal conductivity	2.2	$W\ m^{-1}K^{-1}$	[98]
	Density	4640	$kg\ m^{-3}$	[96][98]
	Electron conductivity	$\frac{9.3 \times 10^5}{T} e^{-1100/T}$	$s\ m^{-1}$	[99]

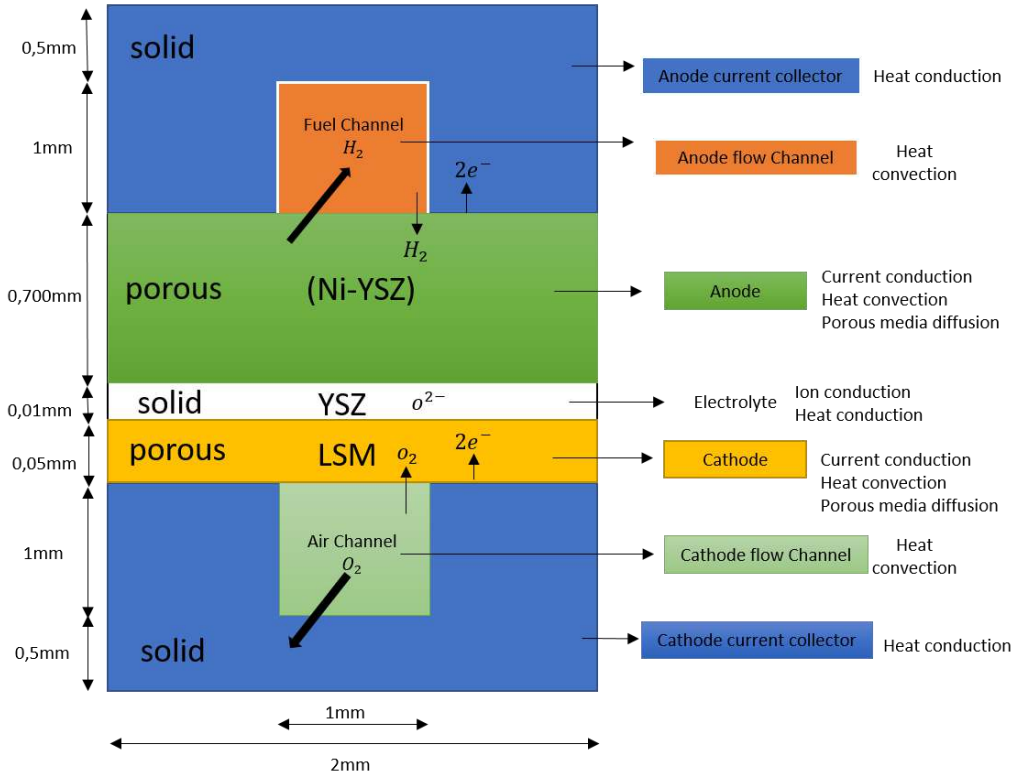

Figure IV.2: Solid oxide fuel cell parts composition.

IV.1.2 Boundary condition

Boundary conditions must be defined for SOFC fuel cell simulations, based on the problem specification. **Table IV.3** gives the input parameters of our fuel cell model.

Table IV.3: Inlet Boundary Conditions for the Anode and Cathode Channels.

	Value	Unit	Ref
Anode mass flow rate	1.141×10^{-8}	$kg\ s^{-1}$	[78]
Cathode mass flow rate	2.287×10^{-7}	$kg\ s^{-1}$	[78]
Anode inlet temperature	1123	K	
Cathode inlet temperature	1123	K	
Anode flow Species(mass fraction)	97% H_2 , 3% H_2O	%	[96]
Cathode flow Species(mass fraction)	100% O_2	%	[100]
External boundaries	Adiabatic		[101][102]

IV.2 Mesh independency

Mesh independency study is the expression utilized to explain the improvement of results by utilizing smaller cell sizes for the calculation to get high quality and acceptable for the simulation study.

In this study, three different meshes are presented and was done by an ANSYS WORKBENCH MESH. The three cases mesh as: coarse mesh (A) with a 76,800 hexahedral cells, medium mesh (B) with a 194,560 hexahedral cells, and fine mesh (C) with a 304,000 hexahedral cells. The simulation was run for each case and compared with experimental data obtained by [103] with the same parametric study listed in Table IV.2.**Figure IV.3** indicates that the polarization curves of meshes B and C are less than 1%. Whereas, Mesh C gives an agreeable precision and is sufficiently fine compared with the experimental data.

The computational time for each case without previous initial data starting condition until there was no change in the current density for cell voltage 0.7 V is show in **Table IV.4.**

Considering the accuracy, the mesh independence analysis and computational time. The mesh C (304,000 hexahedral cells) has been fixed in the current study.

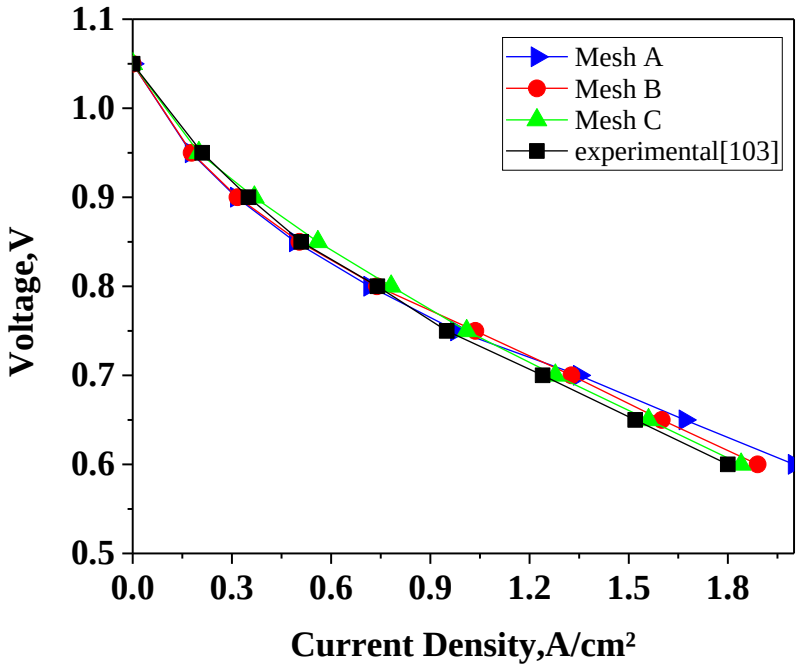

Figure IV.3: Mesh independency analysis and verification.

Table IV.4: computational time for different mesh cases at 0.7V

No. of cells	76,800 hexahedral cells (Mesh A)	194,560 hexahedral cells (Mesh B)	304,000 hexahedral cells (Mesh C)
Current Density at 0.7V	1.351322	1.322505	1.201916
Error %Compared to Numerical results by Ref [78]	13.33	11.36	4.16
Solving time (hour)	7	14	25

IV.3 Model validation

To test the present modeling, the simulation results are compared to the numerical and the experimental data reported by[78][103]. For anode supported SOFC cell, the dimension, and cell components are presented in Table IV.1 and 2. These values are exactly the same as those given by[78][103]. The validation model shows a good agreement between our model and data obtained by [78][103] as presented in **Figure IV.4**. Nevertheless, the

simulation showed different values of current density at lower values of voltage. This is most probably due to errors and hypotheses associated with the SOFC model.

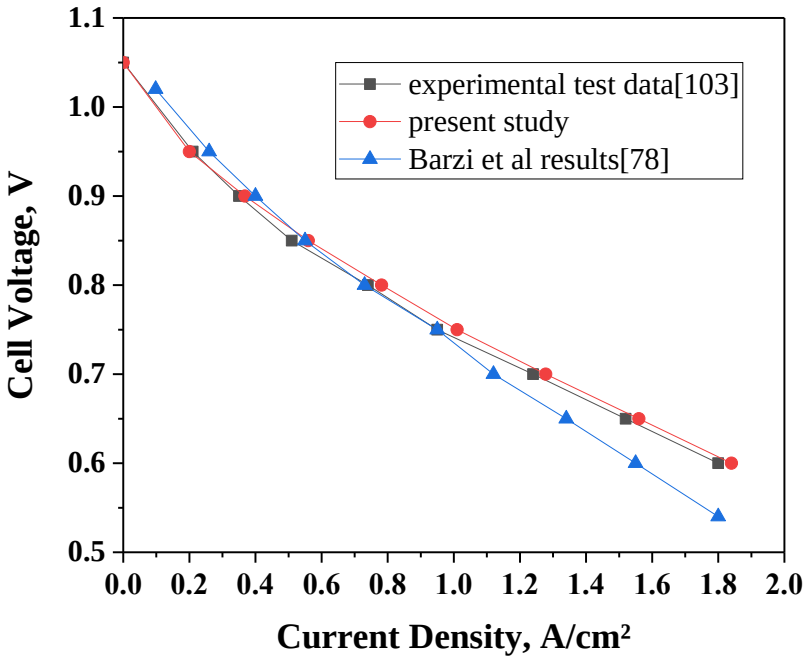

Figure IV.4: j-V curve comparison between present results and both the experimental and the numerical results obtained by[78][103].

IV.4 Results and interpretations

IV.4.1 Operating temperature effect

IV.4.1.1 Activation, Ohmic, and concentration overpotentials at deferent temperature

The performance of SOFC fuel cells is influenced by different processes and operating parameters such as temperature. In the simulation model, all overpotentials, activation, Ohmic, and concentration were measured separately, using the appropriate equations, and were investigated at various temperatures. The Ohmic and activation overpotentials of a SOFC fuel cell operating at 1023, 1123, and 1173 K are shown in **Figure IV.5** and **Figure IV.6**, respectively. As depicted, the ohmic overpotential was reduced with rising temperature due to the influence of temperature on the ionic conductivity of electrolyte

material (YSZ). The most ohmic overpotential appears at 1023 K, though the electrolyte is thin (0.01mm). Consequently, to decrease the Ohmic overpotential, the thickness of the electrolyte must become small and have a great oxygen ion conductivity as reported in the literature. Additionally, it was observed that the activation overpotential was reduced with decreasing temperature. The electrodes displayed more reactive at a greater temperature, thus, the activation overpotential rises. As displayed in **Figure IV.6**. Accordingly, the concentration overpotential rises with temperature. But the difference is approximately low. As presented in **Figure IV.7**.

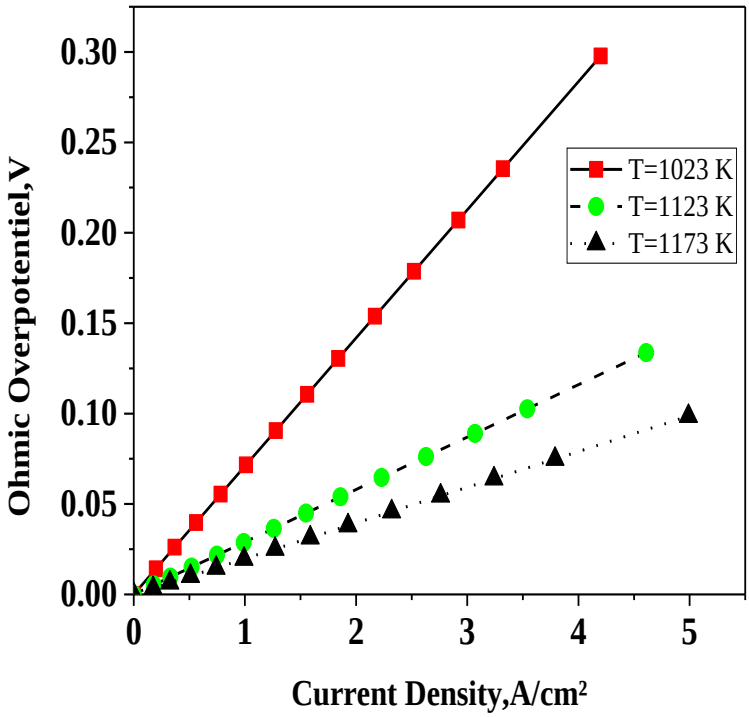

Figure IV.5: Effect of Ohmic overpotentials at deferent temperature.

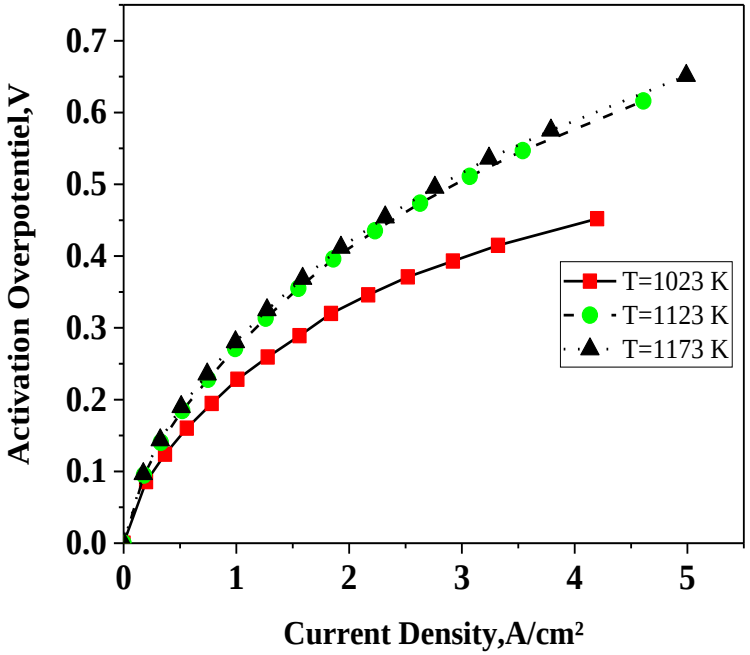

Figure IV.6: Effect of activation overpotentials at deferent temperature.

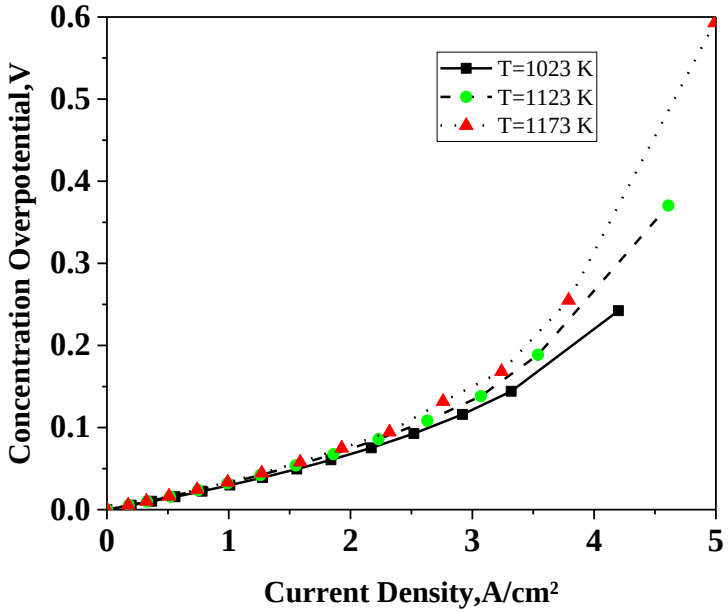

Figure IV.7: Effect of concentration overpotentials at deferent temperature.

IV.4.1.2 Performance at a deferent temperature

Simulation analysis was also carried out to investigate the effect of temperature on the performance of SOFC fuel cell. The predicted performance curves obtained for the operating temperature from 1023 K to 1173 K are shown in **Figure IV.8**, the maximum power densities are 1.328, 1.416, and 1.516 W/cm² at 1023, 1123, and 1173 K respectively. This tendency qualitatively corresponds to the literature; that is due to the electrochemical processes occurring at the electrodes and these effects accelerate the electrode kinetics and chemical reactions when the temperature increases.

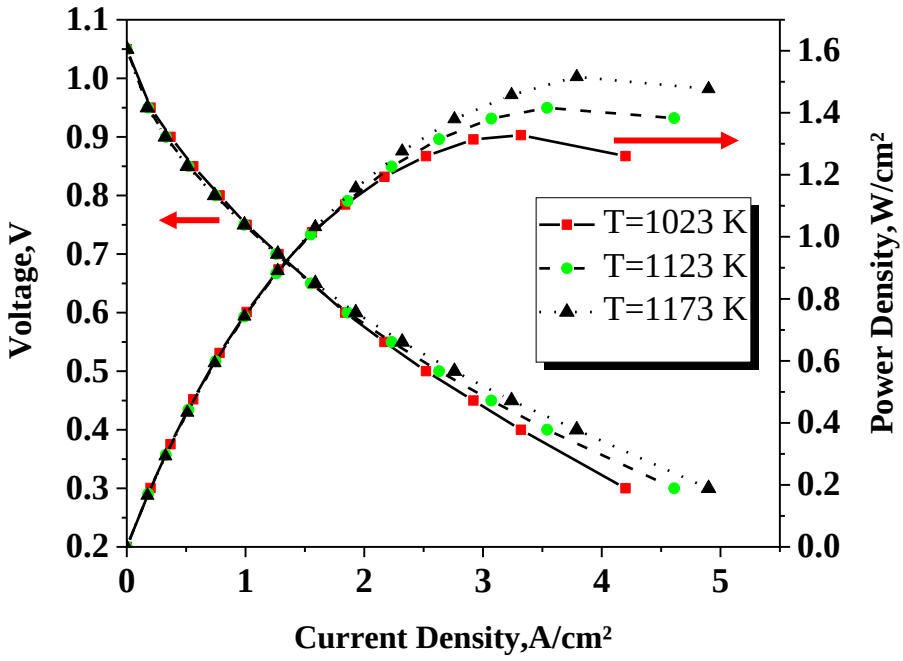

Figure IV.8: polarization characteristics and power density at deferent temperature.

IV.4.1.3 Effect of fuel utilization at a deferent temperature

Figure IV.9 shows the change of fuel utilization factor with power density at various temperatures. As expected, it was found that the fuel utilization factor U_f has a notable impact on cell performance. With increasing power density, the factor fuel utilization has to increase that what mean also the current density increase referring to Figure IV.8 and constantly the voltage decrease. Moreover, the fuel utilization improves with raising the

temperature of the fuel cell, because more of hydrogen quantity is consumed in the electrochemical reactions at a greater operating temperature.

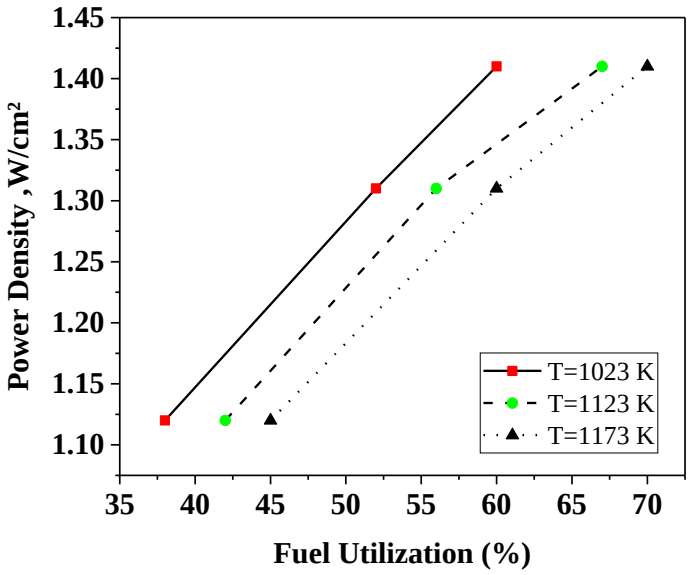

Figure IV.9: Fuel utilization at different temperatures.

IV.4.1.4 H_2 mass fraction at deferent temperatures

Figure IV.10 presents the change of the hydrogen mass fraction on the anode channel length at various temperatures. The H_2 starts at Z=19mm and O_2 starts at Z=0, (counter flow). The hydrogen mass fraction diminished at the anode channel due to electrochemical reactions continuous. The maximum value of hydrogen mass reduces as the temperature rises. According to Figure IV.9, the highest hydrogen consumption produces the highest value of fuel utilization for high temperatures. It is observed that the fuel utilization for the case of T=1173 K is higher than all other cases. Furthermore, fuel utilization for the case of T=1123 K is higher than the case of T=1023K. The higher fuel utilization at higher temperatures is linked to the higher activity of electrochemical reactions that achieve a greater current density compared with other cases.

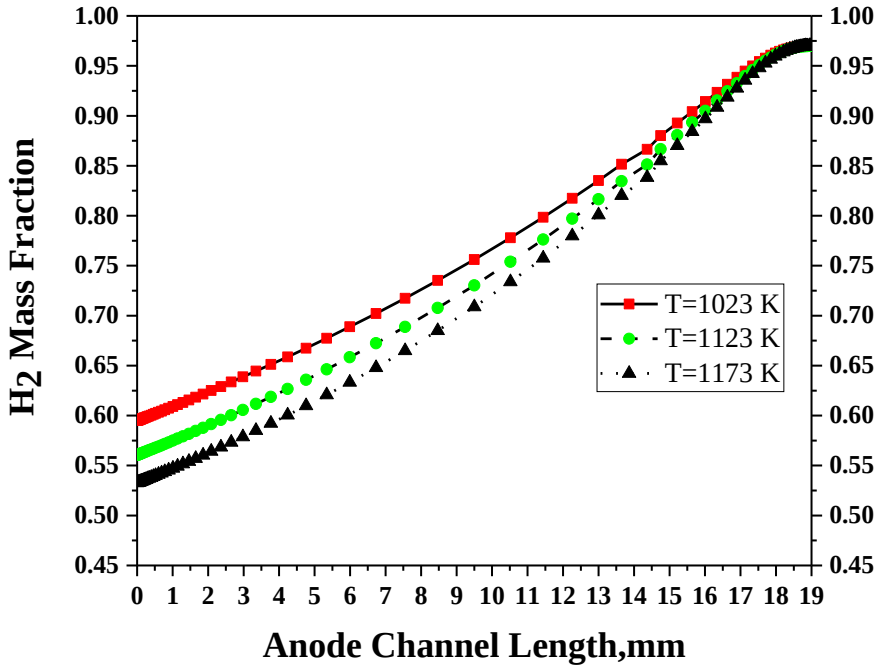

Figure IV. 10: Variation of H_2 mass fraction distribution along the anode channel for different temperatures, at 0.6 V.

IV.4.1.5 H_2O mass fraction at deferent temperatures

Figure IV.11 presents the variation of the water mass fraction at the anode channel with various temperatures. As observed, the highest value of water fraction at the anode channel rises as the temperature rises. Due to the greater inlet fuel temperature, the electrochemical reaction rate is improved and more water is carried at the cell outlet.

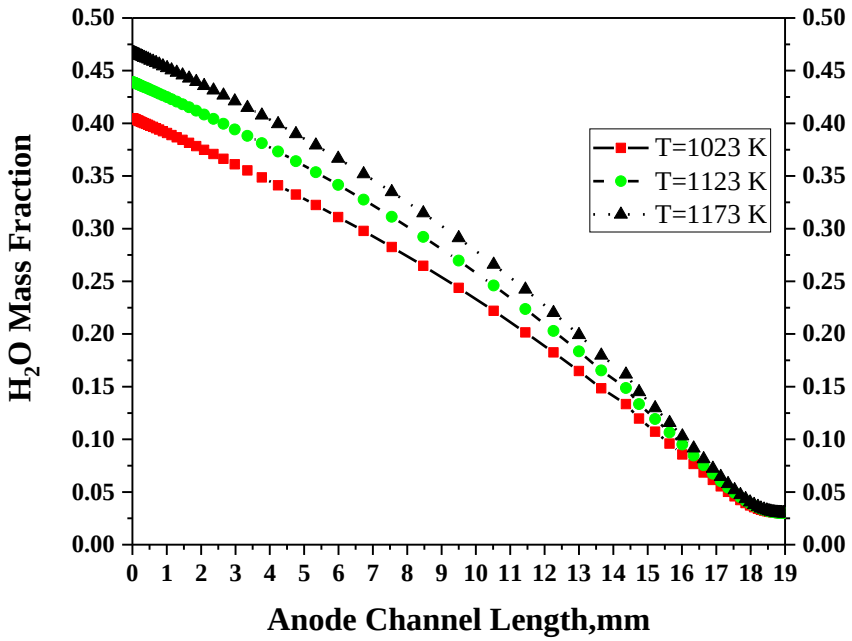

Figure IV.11: Variation of H_2O mass fraction distribution along the anode channel for different temperatures, at 0.6 V.

IV.4.2 Operating pressure effect

IV.4.2.1 Performance and concentration overpotential at various pressure

Figure IV.12 gives the effect of the pressure on the cell polarization curve. Where the operating pressure is changed from 1 atm to 3 atm while all other parameters are held at base conditions. The current density improves when there is an increment in gas pressure. Considering the point of maximum cell efficiency 0.4V and 1 atm of pressure, the power density obtained was 1.416 W/cm². For the gas pressures 2 and 3 atm the power density takes the values 1.668 and1.788 W/cm² respectively; this only corresponds to a relative increment due to pressure variation. The best response of the fuel cell was observed at 3 atm. This last is due to a gas diffusivity raise, improving the exchange current density and the performance of the SOFC fuel cell. Moreover, the concentration overpotential is decreased as shown in **Figure IV.13**.

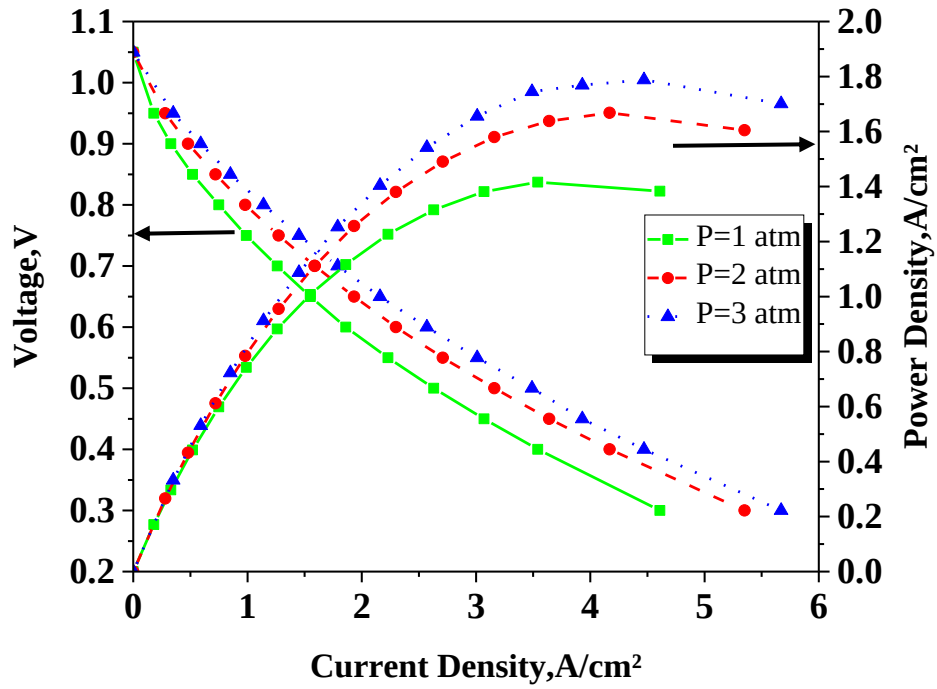

Figure IV.12: polarization characteristics and power density at deferent pressure.

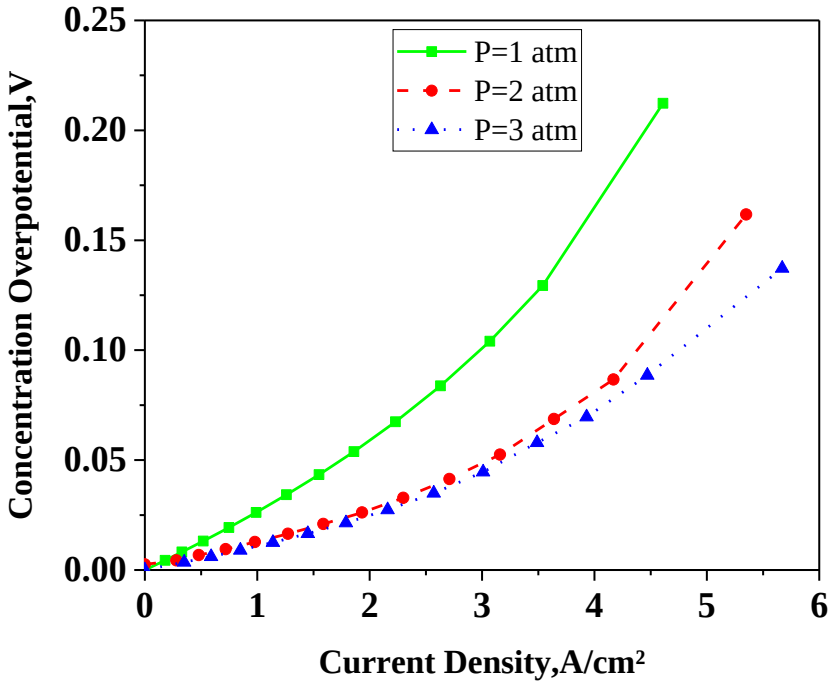

Figure IV.13: Effect: of concentration overpotential at deferent pressure.

IV.4.2.2 Effect of fuel utilization at various pressure

The variations of fuel utilization factor with power density at different pressures are presented in **Figure IV.14**. As expected it was found that, with increasing power density, the fuel utilization has to increase. That is what mean also the current density increase referring to **Figure IV.12** and constantly the voltage decrease. Moreover, the fuel utilization increases with increasing the pressure of the SOFC fuel cell, the increment in fuel utilization may be because of a better supply of reactants at higher pressures.

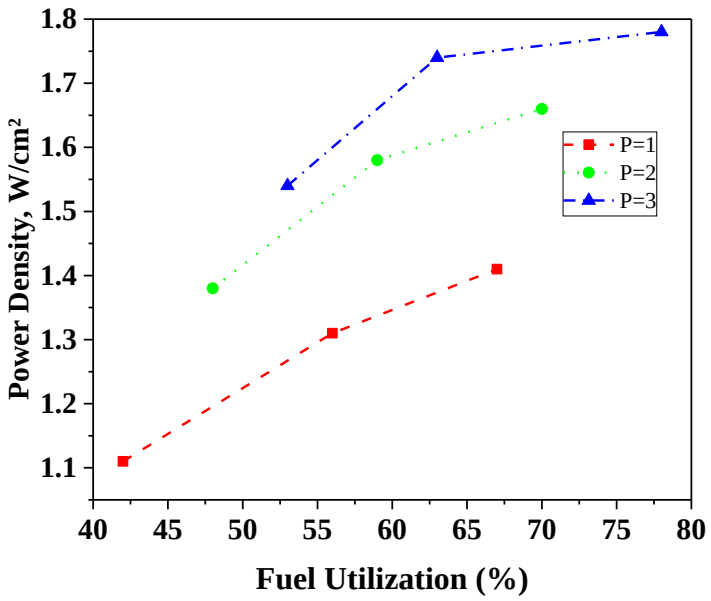

Figure IV.14: Fuel utilization at different pressure.

IV.4.2.3 H_2 mass fraction at various pressure

The counter flow channel at high pressure shows a better mass fraction of the reactants species. **Figure IV.15** presents the change of the hydrogen mass fraction along the anode flow channel at various pressures with T=1123 K. The mass fraction of hydrogen diminishes along the anode channel because hydrogen is reacted by the electrochemical reaction along the length of the channel. It was found that at 3 atm provides a higher level of hydrogen mass fraction consumption. The highest value of hydrogen mass fraction consumed are 40%, 46% and 51% for the operating pressure 1, 2, and 3 atm respectively.

Due to an increment in pressure, hydrogen mass fraction consumption into the GDL increases.

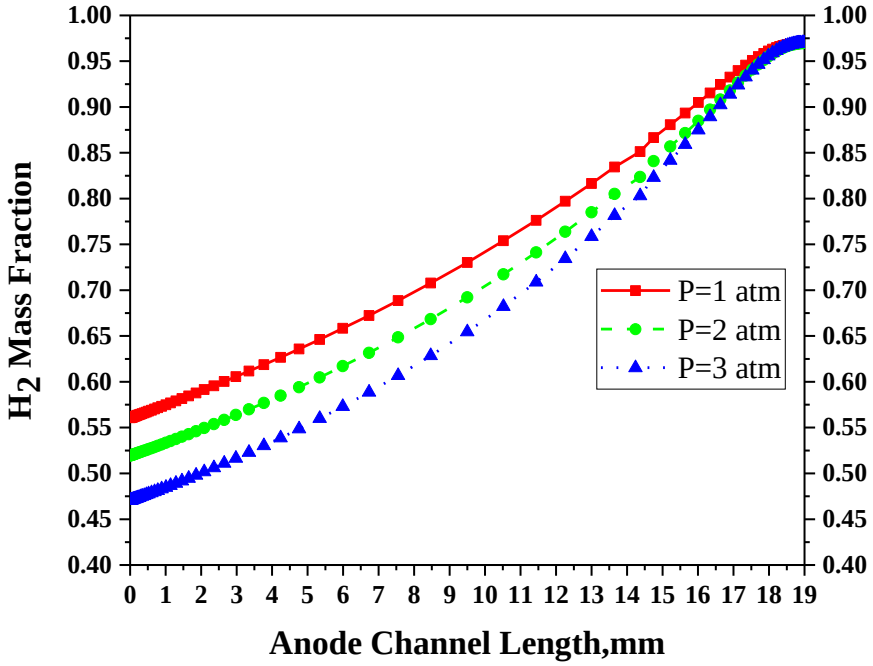

Figure IV.15: Variation of H_2 mass fraction distribution along the anode channel for deferent pressure, at 0.6 V.

IV.4.2.4 H_2O mass fraction at various pressure

On the other hand, increasing hydrogen mass fraction consumption increases water mass fraction produced as shown in **Figure IV.16**.The increase in water mass fraction produced is due to an increase in reaction rate, which is favored by increased operation pressure.

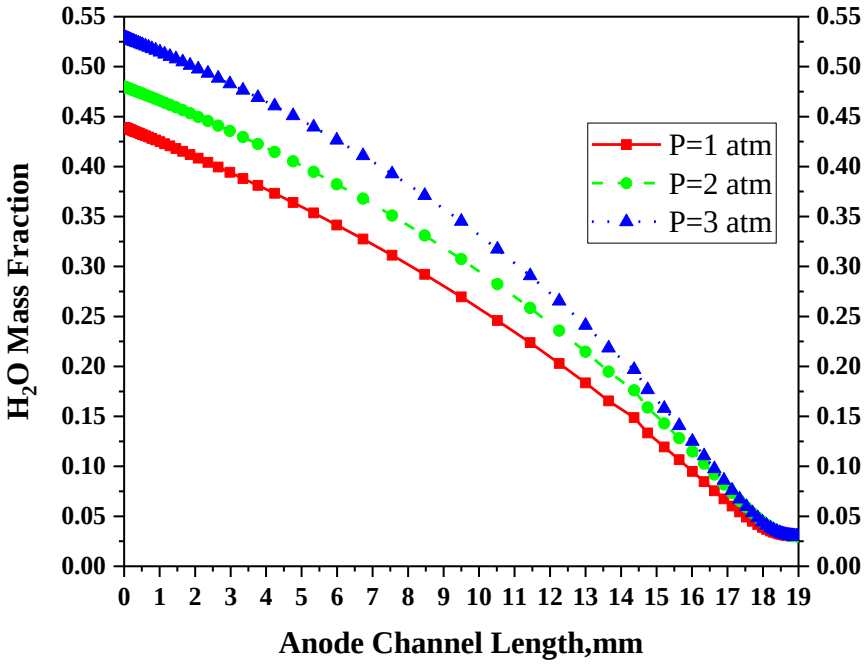

Figure IV.16: Variation of H_2O mass fraction distribution along the anode channel for deferent pressure, at 0.6 V.

IV.4.3 Effect of porosity

IV.4.3.1 Power density for deferent porosity

Figure IV.17 gives the effect of the porosity on the cell polarization curve. Where the porosity is changed from 0.3 to 0.003 while all other parameters are held at base conditions. It can be observed that the maximum power density is 1.41 W/cm^2, 1.37 W/cm^2, and 1.20 W/cm^2 for porosity 0.3, 0.03, and 0.003, respectively. As a result, the performance of an anode-supported SOFC improves as the porosity raise which results in increasing the permeability. This is due to mass transport limitations occurring at higher current densities. Moreover, higher porosity leads to a better flow of reacting gases.

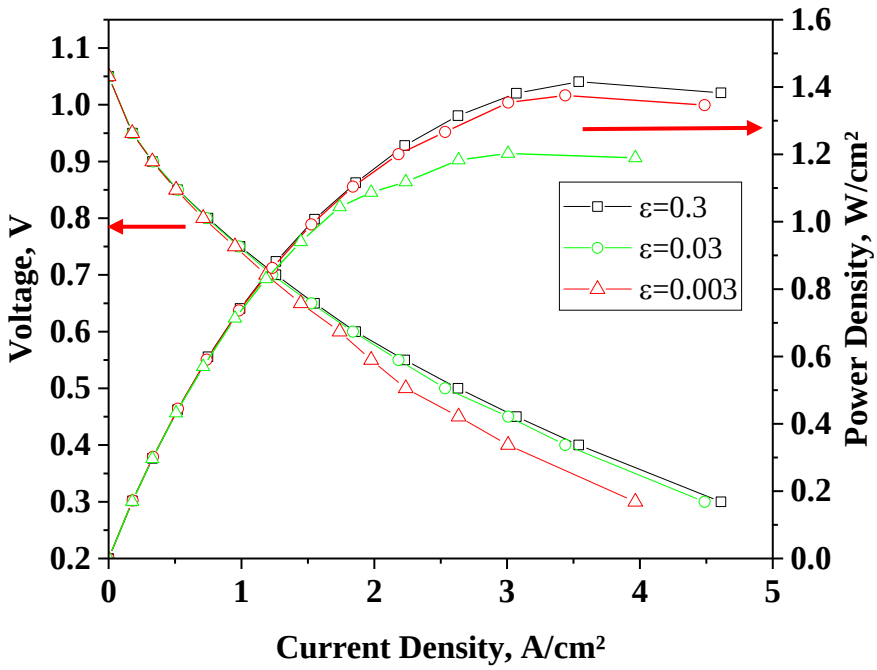

Figure IV.17: polarization characteristics and power density for deferent porosity.

IV.4.3.2 H_2 and H_2O mass fraction for deferent Porosity

Figures IV.18 and **Figure IV.19** represent the profiles of hydrogen and water mass fraction along the anode channel for different porosity values, respectively. The increase in the value of the porosity leads to an easy circulation of hydrogen at the level of the anode. Thus, facilitating the passes of water produced and providing the best diffuse of reactants into the reaction sites as shown in Figure IV.19.

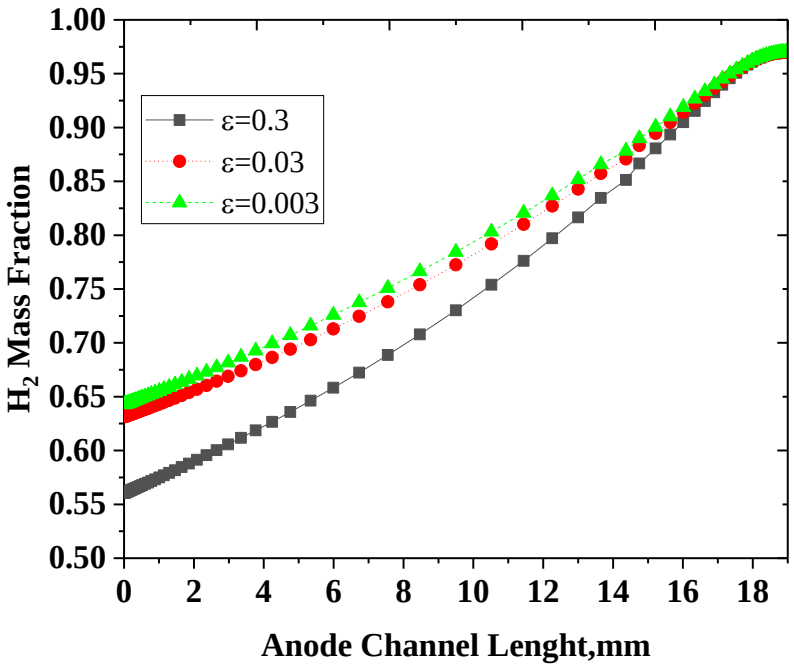

Figure IV.18: Variation of H_2 mass fraction distribution along the anode channel for deferent porosity, at 0.6 V.

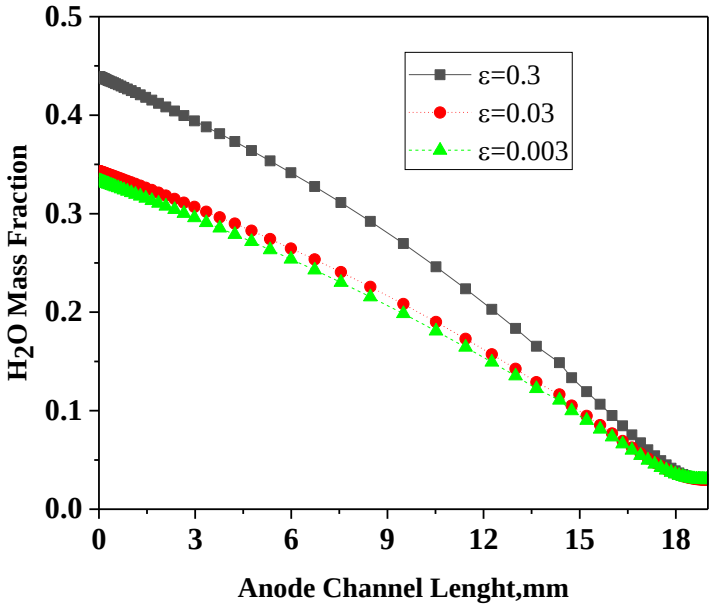

Figure IV.19: Variation of H_2O mass fraction distribution along the anode channel for deferent porosity, at 0.6 V.

IV.4.3.3 Effect of fuel utilization for deferent porosity

The curve of fuel utilization of various porosity is presented in **Figure IV.20**. Improved fuel utilization can be obtained at higher porosity. The increment in fuel utilization maybe because of the best use of reacting gases at higher porosity and thus higher permeability.

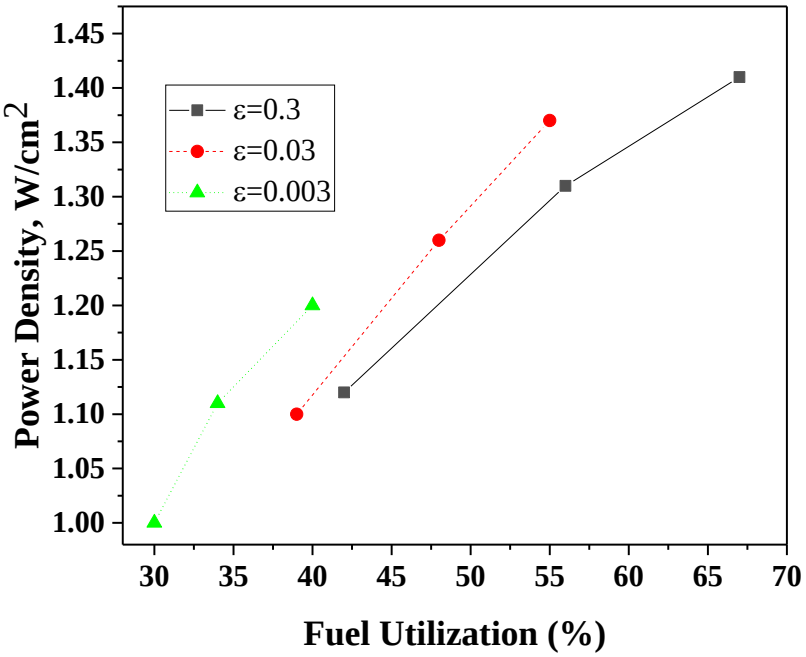

Figure IV.20: Fuel utilization at different porosity.

IV.4.4 The influence of anode/cathode and electrolyte thickness

In order to investigate the influence of thickness on the cell performance, three different SOFC cells were suggested: anode supported (AS), cathode supported (CS), and electrolyte supported (ES) each one is tested by three different thicknesses as illustrated geometrically in **Table IV.5**.

Table IV.5: the Geometrical description of the PEN layers of the SOFCs.

Thickness (mm)									
	Anode supported			**Cathode supported**			**Electrolyte**		
Anode GDL	0.3	0.7	0.9	0.05			0.05		
Cathode GDL	0.05			0.3	0.7	0.9	0.05		
Electrolyte	0.01			0.01			0.2	0.3	0.5

IV.4.4.1 Effect of anode and cathode thickness on the cell performance

The influence of AS and CS on the polarization and power density curves (performance) is tested. The results for supporting layer thickness are shown in **Figure IV.21** and **22** respectively. As can be seen, the cell performance improves as the supporting layer thickness of AS and CS diminishes. That is due to when the anode/cathode thickness has reduced the activation and concentration of the cell diminished.

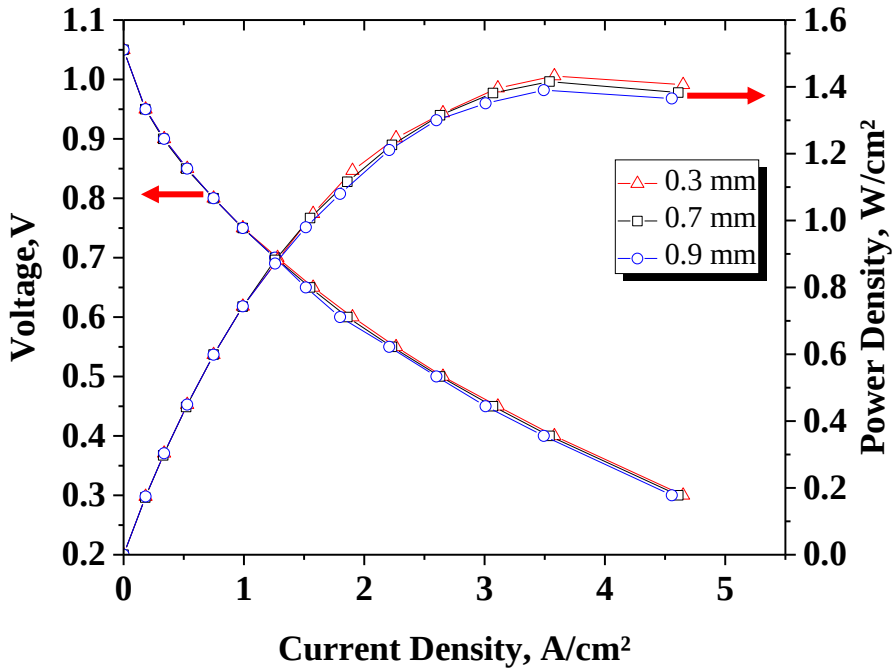

Figure IV.21: The influence of anode supported layer thickness on the performance of cell.

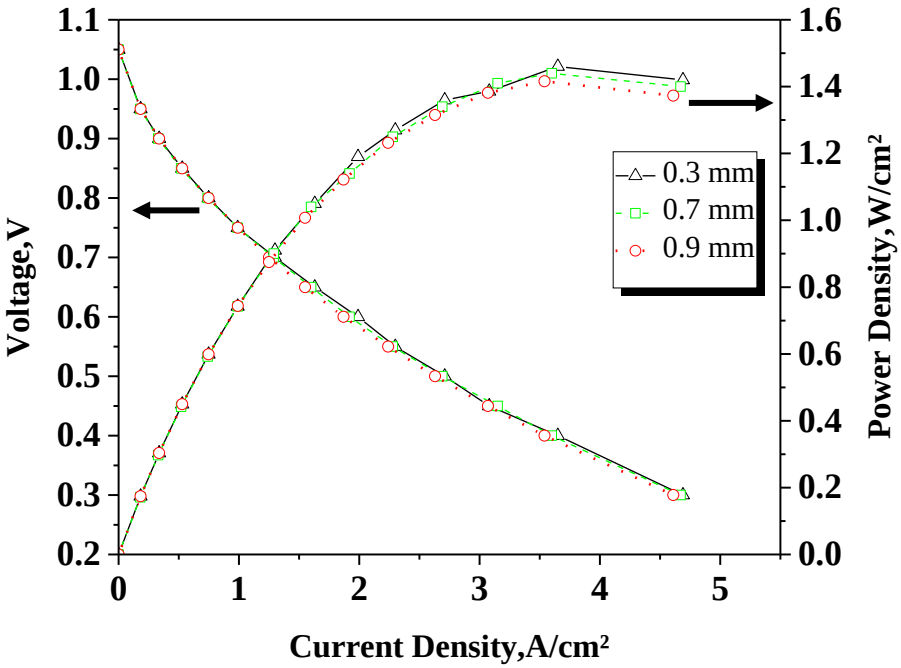

Figure IV.22: The influence of cathode supported layer thickness on the performance of the cell.

IV.4.4.2 The activation and concentration overpotentials for AS and CS

The activation and concentration overpotentials are taken into account, as reported in **Figure IV.23** and **24**, respectively. The effect of AS and CS on activation and concentration overpotentials are given. Furthermore, the activation and concentration overpotential rise as the current density increases. Where the effect of AS is slightly superior to the CS. Due to its lower exchange current density. The AS concentration over potential becomes a more important loss than CS when a thinner electrolyte is used.

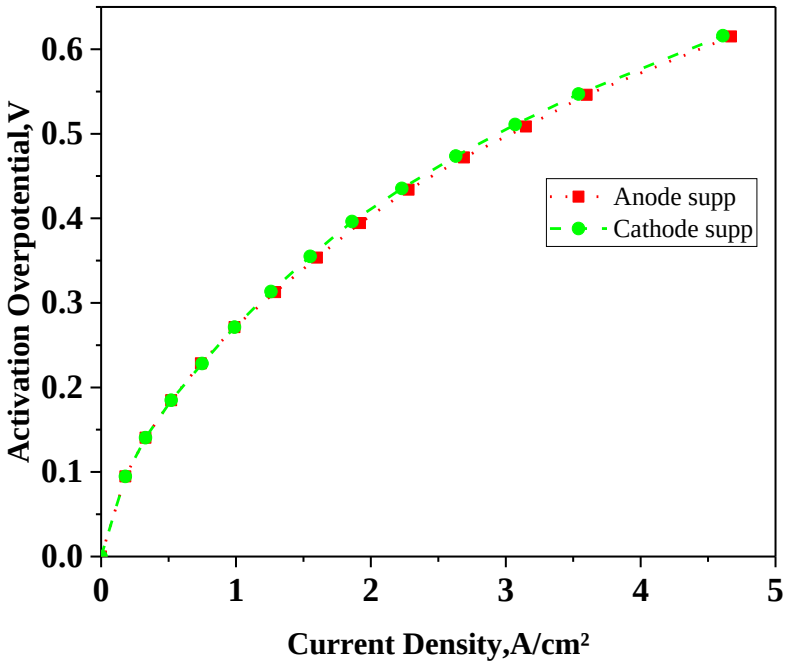

Figure IV.23: Effect of anode and cathode supported activation overpotential at different current densities

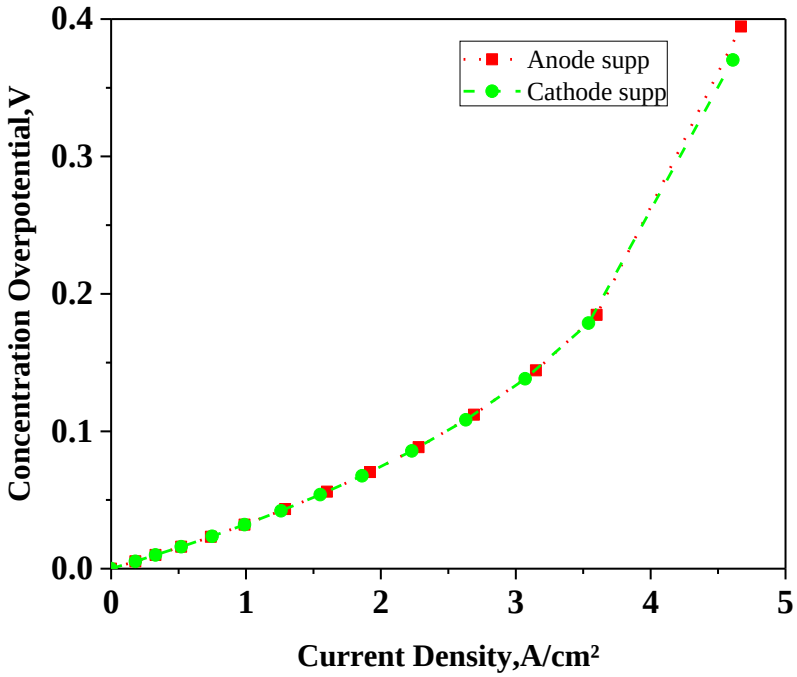

Figure IV.24: Effect of anode and cathode supported concentration overpotential at different current densities.

IV.4.4.3 Effect of electrolyte thickness on the cell performance and Ohmic overpotentials

Simulation analysis was also carried out to examine the effect of ES on the performance of SOFC fuel cell. The electrolyte thickness was varied from 0.2 to 0.5 mm. **Figure IV.25** presents the polarization curve at several electrolyte thicknesses. As expected, it was observed, that the performance diminishes when there is an increase in the electrolyte thickness. This is due to the enhanced Ohmic overpotential when the thickness rises as presented in **Figure IV.26**. Therefore, it can be concluded that decreasing the thickness of the electrolyte enhances Ohmic over potential; consequently making the electrolyte layer thin is necessary to improve the cell performance.

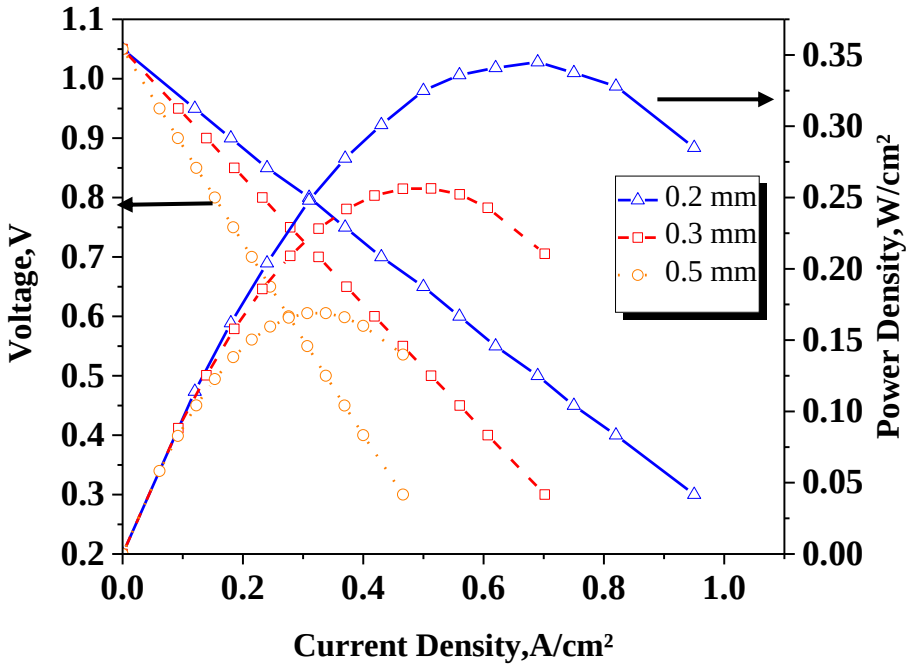

Figure IV.25: cell voltage and power density for electrolyte thickness.

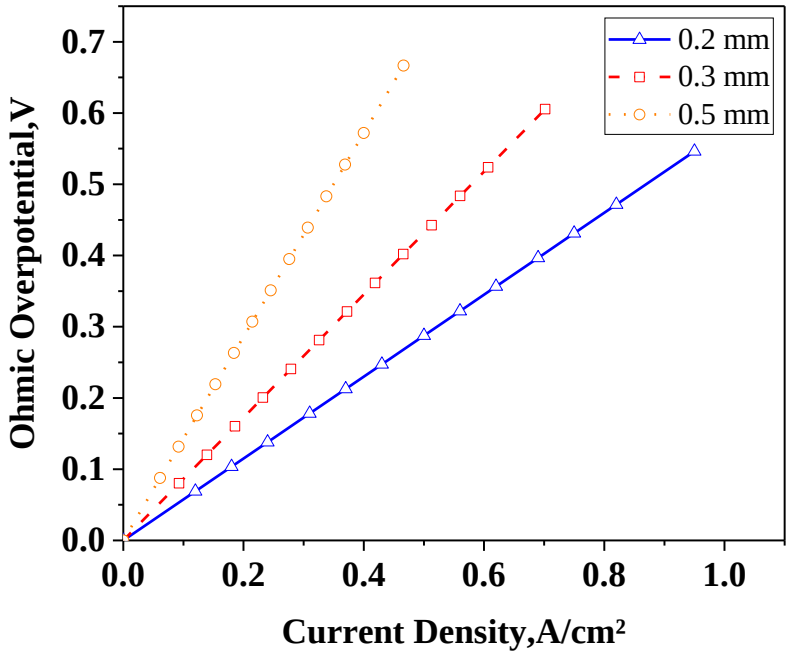

Figure IV.26: Effect of ohmic overpotential for different electrolyte thickness at different current densities.

IV.4.5 Comparison between anode-supported, cathode-supported and electrolyte supported cells

The three various support structures (anode supported AS, cathode supported CS and electrolyte supported ES) were compared so to examine the performance of SOFC cell. These cells are geometrically described in **TableIV.6**.

Table IV.6: the Geometrical description of the PEN layers of the SOFCs.

	Thickness (mm)		
	Anode GDL	**Cathode GDL**	**Electrolyte**
Anode supported	0.7	0.05	0.01
Cathode supported	0.05	0.7	0.01
Electrolyte supported	0.05	0.05	0.2

IV.4.5.1 Performance for anode-supported, cathode-supported and electrolyte supported cells

Three various support structures (anode supported AS, cathode supported CS, and electrolyte supported ES) are compared to examine the performance of SOFC cell as presented in **Figure IV.27**. It was noticed that the performance of the AS/CS was superior to that of the ES. Moreover, AS cell was slightly higher than the CS. Besides, the simulation results confirm that cells with AS/CS with thin electrolyte were better than Cells with ES; consequently this greatly decreases the Ohmic loss connected to the electrolyte thickness, which allows greater performance.

IV.4.5.2 Fuel utilization at a maximum value of current density for deferent support structures

According to **Table IV.7**, the highest value of fuel utilization is obtained for anode supported and that is due to better use diffusion of hydrogen molecules in the case of anode supported and not in a thicker cathode or electrolyte.

Table IV.7: maximum value of current density with maximum factor fuel utilization.

Supporting layer	Maximum Current Density(A/cm^2)	Factor Fuel Utilization (%)
Anode supported	1.863	42%
Cathode supported	1.836	39%
Electrolyte supported	0.294	13%

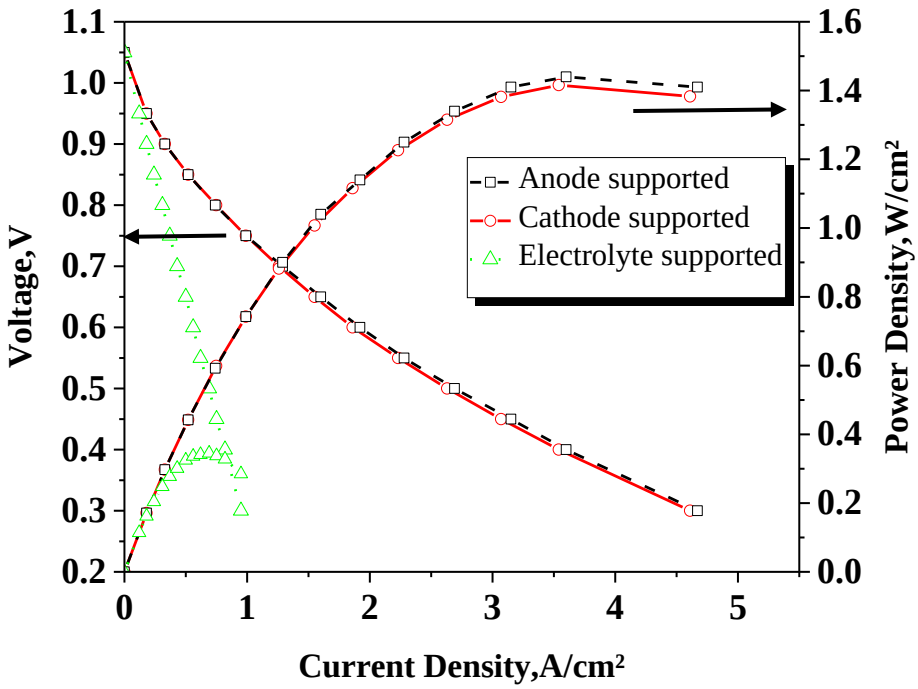

Figure IV.27: Comparison of anode-supported, cathode-supported and electrolyte supported cells.

IV.4.5.3 Activation, concentration, and Ohmic losses effect in AS CS and ES types

Figure IV.28 shows comparison overpotentials of SOFC with different support structures as presented the activation and concentration overpotentials is higher compared to Ohmic for both AS and CS. Whereas, the AS cell has significantly more activation and concentration overpotentials than CS cell. By comparing all the overpotentials, it was noted that the Ohmic loss was relatively small compared to the activation and concentration losses; even though it is a supporting electrode. From simulation analysis, AS-SOFC manifests a great current density and a higher power density compared to the CS and ES. Thus, attained a better performance.

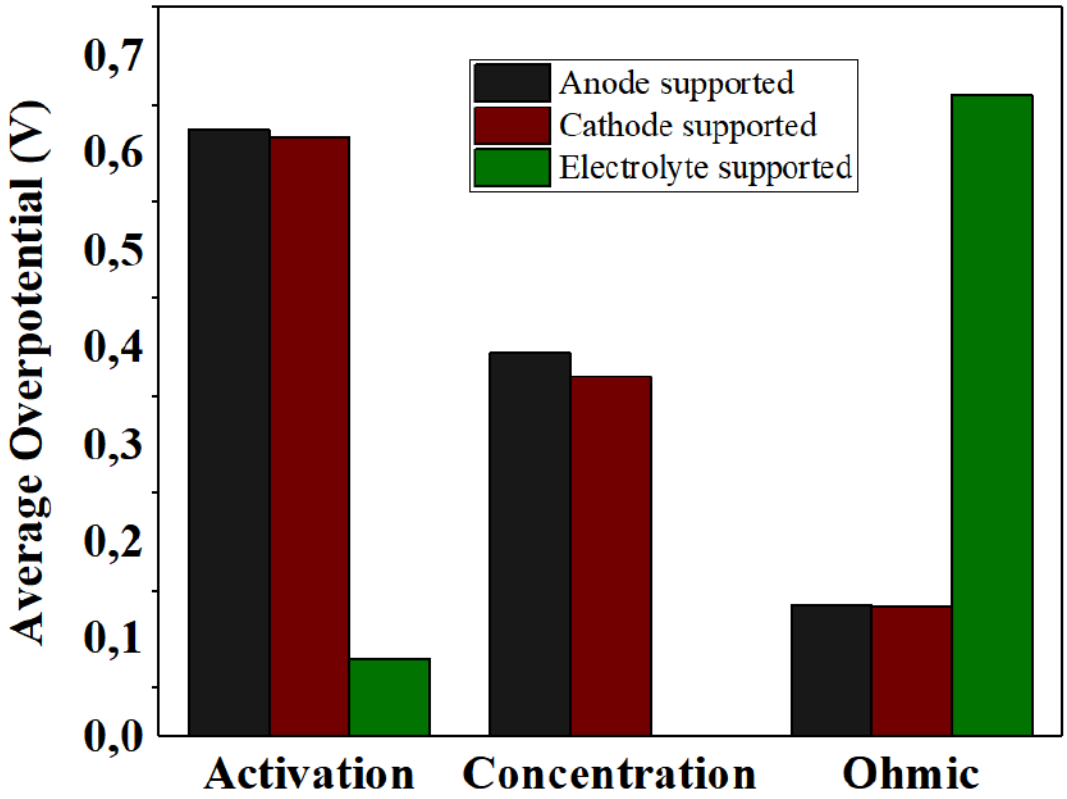

Figure IV.28: Comparison of overpotentials of SOFC with different support structures.

IV.4.5.4 Current density flux magnitude

Figure IV.29 Shows the contours of current density flux magnitude at a different supporting layer thickness of cells. As expected, it was found that the higher current density magnitude of the electrode-supported cases compared to the ES one. The current density flux maximum is $1.815e^{+05}$, $1.721e^{+05,}$ and 3585.2 A/m² in AS, CS, and ES respectively, the ES cell led to the lowest current density flux. Moreover, for the electrode-supported (i.e., AS and CS) cases, the maximum local current density occurred at the non-supporting side.

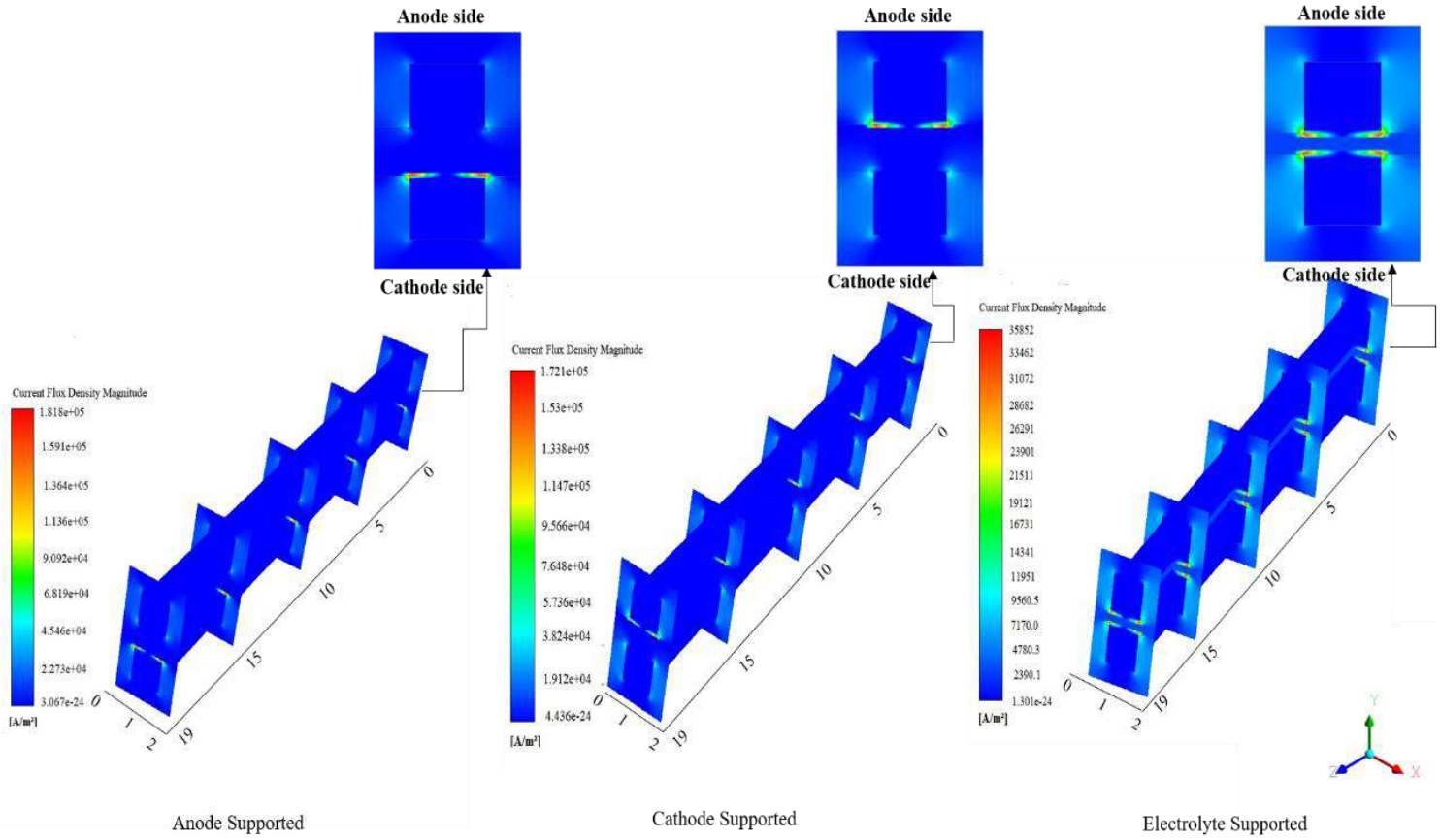

Figure IV.29: The contours of current density flux magnitude at a different supporting layer thickness of cells.

IV.4.6 Locate the optimal operating points

We used the results of our modeling to identify the optimal parameters of the SOFC fuel cell. **Table IV. 8** shows a significant improvement in the power density for a fixed voltage (V=0.6 V). Clearly, we were able to improve the performance starting from the initial operating parameters. The optimized model shows that the use of the optimal parameters compared to the initial operating parameters increases the power density from 1.416 A/cm^2 to 1.801 A/cm^2

From a design point of view: we change the thickness of the anode from the 0.7 mm (initial) value to the optimal 0.3 mm value. With making the electrolyte layer thin is necessary to diminish the Ohmic overpotential and improve the cell performance.

Table IV.8: power density corresponding to the optimal parameters.

Parameter optimization	Initial parameter	Optimal parameter
Temperature	1123 K	1073 K
pressure	1 atm	2 atm
porosity	0.3	0.3
AS	0.7	0.3
Fuel utilization	42%	58%
Power density	1.416 W/cm^2	1.801 W/cm^2

Conclusion

A parametric and geometric study of a SOFC fuel cell was carried out. This model is used to provide a fundamental understanding of the transport phenomena that occur in a fuel cell and identify the optimal parameters of the SOFC fuel cell, the simulation results are summarized in brief:

- Increasing the operating temperature and pressure improved the performance. While the anode supported had significantly better performance than cathode and electrolyte supported.
- The Ohmic and activation overpotentials decrease with increasing temperature while the concentration rises as the temperature rises. That is due to the electrochemical processes occurring at the electrodes and these effects accelerate the electrode kinetics and chemical reactions when the temperature increase.
- The fuel utilization improves with raising the temperature. This, in turn, leads to better consumption of the hydrogen fraction. Consequently, more water is carried at the cell outlet. Due to the greater inlet fuel temperature
- The concentration overpotential dominates the performance of SOFC cell at different pressures. Where the concentration overpotential is decreased as the pressure increases. While the fuel utilization is directly proportional to the pressure. Maybe because of a better supply of reactants at higher pressures.

- The highest value of hydrogen mass fraction consumed are 40%, 46%, and 51% for the operating pressure 1, 2, and 3 atm respectively. Due to an increment in pressure, hydrogen mass fraction consumption into the GDL increases. Consequently, the water fraction produced increases. Due to an increase in reaction rate which is favored by increased operation pressure.
- The cell performance improves as the supporting layer thickness of AS and CS diminishes. That is due when the anode/cathode thickness has reduced the activation and concentration of the cell diminished
- The AS concentration over potential become a more important loss than CS when a thinner electrolyte is used
- The highest value fuel utilization is obtained for anode supported (42%) that is due a more for the hydrogen diffuses in the transversal direction in the case of anode supported and not in a thicker cathode or electrolyte.
- Decreasing the thickness of the electrolyte enhances Ohmic over potential, consequently making the electrolyte layer thin is necessary to improve the cell performance.

Part B: Effect of Cell Design and Performance Considerations

Introduction

The flow field configuration has a vital effect on the performance of the fuel cell and is the key factor in SOFC design optimization. Therefore, further studies on new field designs are recommended to obtain more acute and reliable results on cell performance. The main objective of the present investigation is to enhance the performance of a solid oxide fuel cell (SOFC). Thus, a new flow field based on a sinusoidal flow has been proposed and studied as shown in **Figure IV.30**. The performance of a sinusoidal solid oxide fuel cell (SOFC) was examined using 3D computational fluid dynamics to model mass and heat flows inside the channels and compared to the single cell. By taking into account the concentration, activation, and Ohmic losses.

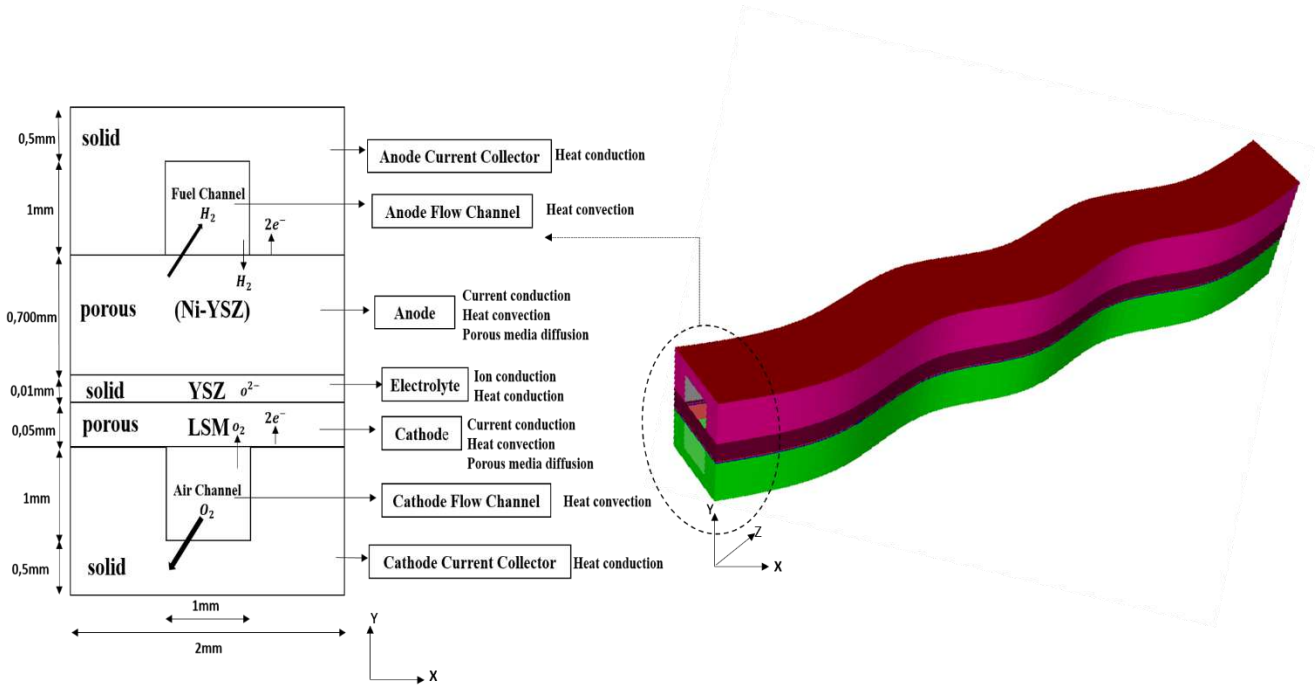

Figure IV.30: Schematic view of sinusoidal SOFC cell.

IV.5 Model description

The dimensions of the sinusoidal cell are similar to the dimensions used of the single-cell and are included in Table IV.2. The geometrical SOFC sinusoidal cell was executed in the commercial software GAMBIT (Version 2.4.6). In order to achieve the best quality mesh was entered in ANSYS WORKBENCH MESH. Once the computational mesh was created, it must be imported into the solver ANSYS FLUENT 18.1. The calculation procedure is given in **Figure IV.31**.

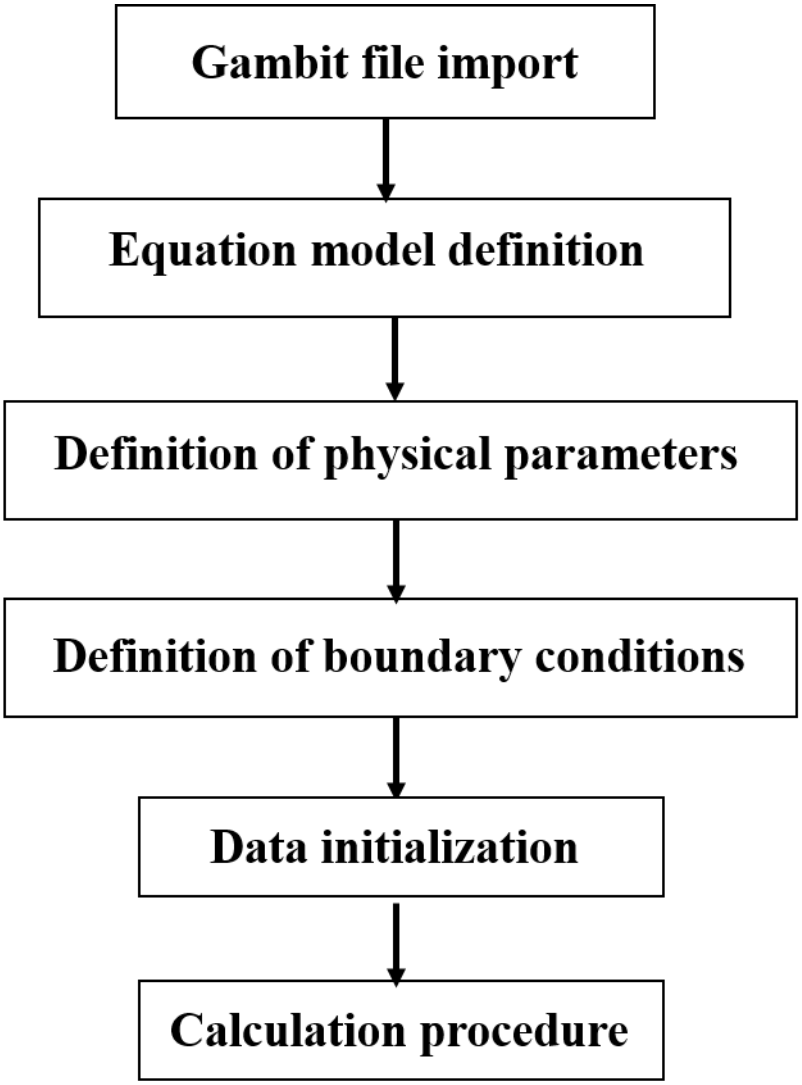

Figure IV.31: General simulation procedure.

IV.6 Result and discussion

IV.6.1 Distribution of hydrogen and water mass fraction

a) H_2

The H_2 mass fraction contours on the anode channel for both designs are represented in **Figure IV.32** and **Figure IV.33** at 0.6 V and 0.5 respectively. The mass fraction reduction along the z-channel is due to the consumption of hydrogen by the electrochemical reaction. It is also found that for 0.6 V, the mass fraction diminished from 0.97 to 0.38 and 0.43 for the sinusoidal and single flow design respectively. For the operating voltage of 0.5 V, the

H_2 mass fraction diminishes from 0.97 to 0.29 and 0.38 for the sinusoidal and single flow field design respectively. These results signify that the reaction rates at the sinusoidal flow design are greater than those detected in the single flow. The maximum use of H_2 mass fraction consumed in the sinusoidal and single flow field designs are 60% and 55% respectively for the operating voltage of 0.6 V, and 68% and 59% respectively for the operating voltage of 0.5 V as given in **Table IV.9**. According to Figure IV.32 and 33 along with Table IV.9, the sinusoidal form gave a greater level of H_2 mass fraction. Consequently, this configuration is considered more uniform in diffusing of H_2 mass fraction because of the best use of the active area in the CL (catalyst layer).

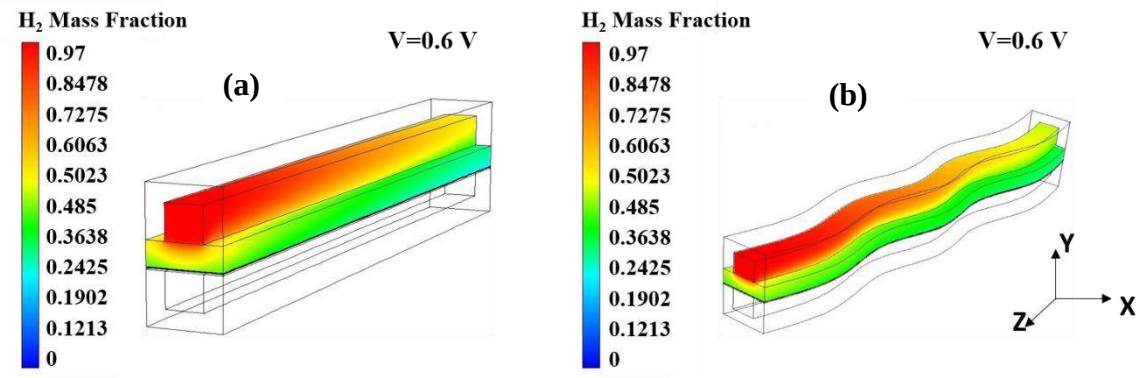

Figure IV.32: Hydrogen mass fraction distribution contour along the anode channel for two different flow designs at 0.6 V.

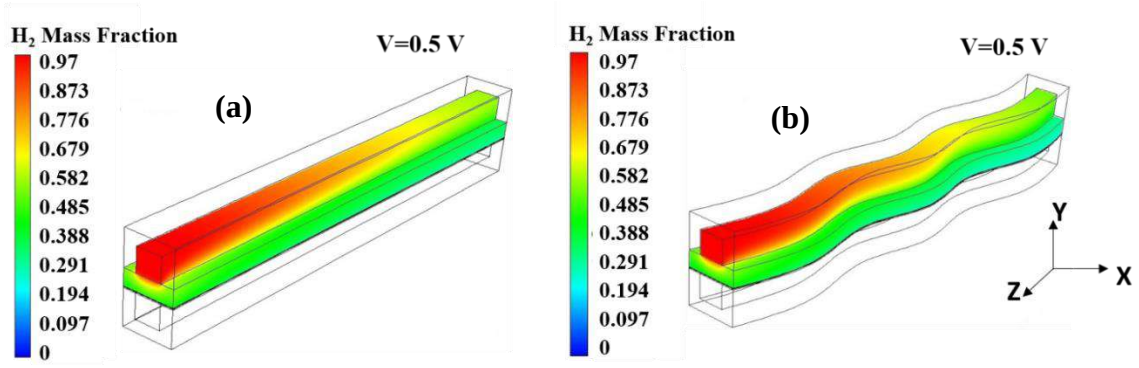

Figure IV.33: Hydrogen mass fraction distribution contour along the anode channel for two different flow designs at 0.5 V.

Table IV.9: Maximum value consumed of hydrogen mass fraction at the anode/ electrolyte interface.

Flow field designs	**Hydrogen mass fraction consumed at anode/electrolyte interface (%)**	
	0.6 V	**0.5 V**
sinusoidal flow field	60%	68%
single flow field	55%	59%

b) H_2O

On the other hand, increasing H_2 mass fraction consumption increases H_2O mass fraction produced as displayed in **Figure IV.34** and **Figure IV.35**. The sinusoidal flow design has a better distribution compared to the single flow field as demonstrated in Figure IV.34 and 35. The highest H_2O mass fraction values produced for the sinusoidal and single flow designs were 42% and 34% respectively for the operating voltage 0.6 V, and for operating 0.5 V are 48% and 39% respectively, as shown in **Table IV.10**. This uniform distribution leads to regularly generates heat and decreases thermal stresses, suggesting that the sinusoidal cell aids in reducing losses. In addition, the maximum value of the H_2O fraction at the anode channel increases as the voltage reduces.

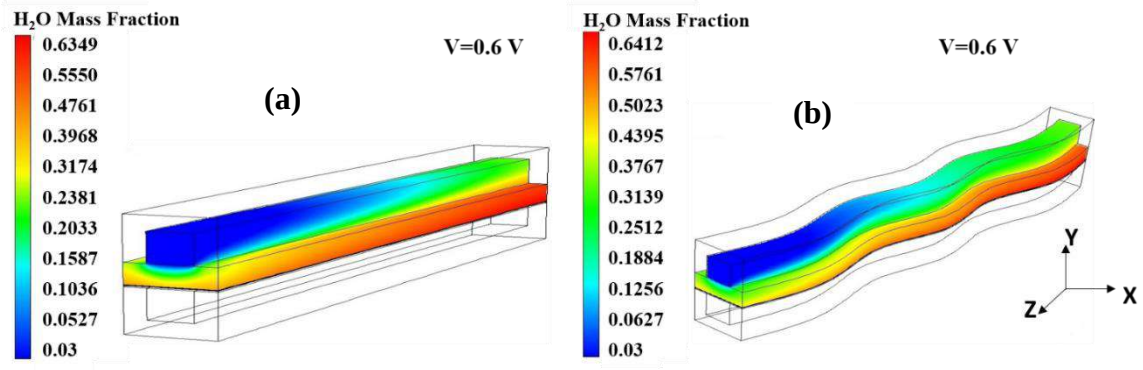

Figure IV.34: Water mass fraction distribution contour along the anode channel for two different flow designs at 0.6 V.

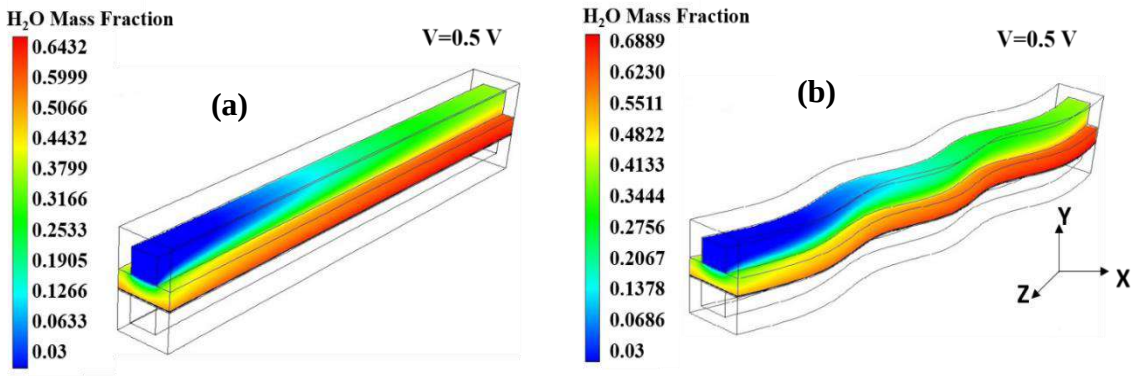

Figure IV.35: Water mass fraction distribution contour along the anode channel for two different flow designs at 0.5 V.

Table IV.10: Maximum value produced of Water mass fraction at the anode/ electrolyte interface.

Flow field designs	**Water mass fraction produced at anode/electrolyte interface (%)**	
	0.6 V	**0.5 V**
sinusoidal flow field	42%	48%
single flow field	34%	39%

IV.6.2 Distribution of velocity

Figure IV.36 and **Figure IV.37** show the anode velocity distribution for both flow field designs at 0.6 V and 0.5 V, respectively. The upmost velocity in the anode channel was 10.63 and 10.35 m/s for sinusoidal and single flow field designs, respectively at 0.6 V, as displayed in Figure IV.36 (a) and (b). These values are 12.03 and 11.54 m/s at 0.5 V for sinusoidal and single flow field designs, respectively as exposed in Figure IV.37 (a) and (b). It could be deduced that the distribution near GDL had improved, due to deflection design which increased the anode velocity as the voltage decreased and augmented the distribution mechanism. As a result, the velocity in the anode channel for the sinusoidal design was higher than the simple single-channel which led to cell performance enhancement.

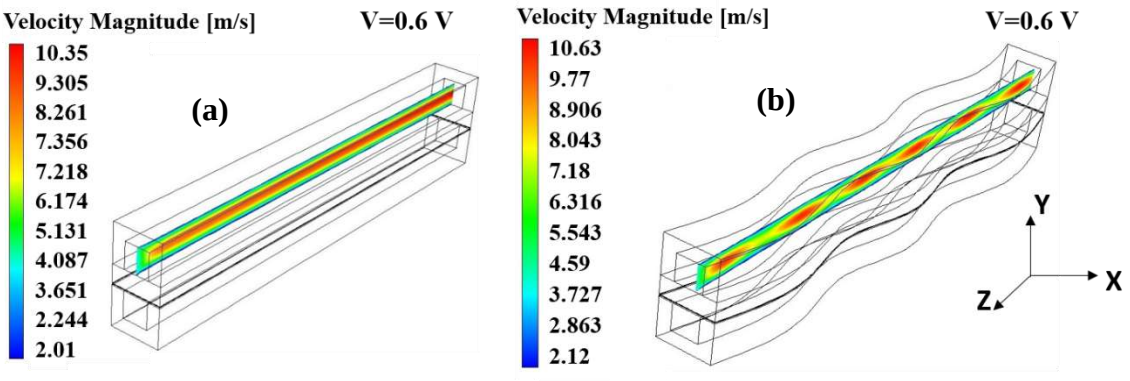

Figure IV.36: Velocity distribution contour along the anode channel for two different flow designs at 0.6 V.

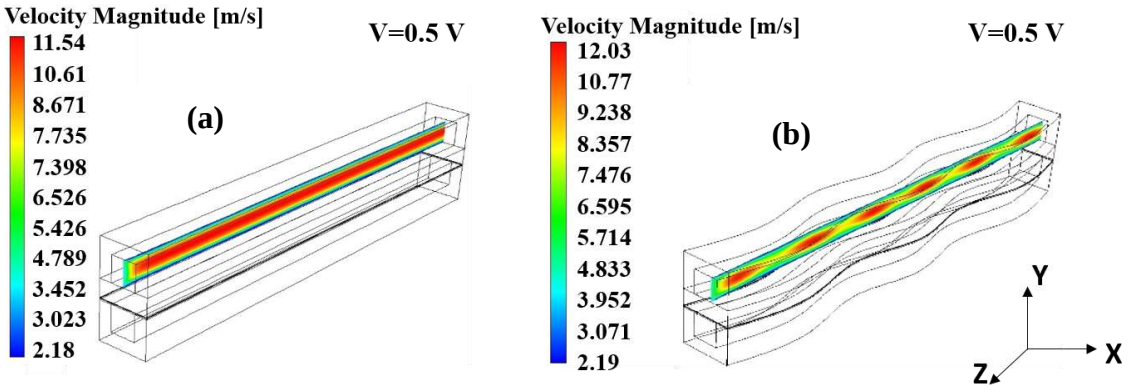

Figure IV.37: Velocity distribution contour along the anode channel for two different flow designs at 0.5 V

IV.6.3 Distribution of temperature

Figure IV.38 and **Figure IV.39** displays temperature contours for the sinusoidal and single flow field designs at 0.6 V and 0.5 V. An increase in temperature values is clearly observable along the cells for both designs. The sinusoidal flow led to greater values as compared to the single flow, as can be seen in the same figure. This could be explicated by the higher rate of reaction. Specifically, the highest temperatures for the sinusoidal and single flow were 1128.30 K and 1126.95 K respectively for the operating voltage 0.6 V as shown in Figure IV.38, and for operating voltage 0.5 V are 1138.22 K and 1134.09 K for the sinusoidal and single flow, respectively as demonstrated in Figure IV.39. For all the geometrical configurations, the highest temperature value was always located in the center

of the cell which represents the electrolyte due to the counter-flow direction as marked in the literature [47].

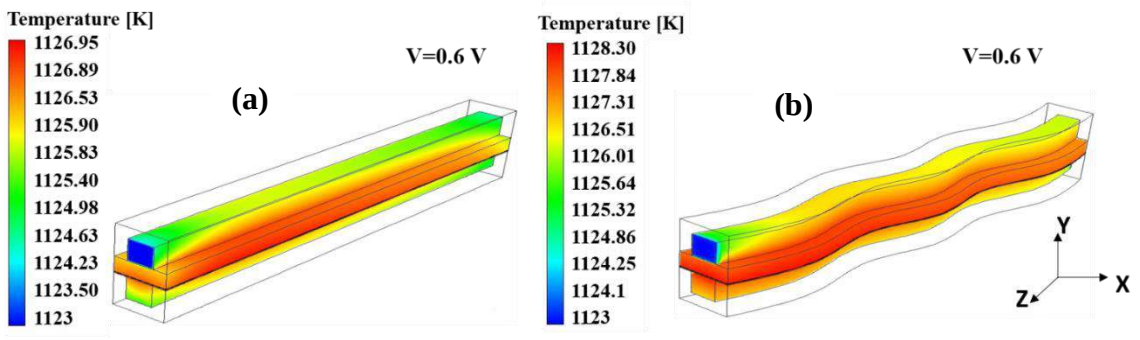

Figure IV.38: Temperature distribution contour along the SOFCs cells for two different flow designs at 0.6 V.

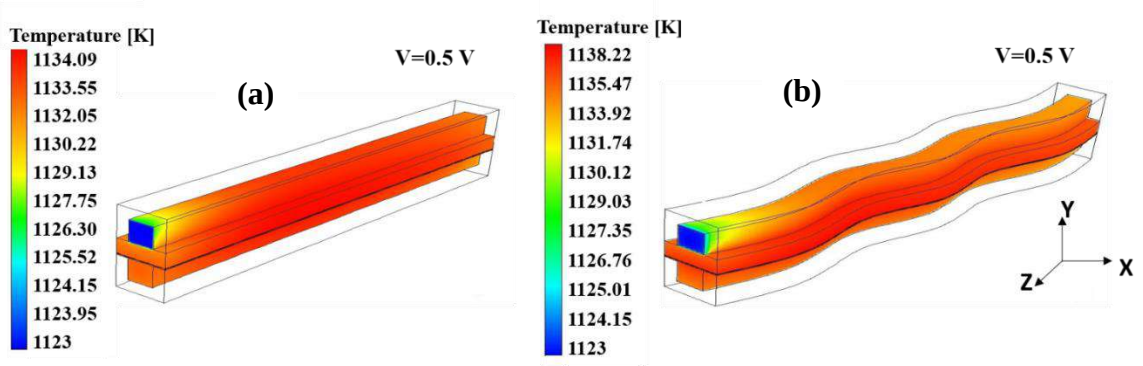

Figure IV.39: Temperature distribution contour along the SOFCs cells for two different flow designs at 0.5 V.

IV.6.4 Concentration, activation, and Ohmic Overpotentials

The mathematical model was able to predict the overpotentials inside the SOFC for both sinusoidal and single cells, which is necessary for testing their performance. As presented in the literature, there are three overpotentials, caused by various mechanisms. The concentration overpotential is based on the resistance to transport the fraction of reactants and oxidant. As shown in **Figure IV.40** the sinusoidal flow field led to a reduction in the concentration overpotential, whereas, the concentration overpotential increased with the current density for both designs. The activation overpotential was slightly higher for the

single cell than the sinusoidal as shown in **Figure IV.41**. This is due to increasing the temperature in the sinusoidal cell which contributed in reducing activation polarization. In addition, the sinusoidal cell took part in minimizing the Ohmic overpotential as displayed in **Figure IV.42**. This is due to the improvement of the operation temperature which raises the conductivity of the electrolyte. From the above mentioned arguments, it could be deduced that the sinusoidal cell significantly contributed to the performance enhancement and to minimization of the concentration, activation, and Ohmic overpotentials compared to the single cell.

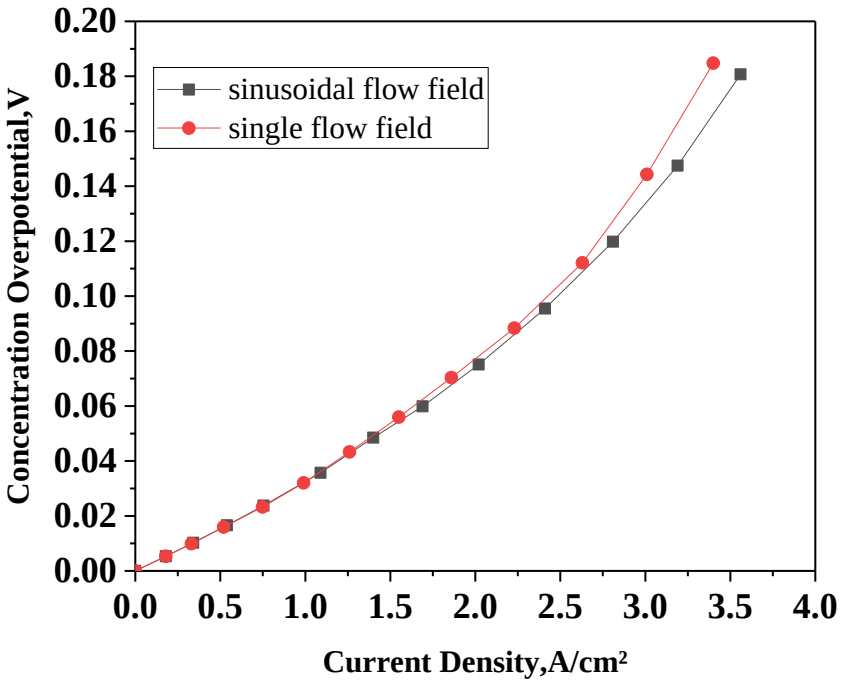

Figure IV.40: The concentration overpotentials curves for two different flow field designs.

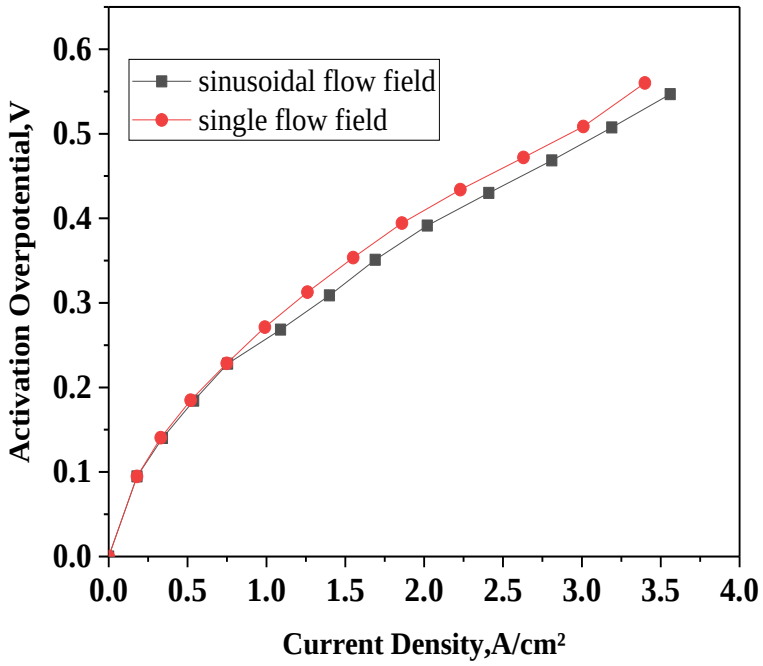

Figure IV.41: The activation overpotentials curves for two different flow field designs

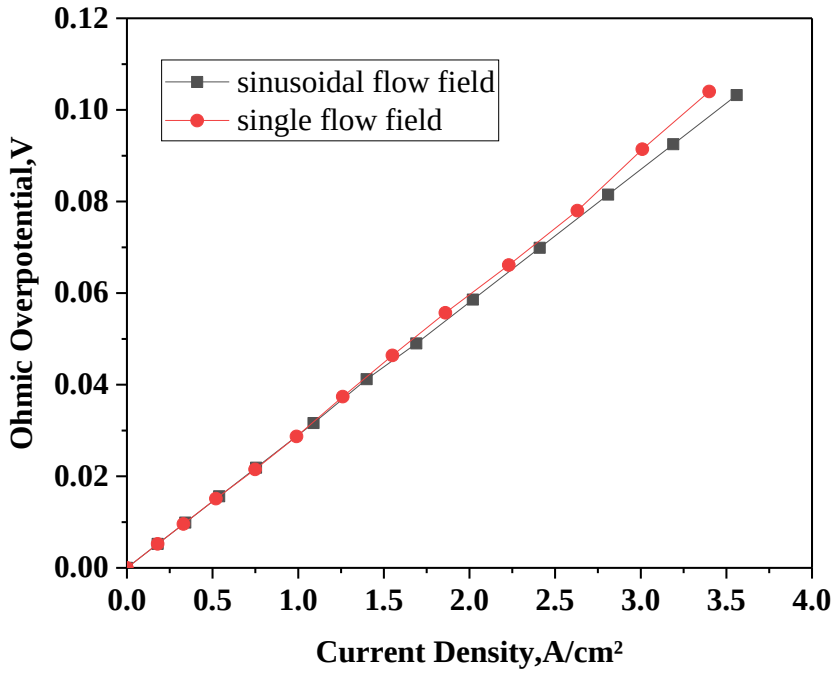

Figure IV.42: The Ohmic overpotentials curves for two different flow field designs.

IV.6.5 SOFC overall performance

Figure IV.43 displays the polarization (j-V) and the power density curves for the two designs; from which it could be readily noticed that the sinusoidal flow design was more performable than the single flow. Additionally, the maximum power densities of the sinusoidal and single flow designs were 1.43 and 1.35 W/cm^2, respectively. This result indicates that the sinusoidal flow design offers the most use of the hydrogen as considered in the previous section. Moreover, the difference in performance between the two designs is well remarked at low voltages due to decreasing in the concentration losses. As a consequence, the sinusoidal flow design has contributed significantly in ameliorating the performance.

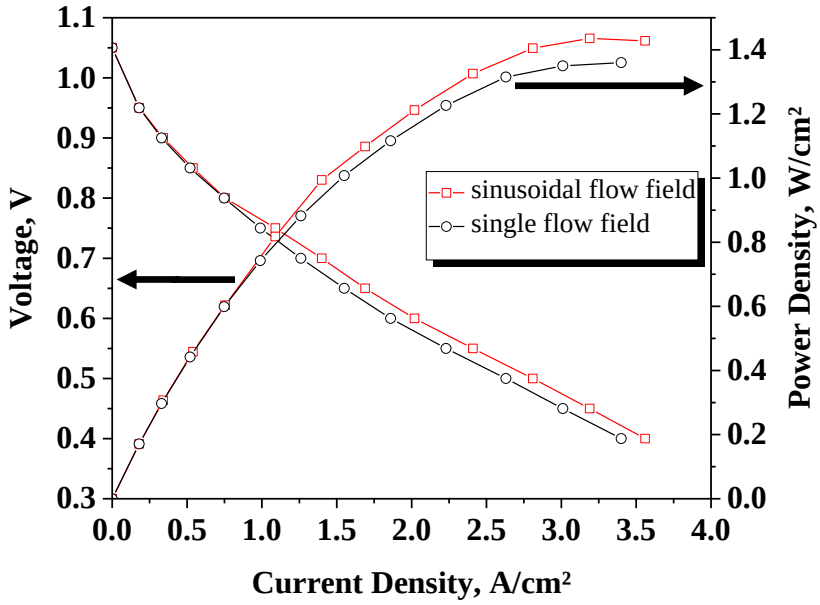

Figure IV.43: The polarization curve (j-V) and power density curve for two different flow designs.

Conclusion

Simulation results including velocity distributions, gas species, temperature, concentration overpotential, activation overpotential, Ohmic overpotential, and cell performance for both flow designs have been introduced and discussed. It was established that the channel design

performed an important role in enhancing the performance and decreasing the overpotentials losses of SOFC fuel cells. The CFD results indicated that, when the cell was run at high voltage, the influence of channel design on the cell performance was negligible; whereas, when treated at the low voltage the channel design influence became significant. On the other hand, the sinusoidal design gave a better distribution of velocities and temperatures than the single flow, which improved the transport of hydrogen of the cell. As a result, more water was produced at the anode channel and accordingly, the cell performance rose. Lastly, it could be concluded that the sinusoidal design has greater performance than the single flow; and this could be useful in choosing the best configuration for certain applications requiring the greatest achievable performance.

References

[1] J. Larminie and A. Dicks, “Fuel Cell Systems Explained Second Edition.” Book Second Edition, Wiley, (2003).

[2] S. Edition and W. Virginia, “Fuel Cell Handbook,” no. November, 2004.

[3] H. Mohcene, “Etude des causes d’augmentation de la température dans une pile à oxyde solide (SOFC): Etude bidimensionnelle du champ de température,” Doctoral thesis at Université Kasdi Merbah Ouargla, 2012.

[4] C. Stiller, “Design , Operation and Control Modelling of SOFC / GT Hybrid Systems,” Doctoral Thesis at Norwegian University of Science and Technology, March 2006.

[5] M. Jourdani, “Simulation Numérique Couplée des Phénomènes Thermo- fluide, Electrochimique et Mécanique dans une Pile à Combustible type PEMFC,” Doctoral Thesis at mohammed v-rabat university mohammadia school of engineers, 2019.

[6] C. Lalanne, “Synthèse et mise en forme de nouveaux matériaux de cathode pour piles ITSOFC : réalisation et tests de cellules", Doctoral Thesis at bordeaux 1 university,2006. HAL Id : tel-00092666

[7] N. Q. Minh, “Solid oxide fuel cell technology features and applications,” Solid State Ionics vol. 174, pp. 271–277, 2004.

[8] A. Mohammadzadeh, S. Kiana, N. Zadeh, M. H. Saidi, and M. Sharifzadeh, Chapter 3. Mechanical engineering of solid oxide fuel cell systems: geometric design, mechanical configuration, and thermal analysis. Book Design and Operation of Solid Oxide Fuel Cells, Elsevier Inc, 2020.

[9] M. Rieu, “Préparation par voie sol-gel et caractérisation d’une cellule complète

SOFC sur support métallique poreux," Doctoral thesis at toulouse university, 2009.

[10] B. Sundén and M. Faghri, TRANSPORT PHENOMENA IN FUEL CELLS. Book, 2005.

[11] T. Besnic, "implementation and validation of the two-potential electrolyte assembly equations in the computational fuel cell model," master's thesis,2016.

[12] S. P. S. Badwal and K. Foger, "Solid Oxide Electrolyte fuel cell review," Journal Ceramics International vol. 8842, no. 95, pp. 257–265, 1996.

[13] J. Fondard, "Elaboration et test d'une pile à combustible IT-SOFC à support métallique poreux par l'intermédiaire de techniques de dépot en voie séche : projection thermique et pulvérisation cathodique magnétron," thése de doctorat à Université de Technologie de Belfort-Montbéliard en Sciences pour l'Ingénieur, 2015.

[14] J. W. Fergus, "Electrolytes for solid oxide fuel cells," Journal of Power Sources vol. 162, no. June, pp. 30–40, 2006.

[15] J. Drennan and G. Auchterlonie, "Microstructural aspects of oxygen ion conduction in solids," journal Solid State Ionics vol. 134, pp. 75–87, 2000.

[16] N. P. Brandon *et al.*, "Development of Metal Supported Solid Oxide Fuel Cells for Operation at 500 – 600 ° C," Journal of Fuel Cell Science and Technology vol. 1 pp. 61–65, November 2004.

[17] J. Molenda, K. Swierczek, and W. Zaj, "Functional materials for the IT-SOFC," Journal of Power Sources vol. 173, pp. 657–670, 2007.

[18] N. Preux, "A la recherche de nouveaux matériaux d ' électrolyte et de cathode pour SOFC : Weberite et Cobaltite," Thèse Pour obtenir le grade de Docteur de l'Université des Sciences et Technologies de Lille, 2011.

[19] L. Spiridigliozzi, "SOFC Components," SpringerBriefs in Applied Sciences and Technology chapter 3 pp. 15–24.

[20] Jeffrey W. Fergus, R. Hui, X. Li, David P. Wilkinson, and J. Zhang, solid oxide

fuel cells Materials Properties and Performance.Book published in Taylor & Francis Group, 2009.

[21] S. Dwivedi, “Solid oxide fuel cell : Materials for anode , cathode and electrolyte,” Int. J. Hydrogen Energy, 2019.

[22] D. Rotureau, “developpement de piles a combustible de type sofc, conventionnelles et mono-chambres, en technologie planaire par serigraphie”,Thése de doctorat de l'ecole nationale superieure des mines de saint-etienne 2005.

[23] B. Hu, M. Keane, M. K. Mahapatra, and P. Singh, “Stability of strontium-doped lanthanum manganite cathode in humidi fi ed air,” Journal of Power Sources vol. 248, pp. 196–204, 2014.

[24] K. Dumaisnil, “Élaboration et caractérisations de matériaux de cathode et d ’ électrolyte pour pile à combustible à oxyde solide Élaboration et caractérisations de matériaux de cathode et d ’ électrolyte pour pile à combustible à oxyde solide,”Thése de doctorat de Université du Littoral Côte d’Opale École, 2015.

[25] E. Lay, “Nouveaux mat´eriaux d’´electrode de cellule SOFC,” thése de doctorat de Université Joseph Fourier - Grenoble I, 2010.

[26] K. Haberko, M. Jasinski, P. Pasierb, M. Radecka, and M. Rekas, “Structural and electrical properties of Ni – YSZ cermet materials,” Journal Power Sources, vol. 195, no. 17, pp. 5527–5533, 2010.

[27] D. J. L. Brett, A. Atkinson, P. Brandon, S. J. Skinner, A. Atkinson, and D. J. L. Brett, “Intermediate temperature solid oxide fuel cells,”Journal Chemical Society Reviews pp. 1568–1578, 2008.

[28] J. Milewski and J. Lewandowski, “Analysis of Design and Construction of Solid Oxide Fuel Cell in Terms of their Analysis of Design and Construction of Solid Oxide Fuel Cell in Terms of their Dynamic Operation,” Journal Archivum Combustionis, vol. 30, pp. 145–153, May 2014.

[29] B. Chong, Y. Chun, Z. Xiang, L. Cai-Bao, and M.-Q. Wu, “Parametric analysis of

solid oxide fuel cell,"Journal Clean Techn Environ Policy pp. 391–399, 2009.

[30] B. Pascal, "synthése par pulvérisation cathodique et caractéisation d'électolytes solides en couches minces pour pile à combustible à oxydes solides (SOFC) fonctionnant à température intermédiaire," Thése de doctorat de université de lorraine 2005.

[31] Zitouni. B, "Etude Numérique des Phénomènes de Transfert dans les Piles à Combustible à Oxyde Solide de Type Planaire,"Thése de doctorat de université de batna 2007.

[32] H. Mounir, "Caractérisation , modélisation thermo fluide et électrochimique , simulation numérique et étude des performances des nouvelles piles à combustible types IP-SOFC (Integrated-Planar Solid Oxide Fuel Cell)," Thése de doctorat ,2010.

[33] M. Halinen, Improving the performance of solid oxide fuel cell systems Improving the performance of solid oxide fuel cell systems. doctoral Thesis, 2015.

[34] A. AMAN, "numerical simulation of electrolyte-supported planar button solid oxide fuel cell," Masters Thesis, 2012.

[35] F. Nandjou, "Étude locale de la thermique dans les piles à combustible pour application automobile ," Thése de doctorat, 2015.

[36] A. Averberg, K. R. Meyer, C. Q. Nguyen, and A. Mertens, "A Survey of Converter Topologies for Fuel Cells in the kW Range," Conference Paper IEEE Energy, Atlanta, Georgia, USA, 17-18 November 2008.

[37] F. RICOUL, "Association d'un procédé de gazéification avec une pile à combustible haute température (SOFC) pour la production d'électricité à partir de biomasse," Thése de doctorat,2016.

[38] D. Roussel, "Optimisation d ' architecture d ' électrode poreuse pour pile à combustible à oxyde solide To cite this version .Thése de doctorat, 29 janvier 2015.

[39] S. Campanari and P. Iora, “Definition and sensitivity analysis of a finite volume SOFC model for a tubular cell geometry,” Journal of Power Sources, vol. 132, pp. 113–126, 2004.

[40] E. Achenbach, “Three-dimensional and time-dependent simulation of a planar solid oxide fuel cell stack,” Journal of Power Sources, vol. 49, pp. 333–348, 1994.

[41] W. Bi, D. Chen, and Z. Lin, “A key geometric parameter for the flow uniformity in planar solid oxide fuel cell stacks,” Int. J. Hydrogen Energy, vol. 34, no. 9, pp. 3873–3884, 2009.

[42] V. A. Danilov and M. O. Tade, “A CFD-based model of a planar SOFC for anode flow field design,” Int. J. Hydrogen Energy, 2009.

[43] M. Saied, K. Ahmed, and M. Ahmed, “Performance study of solid oxide fuel cell with various flow field designs : numerical study ScienceDirect Performance study of solid oxide fuel cell with various flow field designs : numerical study,” Int. J. Hydrogen Energy, vol. 43, no. 45, pp. 20931–20946, 2018.

[44] C. M. Huang, S. S. Shy, and C. H. Lee, “On flow uniformity in various interconnects and its influence to cell performance of planar SOFC,” Journal of Power Sources, vol. 183, pp. 205–213, 2008.

[45] Z. Lin, J. W. Stevenson, and M. A. Khaleel, “The effect of interconnect rib size on the fuel cell concentration polarization in planar SOFCs,” Journal of Power Sources, vol. 117, pp. 92–97, 2003.

[46] Q. Shen, L. Sun, and B. Wang, “Numerical Simulation of the Effects of Obstacles in Gas Flow Fields of a Solid Oxide Fuel Cell,” International Journal of electrochemical science, vol. 14, pp. 1698–1712, 2019.

[47] B. Zitouni, H. Ben, K. Oulmi, S. Saighi, and K. Chetehouna, “Temperature field , H 2 and H 2 O mass transfer in SOFC single cell : Electrode and electrolyte thickness effects,” International Journal of Hydrogen Energy, vol. 34, no. 11, pp. 5032–5039, 2009.

[48] M. Ilbas and B. Kumuk, “Numerical modelling of a cathode-supported solid oxide

fuel cell (SOFC) in comparison with an electrolyte-supported model," Journal Energy Inst., 2018.

[49] S. Koch *et al.*, "Solid Oxide Fuel Cell Performance under Severe Operating Conditions," Journal Fuel Cell, pp. 130–136, 2006.

[50] S. Henning and Mohsen Assadi, "Modeling of Overpotentials in an Anode-Supported Planar SOFC Using a Detailed Simulation Model," Journal of Fuel Cell Science and Technology, vol. 8, no. October 2011, pp. 1–13, 2016.

[51] A. K. Shukla, S. Gupta, S. P. Singh, M. Sharma, and G. Nandan, "Thermodynamic Performance Evaluation of SOFC Based Simple Gas Turbine cycle," International Journal of Applied Engineering Research , vol. 13, no. 10, pp. 7772–7778, 2018.

[52] A. K. Samantaray, "Constant Fuel Utilization Operation of a SOFC System : An Efficiency Viewpoint Constant Fuel Utilization Operation of a SOFC System : An Efficiency Viewpoint," Journal of Fuel Cell Science and Technology , August 2010.

[53] C. W.Tanner, K.-Z. Fung, and A. V.Virkar, "The Effect of Porous Composite Electrode Structure on Solid Oxide Fuel Cell Performance I. Theoretical Analysis," Journal The Electrochemical Society, 1, pp. 21–30, 1997.

[54] M. Farnak, J. A. Esfahani, and S. Bozorgmehri, "An experimental design of the solid oxide fuel cell performance by using partially oxidation reforming of natural gas," Journal Renew. Energy, vol. 147, pp. 155–163, 2020.

[55] K. Zouhri, M. Shinneebb, M. Chikhalsoukb, and J. Cressa, "Solid oxide fuel cell cathode diffusion polarization: materials and exergy study," Journal Energy Conversion and Management, vol. 231,2021.

[56] S. Lee *et al.*, "The effect of fuel utilization on heat and mass transfer within solid oxide fuel cells examined by three-dimensional numerical simulations," Int. Journal of Heat Mass Transf., vol. 97, pp. 77–93, 2016.

[57] J. Zhang, C. Lenser, N. H. Menzler, and O. Guillon, "Comparison of solid oxide fuel cell (SOFC) electrolyte materials for operation at 500 ° C,"Journal Solid

State Ionics, vol. 344, no. October 2019, p. 115138, 2020.

[58] D. Feng, C. Bao, and T. Gao, “Prediction of overpotential and concentration profiles in solid oxide fuel cell based on improved analytical model of charge and mass transfer,” Journal of Power Sources, p. 227499, November 2019.

[59] S. K. Dong, W. N. Jung, K. Rashid, and A. Kashimoto, “Design and numerical analysis of a planar anode-supported SOFC stack,”Journal Renew. Energy, 2016.

[60] F. Calise, M. Dentice, and G. Restuccia, “Simulation of a tubular solid oxide fuel cell through finite volume analysis : Effects of the radiative heat transfer and exergy analysis,” International Journal of Hydrogen Energy vol. 32, pp. 4575–4590, 2007.

[61] W. Kong, Z. Han, S. Lu, X. Gao, and X. Wang, “A novel interconnector design of SOFC,” Int. J. Hydrogen Energy, 2019.

[62] G. Min, Y. J. Park, and J. Hong, “1D thermodynamic modeling for a solid oxide fuel cell stack and parametric study for its optimal operating conditions,” Journal of Energy Convers. Manag., vol. 209 p. 112-614, September 2020.

[63] A. Raj, A. P. Sasmito, and T. Shamim, “Numerical investigation of the effect of operating parameters on a planar solid oxide fuel cell,” Journal Energy Convers. Manag., vol. 90, pp. 138–145, 2015.

[64] H. Xu, B. Chen, P. Tan, J. Xuan, M. M. Maroto-valer, and D. Farrusseng, “Modeling of all-porous solid oxide fuel cells with a focus on the electrolyte porosity design,” Journal Applied Energy, vol. 235 pp. 602–611, September 2019.

[65] D. A. Noren and M. A. Hoffman, “Clarifying the Butler – Volmer equation and related approximations for calculating activation losses in solid oxide fuel cell models,” Journal ofPower Sources, vol. 152, pp. 175–181, 2005.

[66] A. V. Akkaya, “Electrochemical model for performance analysis of a tubular SOFC,” International Journal Of Energy Research, pp. 79–98, 2007.

[67] Y. Wang, R. Zhan, Y. Qin, G. Zhang, Q. Du, and K. Jiao, “Three-dimensional

modeling of pressure effect on operating characteristics and performance of solid oxide fuel cell," International Journal of Hydrogen Energy, 2018.

[68] D. Cui, B. Tu, and M. Cheng, "Effects of cell geometries on performance of tubular solid oxide fuel cell," Journal Power Sources, vol. 297, pp. 419–426, 2015.

[69] M. Kamvar, M. Ghassemi, and R. Steinberger-wilckens, "ScienceDirect The numerical investigation of a planar single chamber solid oxide fuel cell performance with a focus on the support types," Int. J. Hydrogen Energy, 2020.

[70] S. R. Pakalapati, "A new reduced order model for solid oxide fuel cells," Doctoral Thesis, 2006.

[71] P. Aguiar, C. S. Adjiman, and N. P. Brandon, "Anode-supported intermediate temperature direct internal reforming solid oxide fuel cell . I : model-based steady-state performance," Journal ofPower Sources, vol. 138, pp. 120–136, 2004.

[72] M. Chnani, "Modélisation Macroscopique de piles PEFC et SOFC pour l ' étude de leur couplage," Thése de doctorat, 2009.

[73] E. Hern, D. Singh, P. N. Hutton, N. Patel, and M. D. Mann, "A macro-level model for determining the performance characteristics of solid oxide fuel cells," Journal ofPower Sources 138, vol. 138, pp. 174–186, 2004.

[74] I. Smail, "Modélisation d'Une Cellule de Piles à Combustible à Oxyde Solide « Simulation Numérique du Transfert Thermique »," Thése magistère en genie mecanique, 2015.

[75] X. Xue, J. Tang, N. Sammes, and Y. Du, "Dynamic modeling of single tubular SOFC combining heat / mass transfer and electrochemical reaction effects," Journal ofPower Sources ,vol. 142, pp. 211–222, 2005.

[76] O. O. Ighodaro, K. Scott, and L. Xing, "An Isothermal Study of the Electrochemical Performance of Intermediate Temperature Solid Oxide Fuel Cells," Journal of Power and Energy Engineering, pp 97–122, 2017.

[77] H. Xu, B. Chen, P. Tan, J. Xuan, M. M. Maroto-valer, and D. Farrusseng,

"Modeling of all-porous solid oxide fuel cells with a focus on the electrolyte porosity design," Journal Applied Energy, vol. 235 pp. 602–611, 2019.

[78] Y. M. Barzi, A. Raoufi, N. M. Rasi, and S. Davari, "Three Dimensional Simulation of a Counter-flow Planar Solid Oxide Fuel Cell," Journal ECS Trans, vol. 35, no. 1, pp. 1021–1033, 2011.

[79] B. Ghorbani and K. Vijayaraghavan, "3D and simplified pseudo-2D modeling of single cell of a high temperature solid oxide fuel cell to be used for online control strategies," Int. J. Hydrogen Energy, vol. 43, no. 20, pp. 9733–9748, 2018.

[80] M. Ni, "Thermo-electrochemical modeling of ammonia-fueled solid oxide fuel cells considering ammonia thermal decomposition in the anode," Int. J. Hydrogen Energy, vol. 36, no. 4, pp. 3153–3166, 2010.

[81] J. Zhang, L. Lei, D. Liu, F. Zhao, F. Chen, and H. Wang, "Numerical investigation of solid oxide electrolysis cells for hydrogen production applied with different continuity expressions,"Journal Energy Convers. Manag., vol. 149, pp. 646–659, 2017.

[82] M. Ni, "2D thermal-fluid modeling and parametric analysis of a planar solid oxide fuel cell," Journal Energy Convers. Manag., vol. 51, no. 4, pp. 714–721, 2010.

[83] M. E. Chelmehsara and J. Mahmoudimehr, "Techno-economic comparison of anode-supported, cathode-supported, and electrolyte-supported SOFCs," Int. J. Hydrogen Energy, vol. 43, no. 32, pp. 15521–15530, 2018.

[84] T. Wilberforce *et al.*, "Optimization of Fuel Cell Performance Using Computational Fluid Dynamics," Journal Membranes, pp. 1–20, 2021.

[85] S. Zeng, X. Zhang, J. Song, T. Li, and M. Andersson, "Modeling of solid oxide fuel cells with optimized interconnect designs," Int. J. Heat Mass Transf., vol. 125, pp. 506–514, 2018.

[86] S. Cordiner, M. Feola, V. Mulone, and F. Romanelli, "Analysis of a SOFC energy generation system fuelled with biomass reformate,"Journal Applied Thermal Engineering 27 vol. 27, pp. 738–747, 2007.

[87] L. Andreassi, G. Rubeo, S. Ubertini, P. Lunghi, and R. Bove, “Experimental and numerical analysis of a radial flow solid oxide fuel cell,” International Journal of Hydrogen Energy, vol. 32, pp. 4559–4574, 2007.

[88] D. Sànchez, R. Chacartegui, A. M. Oz, and T. Sànchez, “On the effect of methane internal reforming modelling in solid oxide fuel cells,” International Journal of Hydrogen Energy , vol. 33, pp. 1834–1844, 2008.

[89] M. Andersson, J. Yuan, and B. Sundén, “SOFC modeling considering hydrogen and carbon monoxide as electrochemical reactants,” Journal of Power Sources, vol. 232, pp. 42–54, 2013.

[90] S. Yang, T. Chen, Y. Wang, Z. Peng, and W. G. Wang, “Electrochemical Analysis of an Anode-Supported SOFC,” International Journal of Electrochemical Science, vol. 8, pp. 2330–2344, 2013.

[91] R. P. O. Hayre, “Fuel cells for electrochemical energy conversion,” EPJ Web of Conferences, vol. 00013, pp. 1–16, 2017.

[92] S. Youcef and H. Ben Moussa, “Optimization study of the produced electric power by SOFCs,” International Journal of Hydrogen Energy , September 2018.

[93] R. Tchakalov, “Engineering and optimization of electrode/electrolyte interfaces to increase solid oxide fuel cell (SOFC) performances,” Doctoral thesis, 2021.

[94] P. Costamagna, “Modeling of Solid Oxide Heat Exchanger Integrated Stacks and Simulation at High Fuel Utilization,” Journal of Electrochem. Soc., vol. 145, no. 11, p. 3995, 1998.

[95] I. Khazaee and A. Rava, “Numerical simulation of the performance of solid oxide fuel cell with different flow channel geometries,” Journal Energy, 2017.

[96] A. Chaisantikulwat, C. Diaz-Goano, and E. S. Meadows, “Dynamic modelling and control of planar anode-supported solid oxide fuel cell,” Journal Comput. Chem. Eng., vol. 32, no. 10, pp. 2365–2381, 2008.

[97] G. Anandakumar, N. Li, A. Verma, P. Singh, and J. H. Kim, “Thermal stress and

probability of failure analyses of functionally graded solid oxide fuel cells," Journal Power Sources, vol. 195, no. 19, pp. 6659–6670, 2010.

[98] Chyu M, "Numerical modeling of transport phenomena in solid oxide fuel cells," Taiwan Solid Oxide Fuel Cell Symp, 2005.

[99] FergusonJR, F. JM, and H. R, "Three-dimensional numerical simulation for various geometries of solid oxide fuel cells,"Journal power source, vol. 58(2), no. 109–22, 1996.

[100] M. Saied, K. Ahmed, M. Ahmed, M. Nemat-Alla, and M. El-Sebaie, "Investigations of solid oxide fuel cells with functionally graded electrodes for high performance and safe thermal stress," Int. J. Hydrogen Energy, vol. 42, no. 24, pp. 15887–15902, 2017.

[101] Z. Qu *et al.*, "Three-dimensional computational fluid dynamics modeling of anode-supported planar SOFC," Int. J. Hydrogen Energy, vol. 36, no. 16, pp. 10209–10220, 2010.

[102] M. M. Hussain, X. Li, and I. Dincer, "Mathematical modeling of planar solid oxide fuel cells," Journal of Power Sources , vol. 161, pp. 1012–1022, 2006.

[103] K. Keegan, M. Khaleel, L. Chick, K. Recknagle, S. Simner, and J. Deiber, "Analysis of a Planar Solid Oxide Fuel Cell Based Automotive Auxiliary Power Unit," SAE technical paper series, vol. 2002, 2002.

General conclusion

A fuel cell is an electrochemical device that converts chemical energy from a reaction directly into electrical energy. This phenomenon is accompanied by the release of water and heat.

The SOFC solid oxide cell is based on the following mechanism: the oxygen is dissociated at the cathode into O^{2-}, then the anion migrates through the ion-conducting electrolyte at high temperature and will combine with the anode with hydrogen, or carbon monoxide, to form water and release electrons.

On the other hand, the performance of the fuel cell, given by the current-voltage (J-V) curve, is related to the physical parameters (pressure, temperature, mass fractions, etc.), and geometrical parameters. In the first part, it is based on the effect of these parameters that this study is conducted. Whereas the second part evaluates the cell design at different voltages in order to achieve the best performance.

In this study, we developed a numerical model using ANSYS FLUENT 18.1 capable of simulating the main fields that characterize the operation of the fuel cell. The studied phenomena are represented with a mathematical model which allowed us to better know the phenomena taking place inside the cell, so we can predict its behavior under different operating conditions and under the effect of different physical parameters.

The study and simulation of this simultaneous model allowed us to highlight the different operating and geometric parameters, and cell design. In which influence the performance of the fuel cell.

With this in mind, we were able to draw some interesting conclusions:

- The increase in temperature improves the performance. This allows a reduction in the ohmic and activation losses. While the concentration rises as the temperature rises.
- The fuel utilization improves with raising the temperature. This, in turn, leads to better consumption of the hydrogen fraction. Consequently, more water is carried at the cell outlet. Due to the greater inlet fuel temperature
- The increase in the pressure in the cell allows easy diffusion of the gases at the level of the interface electrode/electrolyte, which allows an increase in the concentrations of the reactants to the chemical reaction and consequently decreases the losses of concentration and promotes the performance of the fuel cell. While the fuel utilization is directly proportional to the pressure. Maybe because of a better supply of reactants at higher pressures.
- The reduction in the thickness of the cell electrodes (anode, cathode) allows a reduction in voltage losses and an increase in the power produced at the level of the cell. That is due to when the anode/cathode thickness has reduced the activation

and concentration of the cell diminished. While The AS concentration over potential become a more important loss than CS when a thinner electrolyte is used.

- Reducing electrolyte thickness plays an important role in improving cell performance.
- The highest value fuel utilization is obtained for anode supported that is due a more for the hydrogen diffuses in the transversal direction in the case of anode supported and not in a thicker cathode or electrolyte.
- An increase in temperature, pressure, and porosity corresponds to an increase in reactant consumption.
- An increase in porosity improves the diffusion of species towards the catalyst layer.
- Identify the best configuration and calculate the optimal operating parameters allowing maximum power production.
- The sinusoidal design gave a better distribution of velocities and temperatures than the single flow, which improved the transport of hydrogen of the cell.
- The sinusoidal design has greater performance than the single flow, and this could be useful in choosing the best configuration for certain applications requiring the greatest achievable performance.

The results presented in this thesis are in agreement with the experimental data, and the model is able to analyze the various physical phenomena in SOFC fuel cells which are difficult to realize through the experiments. However, there are still proposals that can improve the present model to achieve a more accurate prediction of all major physical phenomena.

In conclusion, this work has demonstrated the usefulness of modeling for understanding internal physical phenomena, predicting and improving the behavior of SOFC type fuel cells.

International Publications and Communications

Publication article :

- Sabrina Horr et al. Performance analysis of AS-SOFC fuel cell combining single and sinusoidal flow field: numerical study. Renew. Energy Environ. Sustain.6, 18 (2021)

Proceeding:

- Sabrina Horr, Hocine Mohcene, Hamza Bouguettaia et Hocine Ben Moussa. Comparative study of solid oxide fuel cell combined the sinusoidal and single flow fields: numerical study. ISBN: 978-605-66381-7-6. p :510-513. 8th GLOBAL CONFERENCE on GLOBAL WARMING April 22-25, 2019 Doha Qatar.

Communications:

- Sabrina horr, Hocine Mohcene. Les piles à combustible : production de l'électricité à partir des énergies renouvelables. Le Premier Séminaire National de Génie des Procédés (SNGP).Université Hamma Lakhdar El Oued, Algérie, 2017

- Sabrina horr, Hocine Mohcene. Study the effect of gas channel surface on anode supported planar of Solid oxide fuel cell performance. Internaional Symposium on Mechatronics & Renewable Energies (ISMRE). Univ-EL-oued, 2018. http://dspace.univ-eloued.dz/handle/123456789/1524

- Sabrina horr, Hocine Mohcene. The Ohmic and activation over-potential in Anode-Supported Solid Oxide Fuel Cells. International Symposium on Technology & Sustainable Industry Development (ISTSID). Univ-EL-oued, 2019

- Sabrina Horr, Hocine Mohcene, Hamza Bouguettaia and Hocine Ben Moussa. Comparative study of solid oxide fuel cell combined the sinusoidal and single flow fields: numerical study. 8th GLOBAL CONFERENCE on GLOBAL WARMING (GCGW). Doha Qatar, April 22-25, 2019

- Sabrina horr, Hocine Mohcene, Hamza Bouguettaia and Hocine Ben Moussa. Improvement the performance of SOFC fuel cell by optimizing the design of channel. International Conference on Renewable Energy and Energy Conversion (ICREEC). USTO-MB Oran, 11 - 13 November 2019

- Sabrina Horr, Hocine Mohcene**.** Analysis of Mass Transport Characteristics in Anode-Supported Solid Oxide Fuel Cells at Various Designs. The first International Pluridisciplinary PhD Meeting (IPPM). Univ-elouad, 2020